Studies on symbiosis-specific phenotype of *Mesorhizobium loti* and its function to host plant

Yohei TATSUKAMI

2017

Contents

Abbreviations

2D-PAGE	2-dimensional polyacrylamide gel electrophoresis
ABA	abscisic acid
ACP	acyl carrier protein
AON	autoregulation of nodulation
CFU	colony forming unit
CLE	CLAVATA3/ESR-related
CPS	*ent*-copalyl diphosphate synthase
DHAP	dihydroxyacetone phosphate
DMAPP	dimethylallyl pyrophosphate
ED	Entner-Doudoroff
ESI	electrospray ionization
ESR	endosperm surrounding region
EtOAc	ethylacetate
FDR	false-discovery rate
FPP	farnesyl pyrophosphate
GA	gibberellic acid
GAP	glyceraldehyde-3-phosphate
GC/MS	gas chromatography-mass spectrometry
GDH	glutamate dehydrogenase
GGOH	geranylgeraniol
GGPP	geranylgeranyl pyrophosphate
GOGAT	glutamine oxoglutarate aminotransferase
GPP	geranyl pyrophosphate
GS	glutamine synthase
GlcN	glucosamine
GlcNAc	*N*-acetyl-D-glucosamine
HAR	hypernodulation aberrant root
IAA	indole acetic acid

IDI	diphosphate isomerase
IPP	isopentenyl pyrophosphate
IPTG	β-D-1-thiogaractopyranoside
IT	infection thread
JA	jasmonic acid
KA	kaurenoic acid
KDGP	2-dehydro-3-deoxy-phosphogluconate
KEGG	Kyoto Encyclopedia of Genes and Genomes
KS	*ent*-kaurene synthase
LC	liquid chromatography
LC-MS/MS	liquid chromatography-tandem mass spectrometry
LPS	lipopolysaccharide
LysM	lysin motif
MM1	minimal medium 1
MS	mass spectrometry
MSF	major facilitator superfamily
MurNAc	*N*-acetylmuramic acid
NFR	nod factor receptor
NFs	nod factors
NIN	nodule inception
NSP	nodule signaling pathway
PBM	peribacteroid membrane
PBS	phosphate buffer saline
PCA	principal component analysis
TMT	tandem mass tag
PEP	phosphoenolpyruvate
PEPCK	phosphoenolpyruvate carboxykinase
PGPR	plant growth promoting rhizobacteria
PHB	polyhydroxybutyrate
PP	pentose phosphate

ROS	reactive oxygen species
RT-PCR	reverse transcription polymerase chain reaction
SA	salicylic acid
SDR	short-chain type dehydrogenase/reductase
SEM	scanning electron microscopy
SIM	selected ion monitoring
STM	signature-tagged mutagenesis
TCA	tricarboxylic acid
TEAB	triethylammonium bicarbonate
TMS	trimethylsilyldiazomethane
TY	trypton-yeast extract
UDP	uridine diphosphate
WPI	week post inoculation

Introduction

"Symbiosis" was defined by Albert Bernhard Flank in 1877 to describe the mutualistic relationship in *Lichenes*, which is a composite organism that arises from algae or cyanobacteria living among filaments of a fungus (Flank, 1877). "Symbiosis" originally means the living together of two or more dissimilar organisms, as in mutualism, commensalism, amensalism, or parasitism; however, the word is usually narrowed down to mutualism. Symbiosis benefits both species. In the symbiotic relationship, one of the mutualists provides some kind of "service" that its partner cannot provide for itself (e.g. carbon source, nutrients, or dispersal of pollen or seeds) and receives some kind of "reward" (shelter or food) (Bronstein, 1994). It can be observed everywhere; for instance, clownfish and sea anemones, aphids and Buchnera, plants with entomophilous flowers and insects, and humans and its microbiome. Among these symbiotic relationships, the relationship between leguminous plants and rhizobia has been researched for a long time. This relationship is a good model for intracellular symbiosis of bacteria. Since the early 20th century, many researchers have tried to understand the relationship between leguminous plants and rhizobia because it affects both agriculture and biological interactions across the globe (Long, 1989).

Legume-rhizobium symbiosis

Rhizobia are heterotrophic obligate microaerophiles that can assimilate various carbon and nitrogen sources in the rhizosphere to survive in various environments. They are symbiotic nitrogen-fixing bacteria that establish symbiosis with many leguminous (Fabaceae) plants and several other plants by constructing nodules (Fig. 1). This relationship is based on the reciprocal provision of a photosynthetic carbon source from the host and fixed nitrogen sources from the symbiont (Udvardi and Poole, 2013).

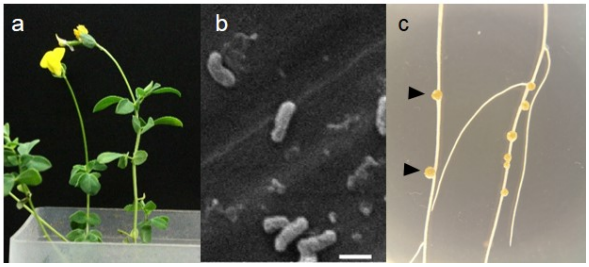

Figure 1 | Legume-rhizobium symbiosis (a) *Lotus japonicus* (Host legume). (b) *Mesorhizobium loti*. Scale bar: 1 μm. (c) Root nodule (arrowhead).

Rhizobial infection of compatible legume strains leads to nodule formation through complex signal exchanges. Leguminous plants release species-specific flavonoids in root

exudates, and compatible rhizobium species show strong chemotaxis towards specific flavonoids (Hassan and Mathesius, 2011). The flavonoids induce the transcription of an important set of nodulation (*nod*) genes of rhizobia, then *nod* genes produce rhizobial symbiotic signal molecules [Nod factors (NFs)], which are lipopolysaccharides (LPS) unique to each rhizobium species (Geurts and Bisseling, 2002; Fig. 2a). The NFs are caught by a specific receptor kinase that contains LysM (lysin motif) domains, such as Nod Factor Receptor 1 (NFR1) and NFR5 in *Lotus japonicus*, and this receptor transmits the signal for symbiosis (Limpens et al., 2003). These unique NF structures determine the strict specificity between rhizobium species and host legume species and elicit both the rhizobial infection process and the initiation of nodule primordia in the roots of the compatible host legumes.

Next, the symbiosis signal is transmitted to a common signaling pathway, inducing Ca^{2+} spiking and influx at the base of the root hair. These Ca^{2+}-dependent signals allow the host cells to support the infection thread (IT) elongation and penetration into cortical cells (Fig. 2b-d). Initiation of ITs requires several sequential steps: attachment of bacteria on the root hairs, root hair curling, and bacterial colonization at the tips of distorted root hairs (Kouchi et al., 2010). The ITs then grow into the developing nodule tissue.

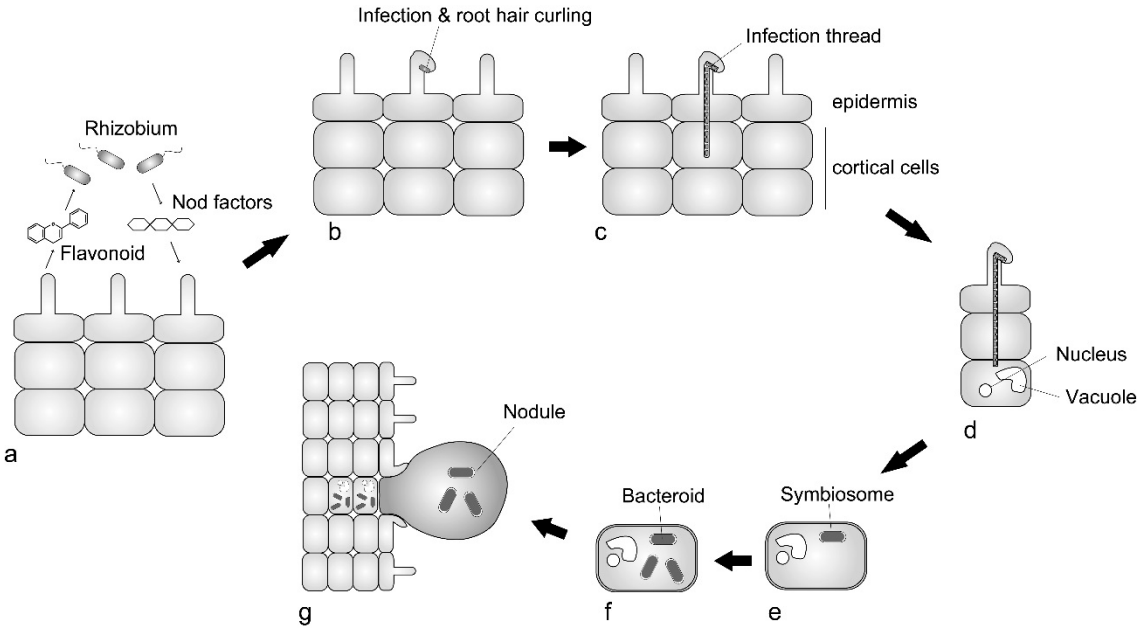

Figure 2 | Nodule formation process (a) The initial signaling in legume-rhizobium interaction. (b) Attachment of rhizobium to the root hair and curled root hair formation. (c) Root hair invasion by elongation of the IT. (d) Endocytosis of bacteria into the plant cell. (e) Formation of symbiosome as an individual bacterium with a surrounding endocytic membrane. (f) Differentiated bacteroid. (g) Nitrogen fixing nodule.

Rhizobia are released from ITs into the nodule cells during nodule appearance, then covered by the peribacteroid membrane (PBM) which is derived from the host plasma membrane. In the PBM, they differentiate into a symbiosis-specific form, the bacteroid, and bacteroid-containing PBM are called 'symbiosomes' (Roth et al., 1988; Fig. 2e). Fully-matured bacteoroids stop cell division and start nitrogen fixation, and nodule development completes (Fig. 2f, g). Most *Rhizobium* species fix nitrogen only in the nodule cells after differentiation into bacteroids. Therefore, bacteroid differentiation and nitrogen fixation are strictly controlled by complex interaction between the host and symbiont.

However, this field of study has focused mainly on the leguminous physiology, and less on rhizobia, whereas the physiology of rhizobia and the mechanisms underlying differentiation of rhizobia into the bacteroid are still largely unknown.

Determinate and indeterminate nodule

There are two major types of leguminous nodules: determinate nodules and indeterminate nodules (Sprent, 2007). Determinate nodules arise from divisions in the root outer cortex, show spherical shape, lack the persistent nodule meristem, and are mainly produced by tropical legumes such as soybean and *L. japonicus*. The mature nodules contain a homogenous central tissue composed of infected cells fully packed with nitrogen-fixing bacteroids and some uninfected cells (Fig. 3). Bacteroids are released after nodule decay, and most of them revert to a free-living lifestyle.

In contrast, indeterminate nodules arise from divisions in the pericycle and root inner cortex, show cylindrical shape, retain a persistent nodule meristem (resulting in elongated nodules), and are mainly produced by temperate legumes such as pea, white clover, and *Medicago truncatula*. The mature nodules contain five histological zones of sequential developmental states (Fig. 3): an apical meristem (zone I), an infection zone

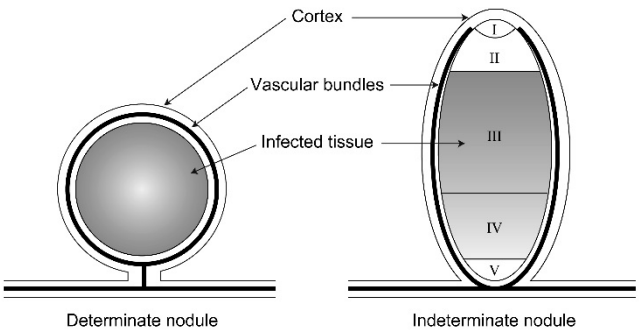

Figure 3 | Schematic representation of determinate (left) and indeterminate nodules (right) I, meristemic zone; II, infection zone; III, nitrogen fixing zone; IV, senescence zone; V, saprophytic zone. This figure was modified from Dupont et al., 2012

where ITs penetrate the plant cells and release rhizobia (zone II), a zone of nitrogen fixation (zone III), a root proximal senescence zone (zone IV), and a saprophytic zone containing undifferentiated bacteria (zone V) (Vasse et al., 1990, Timmers et al., 2000).

While the nodule morphologies and cortical responses are somewhat distinct, almost all known signaling elements have a conserved function between the two types of nodules as described in the former section. However, responses against certain phytohormones appear to have distinct or even opposite roles during the development of these two types of nodules (Subramanian, 2013).

Mechanism and regulation of nodulation

Nodule number is controlled to balance nitrogen income and energy loss. Appropriate nodule formation is a very effective means of host survival in nitrogen-deficient soil; however, over-nodulation consumes too much energy for nitrogen fixation and nodule organogenesis (Fig. 4). To optimize the ratio of nitrogen income to carbon-based energy loss, the host plant tightly regulates nodule organogenesis. Nodule development is locally and systemically controlled (Ryu et al., 2012, Ferguson & Mathesius, 2014).

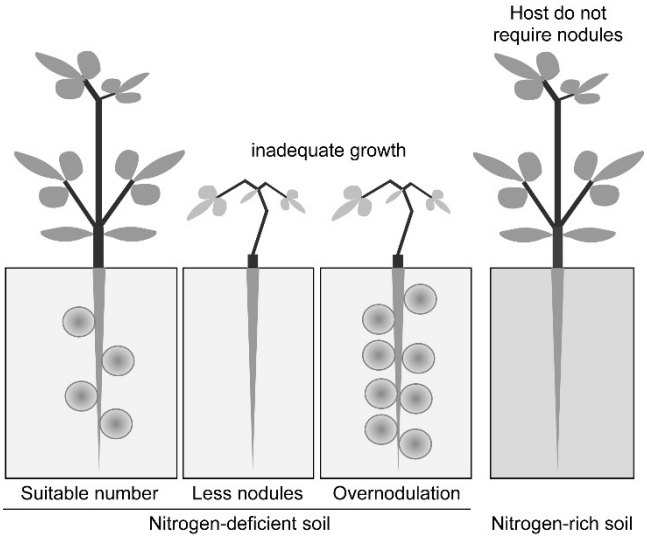

Figure 4 | Regulation of nodule number Nodule number is controlled to grow appropriately. Nodule deficiency and over- nodulation lead to inadequate growth. No nodules are formed in nitrogen-rich soil.

In local control, several phytohormones are induced in the plant in response to rhizobial Nod-factors (NFs) such as LPS and exopolysaccharides secreted by rhizobia, then phytohormones regulate several nodulation processes (Ferguson & Mathesius, 2014; Fig. 5a). In the stage of nodule initiation, ethylene, Jasmonic acid (JA), and abscisic acid (ABA) inhibit root hair response and Ca^{2+} spiking (Nukui et al., 2000, Peters & Crist- Estes, 1989, Oldroyd et al., 2001, Sun et al., 2006, Nakagawa et al., 2006, Suzuki et al., 2004, Ding et al., 2004). Salicylic acid (SA) inhibits rhizobial association with root hairs and nodule primordium

formation only in indeterminate nodule-forming legumes (van Spronsen et al., 2003). In contrast, gibberellic acid (GA) inhibits root hair deformation, nodule formation, and Ca^{2+} spiking only in determinate nodule-forming legumes (Maekawa et al., 2009). Cytokinin might play an important role in cortex cell division during nodule development because the expression of key transcriptional factors associated with nodule initiation such as Nodule Inception (NIN) and Nodule Signaling Pathway 1 (NSP1) act downstream of cytokinin (Madsen et al., 2010). Auxin, which is a central regulator of plant development, has a crucial role for nodule development because auxin accumulation has been observed in early developing nodule primordia in both determinate and indeterminate nodule-forming hosts (van Noorden et al., 2007, Suzaki et al., 2012).

In systemic control, plants perform autoregulation of nodulation (AON), which is a long-distance root-to-shoot-to-root negative feedback system (Caetano-Anolles & Gresshoff, 1991, Oka-Kira & Kawaguchi, 2006, Ferguson et al., 2010; Fig. 5b). In this system, plants use CLAVATA3/ESR (endosperm surrounding region)-related (CLE) glycopeptides as root-to-shoot signal molecules in response to high nitrate conditions and infection of rhizobia (Okamoto et al., 2009, 2013). Root-derived CLE peptides are transported to the shoot and are then recognized by the hypernodulation aberrant root (HAR1) receptor kinase. Recognition by

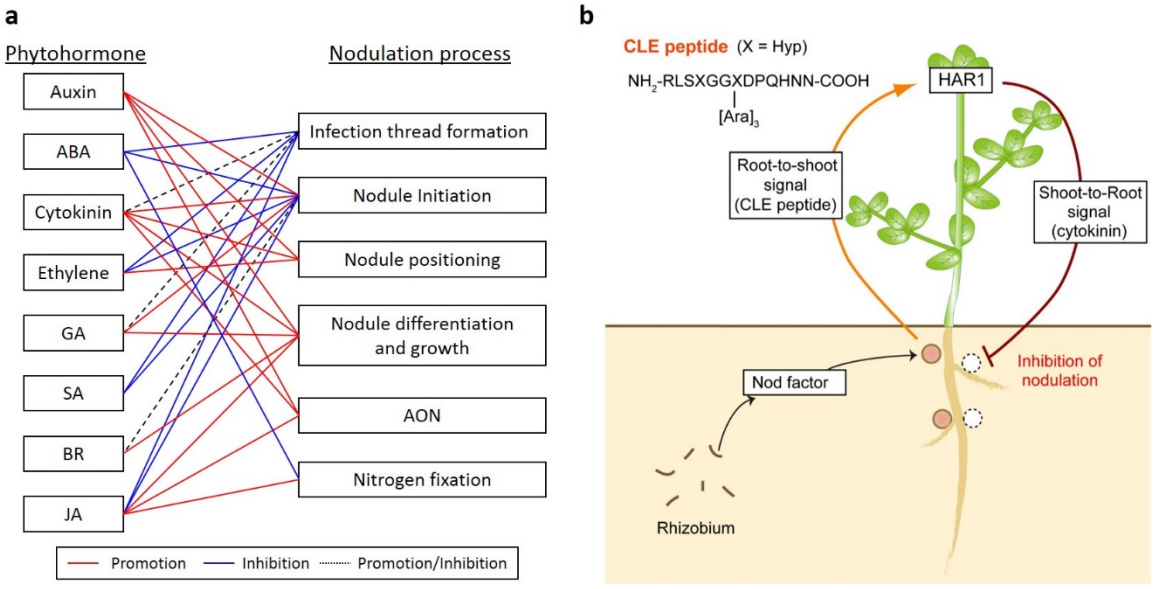

Figure 5 | Regulation of nodulation (a) Phytohormonal regulation of nodulation. Seven phytohormones (Auxin, ABA, Cytokinin, Ethylene, GA, Brassinosteroid (BR), JA) and a phytohormone- like compound (SA) are associated with the nodulation process. (b) Autoregulation of nodulation. NFs from rhizobia induce the root-to-shoot-to-root signal, and the nodulation process is inhibited.

HAR1 results in cytokinin production in the shoot, and the produced cytokinins are transported to the root, as a shoot-to-root signal, where they systemically suppress nodulation (Sasaki et al., 2014).

In both cases, nodule organogenesis is reported to be controlled by plant-derived phytohormones and peptides. In other words, regulation of nodulation has been thought to be the plant-responsible event. However, symbiont-derived signals that regulate the host nodule number have not reported.

Phytohormone biosynthesis in bacteria

Some soil bacteria promote plant growth by synthesizing phytohormones as well as other regulatory chemicals such as siderophores and exo-polysaccharides. These bacteria are called 'plant growth promoting rhizobacteria (PGPRs)'. It is reported that 80% of bacteria isolated from the rhizosphere of various crops possess the ability to synthesize the phytohormone auxin (Patten and Glick, 1996). Auxin affects various plant developmental processes such as plant cell division and differentiation, root development, vegetative growth, biosynthesis of various metabolites, and resistance to stressful conditions. Bacterial auxin interferes with the above events by altering the endogenous pool of plant auxin (Glick, 2012, Spaepen et al., 2007). *Rhizobium* species also synthesize auxin, and the artificially-prepared auxin-overproduction mutant of *Sinorhizobium meliloti* increased nodulation in *Medicago* species, whereas the auxin-overproduction mutant of *Rhizobium leguminosarum* had no effect on nodulation in *Paseolus vulgaris* (Pii et al., 2007). *Bradyrhizobium japonicum* is reported to have the ability to synthesize indole acetic acid, (IAA; auxin), zeatin (cytokinin), GA, ABA, and ethylene under cultivation (Boiero et al., 2007). However, detailed knowledge of the function of rhizobial phytohormone is still mostly unknown.

Proteomics

Rhizobia are typical PGPRs, and it seems very important for agriculture and ecology to clarify the physiology of rhizobia. In legume-rhizobium symbiosis, numerous studies have been performed from the perspective of genetics, biochemistry, molecular biology, cell biology, and so on. These studies have provided many beneficial findings but have focused mostly on clarifying the physiology of the host plant, whereas the physiology of rhizobia is still largely unknown. For

example, elucidating the difference between free-living and symbiotic rhizobia as well as the changes that take place during nodule maturation would be interesting research objectives.

Proteomics holds the potential to comprehensively disclose the physiology of rhizobia on the molecular level. Proteomic studies of many *Rhizobium* species have already been performed. Proteome analysis of *Mesorhizobium loti* in mid-growth phase has been reported (Kajiwara et al., 2003), but it has not been performed for the symbiotic phase. Proteome analyses of other rhizobia, such as *B. japonicum* (Nomura et al., 2010, Delmonte et al., 2010, Hampel et al., 2009, Sarma et al., 2005, 2006) and *S. meliloti* (Barra-Bily et al., 2010, Chen et al., 2003, Djordjevic, 2004, Gao et al., 2005, 2007, Torres-Quesada et al., 2010), have previously been reported. They employed 2-dimensional polyacrylamide gel electrophoresis (2D-PAGE)-based analysis combined with matrix-assisted laser desorption and ionization time-of-flight mass spectrometry, but time-consuming steps, such as gel spot isolation and individual measurement, are necessary with this method. In addition, previous 2D-PAGE-based analyses have only identified up to 500 proteins (Sarma et al., 2005). Another report employed liquid chromatography-tandem mass spectrometry (LC-MS/MS)-based technology combined with prefractionation, such as multidimensional chromatography (Larrainzar et al., 2007) or gel-based separation (Knief et al., 2011), but these prefractionation steps decreased throughput. Furthermore, all of them included a complicated isolation step of the bacteroid (a symbiotic form of rhizobia) from the nodule, and the step required a large number of biological samples, such as 1–5 g nodules collected from approximately 40 plants (Koch et al., 2010). Detection of small amount of proteins present in complex biological samples remains difficult and requires a combination of prefractionation steps.

However, the recent development of shotgun proteomics approaches may hold the potential for solving the problem. Orbitrap mass spectrometers (Shannon and Makarov, 2015) have been used to identify small amounts of proteins by acquiring the mass-to-charge ratio in a high-throughput manner with much higher resolution than conventional ion traps or other MS devices. In addition, a long capillary monolithic column showed much higher separation ability than is possible with conventional packed columns (Iwasaki et al., 2010, Morisaka et al., 2012). Using the equipment, I can perform proteomics of rhizobium in symbiosis with host plants by identifying a large number of proteins including proteins in low abundance in complex biological samples.

The purpose of this study is to clarify the physiology of rhizobia during symbiosis on the

molecular level. I use *L. japonicus* and *M. loti*, both of which are model organisms for the study of legume-rhizobia symbiosis. The entire genome structures of *L. japonicus* MG-20 and *M. loti* MAFF303099 have been reported previously (Kaneko et al., 2000, Sato et al., 2008). In this study, I mainly use proteomics as a tool for the clarification of rhizobial physiology, because it enables me to comprehensively understand the physiological changes of *M. loti* during symbiosis at the protein level and to find a novel phenotype of *M. loti*. Moreover, in this issue, I further investigate the rhizobial biosynthesis of phytohormones revealed by proteomics.

References

1. Ahemad M, Kibret M, Mechanisms and applications of plant growth promoting rhizobacteria: Current perspective. *J. King Saud Univ. Sci*., **26**, 1-20 (2014)
2. Barra-Bily L, Fontenelle C, Jan G, Flechard M, Trautwetter A, Pandey SP, Walker GC, Blanco C, Proteomic alterations explain phenotypic changes in *Sinorhizobium meliloti* lacking the RNA chaperone Hfq. *J. Bacteriol*., **192**, 1719-1729 (2010)
3. Boiero L, Perrig D, Masciarelli O, Penna C, Cassán F, Luna V, Phytohormone production by three strains of *Bradyrhizobium japonicum* and possible physiological and technological implications. *Appl. Microbiol. Biotechnol*., **74**, 874-880 (2007)
4. Bronstein JL, Our current understanding of mutualism, *Q. Rev. Biol.,* **69**, 31-51 (1994)
5. Caetano-Anolles G, Gresshoff PM, Plant genetic control of nodulation. *Annu. Rev. Microbiol.,* **45**, 345–382 (1991)
6. Chen H, Teplitski M, Robinson JB, Rolfe BG, Bauer WD, Proteomic analysis of wild-type *Sinorhizobium meliloti* responses to N-acyl homoserine lactone quorum-sensing signals and the transition to stationary phase. *J. Bacteriol*., **185**, 5029-5036 (2003)
7. Delmotte N, Ahrens CH, Knief C, Qeli E, Koch M, Fischer HM, Vorholt JA, Hennecke H, Pessi G, An integrated proteomics and transcriptomics reference data set provides new insights into the *Bradyrhizobium japonicum* bacteroid metabolism in soybean root nodules. *Proteomics*, **10**, 1391-1400 (2010)
8. Ding Y, Kalo P, Yendrek C, Sun J, Liang Y, Marsh JF, Harris JM, Oldroyd GE, Abscisic acid coordinates nod factor and cytokinin signaling during the regulation of nodulation in

Medicago truncatula. *Plant Cell*, **20**, 2681-2695 (2008)

9. Djordjevic MA, *Sinorhizobium meliloti* metabolism in the root nodule: a proteomic perspective. *Proteomics*, **4**, 1859-1872 (2004)
10. Dupont L, Alloing G, Pierre O, Msehli SE, Hopkins J, Hérouart D, Frendo P, The legume root nodule: from symbiotic nitrogen fixation to senescence. *Senescence*, 137-168 (2012)
11. Ferguson BJ, Indrasumunar A, Hayashi S, Lin MH, Lin YH, Reid DE, Gresshoff PM, Molecular analysis of legume nodule development and autoregulation. *J. Integr. Plant Biol.*, **52**, 61–76 (2010).
12. Ferguson BJ, Mathesius U, Phytohormone regulation of legume-rhizobia interactions. *J. Chem. Ecol.*, **40**, 770–790 (2014).
13. Flank AB, Über die biologischen verhältnisse des thallus einiger krustflechten. *Cohn Beitr. Biol. Pflanz*, **2**, 123–200 (1877)
14. Gao M, Chen H, Eberhard A, Gronquist MR, Robinson JB, Rolfe BG, Bauer WD, sinI- and expR-dependent quorum sensing in *Sinorhizobium meliloti*. *J. Bacteriol*., **187**, 7931-7944 (2005)
15. Gao M, Chen H, Eberhard A, Gronquist MR, Robinson JB, Connolly M, Teplitski M, Rolfe BG, Bauer WD, Effects of AiiA-mediated quorum quenching in *Sinorhizobium meliloti* on quorum-sensing signals, proteome patterns, and symbiotic interactions. *Mol. Plant Microbe Interact.*, **20**, 843-856 (2007)
16. Geurts R, Bisseling T, *Rhizobium* Nod factor perception and signaling. *Plant Cell*, **14**, 239-249 (2002)
17. Hassan S, Mathesius U, The role of flavonoids in root-rhizosphere signaling: opportunities and challenges for improving plant-microbe interaction. *J. Exp. Bot.*, **63**, 3429-3444 (2012)
18. Hempel J, Zehner S, Goettfert M, Patschkowski T, Analysis of the secretome of the soybean symbiont *Bradyrhizobium japonicum*. *J. Biotechnol*., **140**, 51-58 (2009)
19. Iwasaki M, Miwa S, Ikegami T, Tomita M, Tanaka N, Ishihama Y, One-dimensional capillary liquid chromatographic separation coupled with tandem mass spectrometry unveils the *Escherichia coli* proteome on a microarray scale. *Anal. Chem*., **82**, 2616-2620 (2010)
20. Kajiwara H, Kaneko T, Ishizaka M, Tajima S, Kouchi H, Protein profile of symbiotic bacteria *Mesorhizobium loti* MAFF303099 in mid-growth phase. *Biosci. Biotechnol. Biochem*., **67**,

2668-2673 (2003)

21. Kaneko T, Nakamura Y, Sato S, Asamizu E, Kato T, Sasamoto S, Watanabe A, Idesawa K, Ishikawa A, Kawashima K, Kimura T, Kishida Y, Kiyokawa C, Kohara M, Matsumoto M, Matsuno A, Mochizuki Y, Nakayama S, Nakazaki N, Shimpo S, Sugimoto M, Takeuchi C, Yamada M, Tabata S: Complete genome structure of the nitrogen-fixing symbiotic bacterium *Mesorhizobium loti*. *DNA Res.*, **7**, 381-406 (2000)
22. Knief C, Delmotte N, Vorholt JA, Bacterial adaptation to life in association with plants - A proteomic perspective from culture to *in situ* conditions. *Proteomics*, **11**, 3086-3105 (2011)
23. Koch M, Delmotte N, Rehrauer H, Vorholt JA, Pessi G, Hennecke H, Rhizobial adaptation to hosts, a new facet in the legume root-nodule symbiosis. *Mol. Plant Microbe Interact.*, **23**, 784-790 (2010)
24. Kouchi H, Imaizumi-Anraku H, Hayashi M, Hakoyama T, Nakagawa T, Umehara Y, Suganuma N, Kawaguchi M, How many peas in a pod? Legume genes responsible for mutualistic symbioses underground. *Plant Cell Physiol.*, **51**, 1381-1397 (2010)
25. Larrainzar E, Wienkoop S, Weckwerth W, Ladrera R, Arrese-Igor C, Gonzalez EM, *Medicago truncatula* root nodule proteome analysis reveals differential plant and bacteroid responses to drought stress. *Plant Physiol.*, **144**, 1495-1507 (2007)
26. Limpens E, Franken C, Smit P, Willemse J, Bisseling T, Geurts R, LysM domain receptor kinases regulating rhizobial Nod factor-induced infection. *Science*, **302**, 630-633 (2003)
27. Long SR, Rhizobium-legume nodulation: Life together in the underground. *Cell*, **56**, 203-204 (1989)
28. Madsen LH, Tirichine L, Jurkiewicz A, Sullivan JT, Heckmann AB, Bek AS, Ronson CW, James EK, Stougaard J, The molecular network governing nodule organogenesis and infection in the model legume *Lotus japonicus*. *Nat. Commun.*, **1**, 10 (2010)
29. Maekawa T, Maekawa-Yoshikawa M, Takeda N, Imaizumi-Anraku H, Murooka Y, Hayashi M, Gibberellin controls the nodulation signaling pathway in *Lotus japonicus*. *Plant J.*, **58**, 183-194 (2009)
30. Morisaka H, Matsui K, Tatsukami Y, Kuroda K, Miyake H, Tamaru Y, Ueda M, Profile of native cellulosomal proteins of *Clostridium cellulovorans* adapted to various carbon sources. *AMB Express*, **2**, 37-41 (2012)

31. Nakagawa T, Kawaguchi M, Shoot-applied MeJA suppresses root nodulation in *Lotus japonicus*. *Plant Cell Physiol.*, **47**, 176-180 (2006)
32. Nomura M, Arunothayanan H, Dao TV, Le HTP, Kaneko T, Sato S, Tabata S, Tajima S, Differential protein profiles of *Bradyrhizobium japonicum* USDA110 bacteroid during soybean nodule development. *Soil Sci. Plant. Nutr*., **56**, 579-590 (2010)
33. Nukui N, Ezura H, Yuhashi K, Yasuta T, Minamisawa K, Effects of ethylene precursor and inhibitors for ethylene biosynthesis and perception on nodulation in *Lotus japonicus* and *Macroptilium atropurpureum*. *Plant Cell Physiol*., **41**, 893-897 (2000)
34. Oka-Kira E, Kawaguchi M, Long-distance signaling to control root nodule number. *Curr. Opin. Plant Biol.* **9**, 496–502 (2006).
35. Okamoto S, Ohnishi E, Sato S, Takahashi H, Nakazono M, Tabata S, Kawaguchi M, Nod factor/nitrate-induced *CLE* genes that drive HAR1-mediated systemic regulation of nodulation. *Plant Cell Physiol.*, **50**, 67–77 (2009).
36. Okamoto S, Shinohara H, Mori T, Matsubayashi Y, Kawaguchi M, Root-derived CLE glycopeptides control nodulation by direct binding to HAR1 receptor kinase. *Nat. Commun.*, **4**, 2191 (2013).
37. Oldroyd GE, Engstrom EM, Long SR, Ethylene inhibits the Nod factor signal transduction pathway of *Medicago truncatula*. *Plant Cell*, **13**, 1835-1849 (2001)
38. Patten CL, Glick BR, Bacterial biosynthesis of indole-3-acetic acid. *Can. J. Microbiol*., **42**, 207-220 (1996)
39. Peters NK, Crist-Estes DK, Nodule formation is stimulated by the ethylene inhibitor aminoethoxyvinylglycine. *Plant Physiol*., **91**, 690-693 (1989)
40. Pii Y, Crini M, Cremonese G, Spena A, Pandolfini T, Auxin and nitroc oxide control indeterminate nodule formation. *BMC Plant Biol*., **7**, 21 (2007)
41. Roth KE, Jeon K, Stacey G, Homology in endosymbiotic systems: the term “Symbiosome.” *Mol. Genet. Plant Microbe Interact.*, 220-225 (1988)
42. Ryu H, Cho H, Choi D, Hwang I. Plant hormonal regulation of nitrogen-fixing nodule organogenesis. *Mol. Cells*, **34**, 117–126 (2012)
43. Sasaki T, Suzaki T, Soyano T, Kojima M, Sakakibara H, Kawaguchi M, Shoot-derived cytokinins systemically regulate root nodulation. *Nat. Commun.*, **5**, 4983 (2014)

44. Sarma AD, Emerich DW, Global protein expression pattern of *Bradyrhizobium japonicum* bacteroids: a prelude to functional proteomics. *Proteomics*, **5**, 4170-4184 (2005)
45. Sarma AD, Emerich DW, A comparative proteomic evaluation of culture grown vs nodule isolated *Bradyrhizobium japonicum*. *Proteomics*, **6**,3008-3028 (2006)
46. Sato S, Nakamura Y, Kaneko T, Asamizu E, Kato T, Nakao M, Sasamoto S, Watanabe A, Ono A, Kawashima K, Fujishiro T, Katoh M, Kohara M, Kishida Y, Minami C, Nakayama S, Nakazaki N, Shimizu Y, Shimpo S, Takahashi C, Wada T, Yamada M, Ohmido N, Hayashi M, Fukui K, Baba T, Nakamichi T, Mori H, Tabata S, Genome structure of the legume, *Lotus japonicus*. *DNA Res*., **15**, 227-239 (2008)
47. Shannon E, Makarov A, Evolution of orbitrap mass spectrometry instrumentation, *Annu. Rev. Anal. Chem.*, **8**, 61-80 (2015)
48. Spaepen S, Vanderleyden J, Remans R, Indole-3-acetic acid in microbial and microorganism-plant signaling. *FEMS Microbiol. Rev*., **31**, 425-448 (2007)
49. Sprent JI, Evolving ideas of legume evolution and diversity: a taxonomic perspective on the occurrence of nodulation. *New Phytol*., **174**, 11-25 (2007)
50. Subramanian S, Distinct Hormone regulation of determinate and indeterminate nodule development in legumes, *Plant Biochem. Physiol*., **1**, 110-114 (2013)
51. Sun J, Cardoza V, Mitchell DM, Bright L, Oldroyd G, Harris JM, Crosstalk between jasmonic acid, ethylene and Nod factor signaling allows integration of diverse inputs for regulation of nodulation. *Plant J.*, **46**, 961-970 (2006)
52. Suzaki T, Yano K, Ito M, Umehara Y, Suganuma N, Kawaguchi M, Positive and negative regulation of cortical cell division during root nodule development in *Lotus japonicus* is accompanied by auxin response. *Development*, **139**, 3997–4006 (2012)
53. Suzuki A, Akune M, Kogiso M, Imagama Y, Osuki K, Uchiumi T, Higashi S, Han SY, Yoshida S, Asami T, Abe M, Control of nodule number by the phytohormone abscisic acid in the roots of two leguminous species. *Plant Cell Physiol.*, **45**, 914-922 (2004)
54. Timmers AC, Soupene E, Auriac MC, de Billy F, Vasse J, Boistard P, Truchet G, Saprophytic intracellular rhizobia in alfalfa nodules. *Mol. Plant Microbe Interact.*, **13**, 1204-1213 (2000)
55. Torres-Quesada O, Oruezabal RI, Peregrina A, Jofre E, Lloret J, Rivilla R, Toro N, Jimenez-Zurdo JI, The *Sinorhizobium meliloti* RNA chaperone Hfq influences central carbon

metabolism and the symbiotic interaction with alfalfa. *BMC Microbiol*., **10**, 71 (2010)

56. Udvardi M, Poole PS, Transport and metabolism in legume-rhizobia symbiosis. *Annu. Re. Plant Biol.,* **64**, 781-805 (2013)
57. van Noorden GE, Kerim T, Goffard N, Wiblin R, Pellerone FI, Rolfe BG, Mathesius U, Overlap of proteome changes in *Medicago truncatula* in response to auxin and *Sinorhizobium meliloti*. *Plant Physiol*., **144**, 1115–1131 (2007)
58. van Spronsen PC, Tak T, Rood AM, van Brussel AA, Kijne JW, Boot KJM, Salicylic acid inhibits indeterminate-type nodulation but not determinate-type nodulation. *Mol. Plant Microbe Interact.,* **16**, 83-91 (2003)
59. Vasse J, de Billy F, Camut S, Truchet G, Correlation between ultrastructural differentiation of bacteroids and nitrogen fixation in alfalfa nodules. *J. Bacteriol*, **172**, 4295-4306 (1990)

Chapter I Comparison of proteomes in *Mesorhizobium loti* under free-living and symbiotic conditions

Rhizobia are nitrogen-fixing soil bacteria that show intracellular symbiosis with their host legume. This symbiotic interaction has become a model system to identify and characterize the attractive mechanism employed by invasive bacteria during chronic host interactions (Gibson et al., 2008). Rhizobia have two physiological phases; free-living phase in soil, and the symbiotic nitrogen-fixing phase. In nodule, host provides nutrients to the bacteroid (symbiotic form of rhizobia), and bacteroid provides nitrogen sources. The lifestyle of rhizobia remains largely unknown, although genome and transcriptome analyses have been carried out.

Lotus japonicus and *Mesorhizobium loti* are model organisms of legume-rhizobia symbiosis. In this chapter, I performed proteome analysis of *M. loti* to compare the protein profile between *M. loti* under free-living and symbiotic phases to disclose the difference of the physiology in the two phases. Especially, I used a liquid chromatography-tandem mass spectrometry system, equipped with a long monolithic silica capillary column (Miyamoto et al., 2008, Morisaka et al., 2012), which is superior to conventional columns. This high performance proteomics system allowed me to perform proteomics of symbiotic *M. loti* without any additional prefractionation prior to the separation and detection step by liquid chromatography- tandem mass

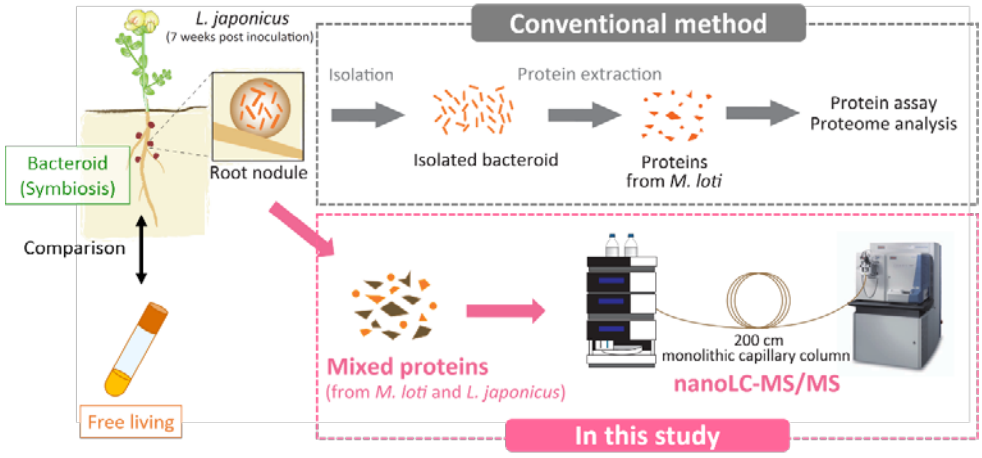

Figure 1 | Analytical method in this study In conventional system, bacteroids were isolated from root nodules with troublesome steps, then the extracted proteins were applied for low-throughput protein assays such as two-dimensional polyacrylamide gel electrophoresis (2D-PAGE). In this study, proteins were directly extracted from fractured nodules, and applied to the nanoLC-MS/MS system equipped with monolithic silica capillary column.

spectrometry (LC-MS/MS) different from the conventional system (Fig. 1). This approach can simplify the workflow of shotgun proteomics and minimize the sample amount, as well as total analysis time.

Materials and Methods

Strains and media

M. loti MAFF303099 was cultured in tryptone-yeast extract (TY) medium (Beringer, 1974) at 28°C. Cells were harvested in the early stationary phase for 72 h. Cells were subjected to sample preparation in the free-living condition.

For the symbiotic condition, *L. japonicus* MG-20 Miyakojima (Kawaguchi, 2000) seeds were sterilized, germinated, and inoculated with *M. loti* and grown in minimal medium 1 (MM1; Becard and Fortin, 1988) medium at 25°C with a 16-h light/8-h dark cycle. Root nodules from several plants were harvested at 7 weeks post-inoculation. Nodules from 3 independently grown pools of plants were collected and processed in parallel.

Sample preparation

Free-living cells were collected with centrifuge at 10,000 × g for 5 min. Less than 20 mg of nodules were frozen with liquid nitrogen, homogenized with an ice-cold mortar, and subjected to sample preparation. Collected cells or nodule homogenates were resuspended with 500 μL of lysis buffer (2% (w/v) 3-(3-cholamidopropyl)dimethylammonio-1-propanesulfonate, 10 mM dithiothreitol, 1% (v/v) protease inhibitor cocktail (Sigma-Aldrich, St. Louis, MO, USA), 7 M urea, and 2 M thiourea in 50 mM Tris–HCl (Nacalai tesque, Kyoto, Japan)). The solution was mixed with an equal volume of 0.5-mm glass beads (Tomy Seiko, Tokyo, Japan). The cells were then disrupted mechanically in triplicate by using BeadSmash 12 (Wakenyaku, Kyoto, Japan) at 4°C, 4,000 × g for 1 min. The solution was centrifuged at 14,000 × g for 10 min, and the supernatant was collected. The supernatant was filtered by 0.45 μm Ultrafree-MC (Millipore, Billerica, MA, USA). The filtered solution was subjected to ultrafiltration using Amicon Ultra YM-10 (Millipore) and buffer-exchanged by 200 mM triethylammonium bicarbonate (TEAB; Sigma-Aldrich). The proteins were reduced by adding 10 mM tris-(2-carboxyethyl)phosphine

(Thermo Fisher Scientific, Waltham, MA, USA) and incubated at 55°C for 1 h. After the reaction, 20 mM iodoacetamide was added to the solution, and incubated for 30 min. The reactant was mixed with 1 mL of ice-cold acetone and incubated at −20°C for 3 h to precipitate proteins. The precipitated proteins were resuspended with 100 μL of 200 mM TEAB and mixed with 2 μl (1 μg μL^{-1}) of sequencing grade modified trypsin (Promega, Madison, WI, USA) at 37°C overnight. The peptide concentration of the tryptic digests was measured using Protein Assay Bicinchoninate Kit (Nacalai tesque). The concentrations of the injected digests were 1.06 ± 0.12 μg μL^{-1} digest for free-living *M. loti* and 4.96 ± 0.90 μg μL^{-1} digest for nodules, respectively. (mean ± SD, N = 3).

LC-MS/MS analysis

Proteome analyses were performed by a liquid chromatography (UltiMate3000 RSLCnano system (Thermo Fisher Scientific))/mass spectrometry (LTQ Velos mass spectrometer (Thermo Fisher Scientific)) system equipped with a long monolithic silica capillary column (200-cm long, 0.1-mm ID) (Motokawa et al., 2002). 10 and 5 μL of tryptic digests were injected for free-living and symbiotic conditions, respectively, and separated by reversed-phase chromatography at a flow rate of 500 nL min^{-1}. The gradient was provided by changing the mixing ratio of the 2 eluents: A, 0.1% (v/v) formic acid and B, 80% (v/v) acetonitrile containing 0.1% (v/v) formic acid. The gradient was started with 5% B, increased to 50% B for 600 min, further increased to 95% B to wash the column, then returned to the initial condition, and held for re-equilibration. The separated analytes were detected on a mass spectrometer with a full scan range of 350–1,500 m/z. For data-dependent acquisition, the method was set to automatically analyze the top 5 most intense ions observed in the MS scan. An electrospray ionization (ESI) voltage of 2.4 kV was applied directly to the LC buffer end of the chromatography column by using a MicroTee (Upchurch Scientific, Oak Harbor, WA, USA). The ion transfer tube temperature was set to 300°C. Triplicate analyses were done for each sample of 3 biological replicates, and blank runs were inserted between different samples.

Data analysis

The mass spectrometry data of each sample were used for protein identification using

MASCOT (Matrix Science, London, UK), working on Proteome Discoverer (Thermo Fisher Scientific) against the database at Rhizobase containing 7,283 sequences with a peptide tolerance of 1.2 Da, MS/MS tolerance of 0.8 Da, and maximum number of missed cleavages of 2. For trypsin digestion, cysteine carbamidomethylation (+57.021 Da) and methionine oxidation (+15.995 Da) were set as a variable modification. The data were then filtered at a q-value ≤ 0.01 corresponding to 1% false discovery rate on a spectral level. Moreover, proteins identified by at least 2 peptides per protein or identified by a single peptide per protein at any 3 data points were accepted as 'identified proteins.'

The pathway analysis of identified proteins is performed by using the pathway mapping tool on the Kyoto Encyclopedia of Genes and Genomes (KEGG; http://www.genome.jp/kegg/). The functional classification of proteins was performed by using Rhizobase (http://genome.microbedb.jp/rhizobase/) at Kazusa DNA Research Institute.

Results

Identification of proteins extracted from free-living and symbiotic M. loti

The tryptic digests were injected to a LC-MS/MS system equipped with a long monolithic silica capillary column; 1,658 proteins were successfully identified by efficient separation. Specifically, 1,533 proteins were identified under the free-living condition, and 847 proteins were identified by the analytes extracted from nodules without bacteroid isolation and prefractionation (Fig. 2a). Many proteins encoded in the symbiosis island were also identified. The symbiosis island of *M. loti* MAFF303099 is one of the notable features, which occurs by integration of a horizontally transferred DNA segment, and is located on a 610,975-bp DNA segment of the chromosome at coordinates 4,644,702 to 5,255,766 (Kaneko et al., 2000). A total of 582 protein-encoding genes were located on the symbiosis island. Mapping the identified proteins to the symbiosis island showed that 74 proteins (8.7% of 847 proteins) were produced under the symbiotic condition, whereas only 22 proteins (1.4% of 1,533 proteins) were produced under the free-living condition. From the viewpoint of reproducibility, my data show highly-reproducible result with the strict criteria for protein identification (Fig. 2b). As shown in this figure, 87% of

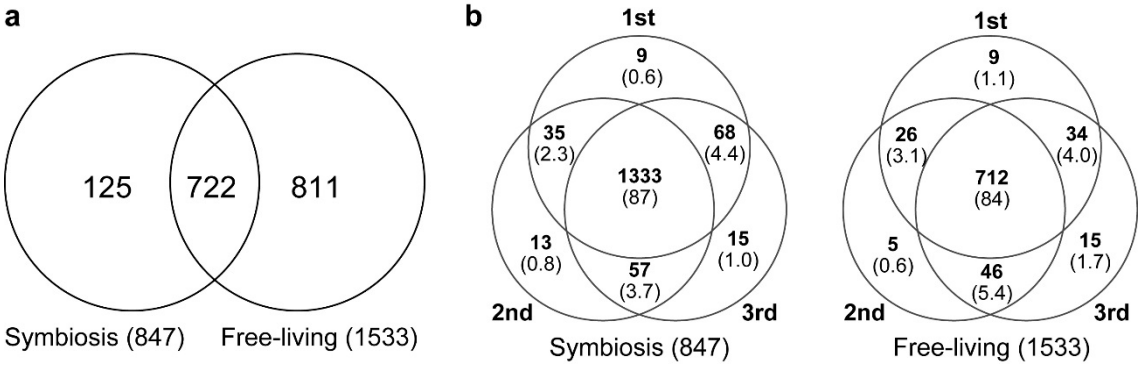

Figure 2 | The Venn diagram of proteins identified in *M. loti* (a) A total of 1,658 proteins were identified. Although 733 proteins were commonly identified under the free-living and symbiotic conditions, 811 and 125 proteins were uniquely identified under the free-living and symbiotic conditions, respectively. (b) Protein identification at each measurement (N = 3). The number of identified proteins were shown in bold, and percentages were indicated between brackets.

proteins were identified from 3 data set under the free-living conditions, although the previous report indicated that protein profile of free-living *M. loti* in stationary phase was not reproducible (Kajiwara et al., 2003). And identified proteins under the symbiotic condition also show high-reproducibility because 84% of proteins were identified at all measurements. These results indicated that the protein profile successfully obtained with my system reflected the free-living and the symbiotic conditions.

KEGG pathway analysis

For further investigation about the lifestyle of rhizobia under each condition, the identified proteins were classified according to KEGG, and metabolic pathways were compared under the free-living and symbiotic conditions. The number of classified enzymes in each pathway is shown in Figure 3a.

To investigate the functional distribution, identified proteins under each condition were classified into 15 major functional categories according to Rhizobase (Fig. 3b). There was no significant difference between the functional profiles under each condition. This indicated that the metabolic pathways, which constitute the backbone of life, were commonly used under both conditions.

a

Pathway	Symbiotic condition	Free-living condition	Genes*
Central carbon metabolism	49	56	77
Nitrogen fixation	8	2	6
Ubiquinone biosynthesis	6	5	9
Nucleotide sugar metabolism	1	6	13
Peptideglycan biosynthesis	2	7	15

b

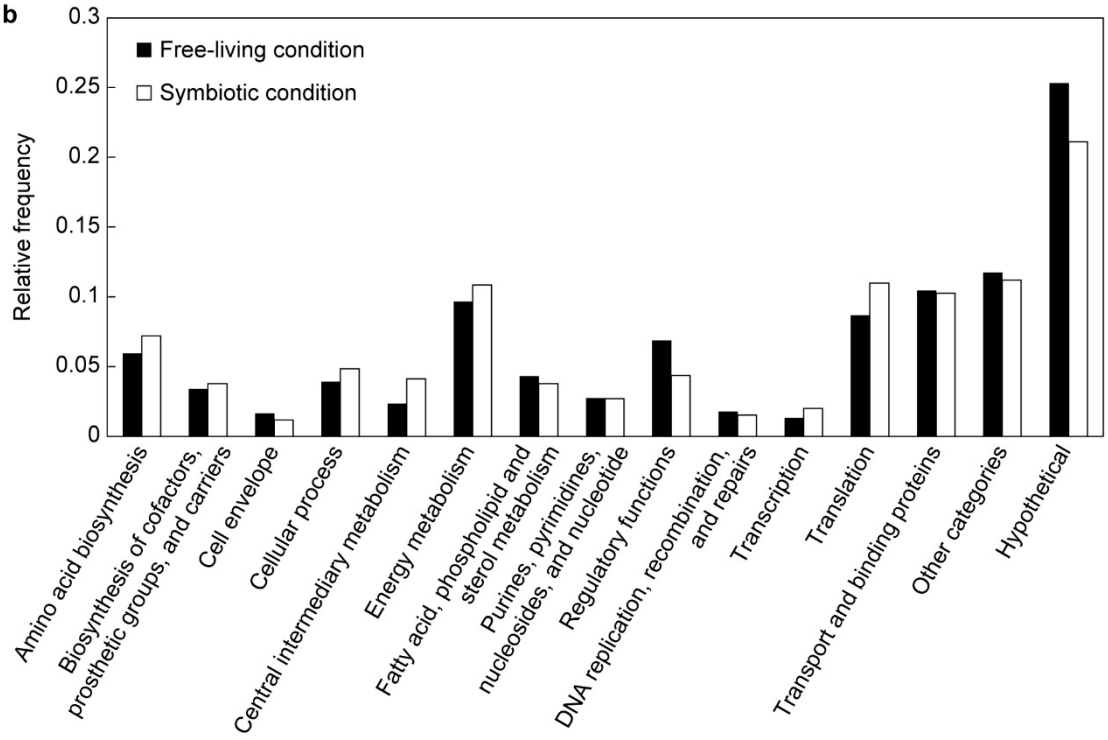

Figure 3 | Functional classification according to KEGG and Rhizobase (a) The number of classified enzymes detected by proteome analysis. Asterisk shows the number of genes proposed by KEGG pathway analysis. (b) Functional classification by Rhizobase. Relative frequency of proteins belonging to a category is given for 2 data sets: the proteins detected under the free-living condition (1,533; closed black bar) and in the *L. japonicus* nodule (847; open black bar). The relative frequencies are calculated by dividing the number of proteins in each category by the total number of identified proteins.

Central carbon metabolism

Most enzymes classified in carbon metabolism, such as glycolysis, gluconeogenesis, tricarboxylic acid (TCA) cycle, pentose phosphate (PP), and Entner-Doudoroff (ED) pathways, were commonly identified (Fig. 4). It is assumed that the same pathways located in central carbon metabolism remained largely unchanged, irrespective of condition.

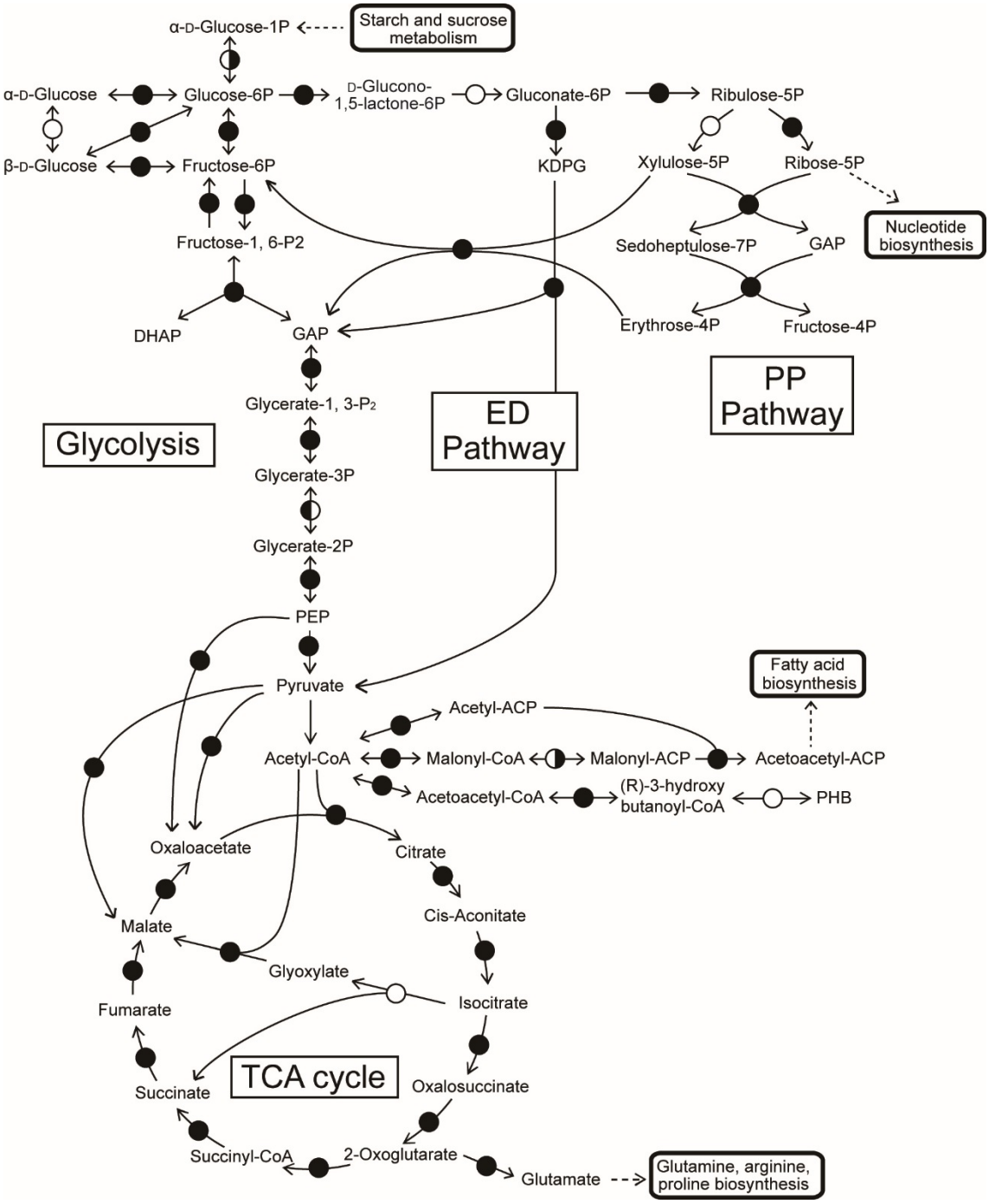

Figure 4 | The map of central carbon metabolic pathways under the free-living and/or symbiotic conditions The map of central carbon metabolic pathways involving glycolysis, gluconeogenesis, the ED pathway, the PP pathway, and the TCA cycle are shown. Symbols represent the following: fully-filled circle (●), enzymes that were commonly identified under each condition; right side-fulled circle (◑), enzyme identified only under the free-living condition; left side-filled circle (◐), enzymes that were identified only under the symbiotic condition; open circle (○), enzymes not identified in this study but proposed in *M. loti* by KEGG pathway analysis. Abbreviations are as follows: DHAP, dihydroxyacetone phosphate; GAP, glyceraldehyde-3-phosphate; PEP, phosphoenolpyruvate; KDPG, 2-dehydro-3-deoxy- phosphogluconate; ACP, acyl carrier protein; PHB, polyhydroxybutyrate

Nitrogen fixation

Nitrogenase complex core subunits (NifH, NifD, NifK) and the electron donor proteins (FixA, FixB, FixC), which transfer electrons to the nitrogenase complex, were detected only under the symbiotic condition (Fig. 5a). Fixation of atmospheric nitrogen is a characteristic feature of rhizobia only under the symbiotic condition (Uchiumi et al., 2004). The proteins related to nitrogen fixation, such as nitrogenase construction (NifN, NifX, NifS, NifW) (Masson-Boivin et al., 2009), electron donation (FixX, FixP), and symbiosis-unique ferredoxins (mlr5869, mlr5930, msl8750), were also found to be unique to the symbiotic condition. In addition, NifA and RpoN, which are known to cooperatively regulate nif and fix genes, were detected only under the symbiotic condition (Shingler, 2011). The protein profile strongly reflected the phenotype that was predicted by transcriptome analysis (Uchiumi et al., 2004).

Terpenoid biosynthesis

It is generally known that rhizobia provide ammonia and other amino acids as a nitrogen source to the host (Prell and Poole, 2006), while no other compound is known to be provided. However, the obtained protein profile suggested that terpenoid derivatives might be provided from rhizobia to plant root cells. In the quinone biosynthetic pathway, the enzymes necessary to farnesyl pyrophosphate (FPP) biosynthesis, such as isopentenyl pyrophosphate isomerase (mlr6371) and geranyltransferase (mlr6368), which are located in the rhizobia symbiosis island, were uniquely detected under the symbiotic condition (Fig. 5b). These enzymes produce isoprenoid precursors such as geranyl pyrophosphate (GPP), FPP, and geranylgeranyl pyrophosphate (GGPP) from isopentenyl diphosphate and dimethyl allyl diphosphate. GPP, FPP, and GGPP are the intermediates in the mevalonate pathway, which is present in all higher eukaryotes and many bacteria. FPP is used for the biosynthesis of ubiquinone in *M. loti*. However, the enzymes which catalyze the ubiquinone biosynthesis reactions from FPP (shown in asterisks in Fig. 5b) were not detected at the protein level. Additionally, the symbiosis island does not include genes encoding octaprenyl-diphosphate synthase (mlr7426) and 4-hydroxybenzoate polyprenyltransferase (mll7442), which are involved in the pathway of ubiquinone biosynthesis. On the other hand, both bacteria and higher plants utilize GPP, FPP, and GGPP as the intermediates of many secondary metabolites, such as monoterpenes, sesqui terpenes, diterpenes,

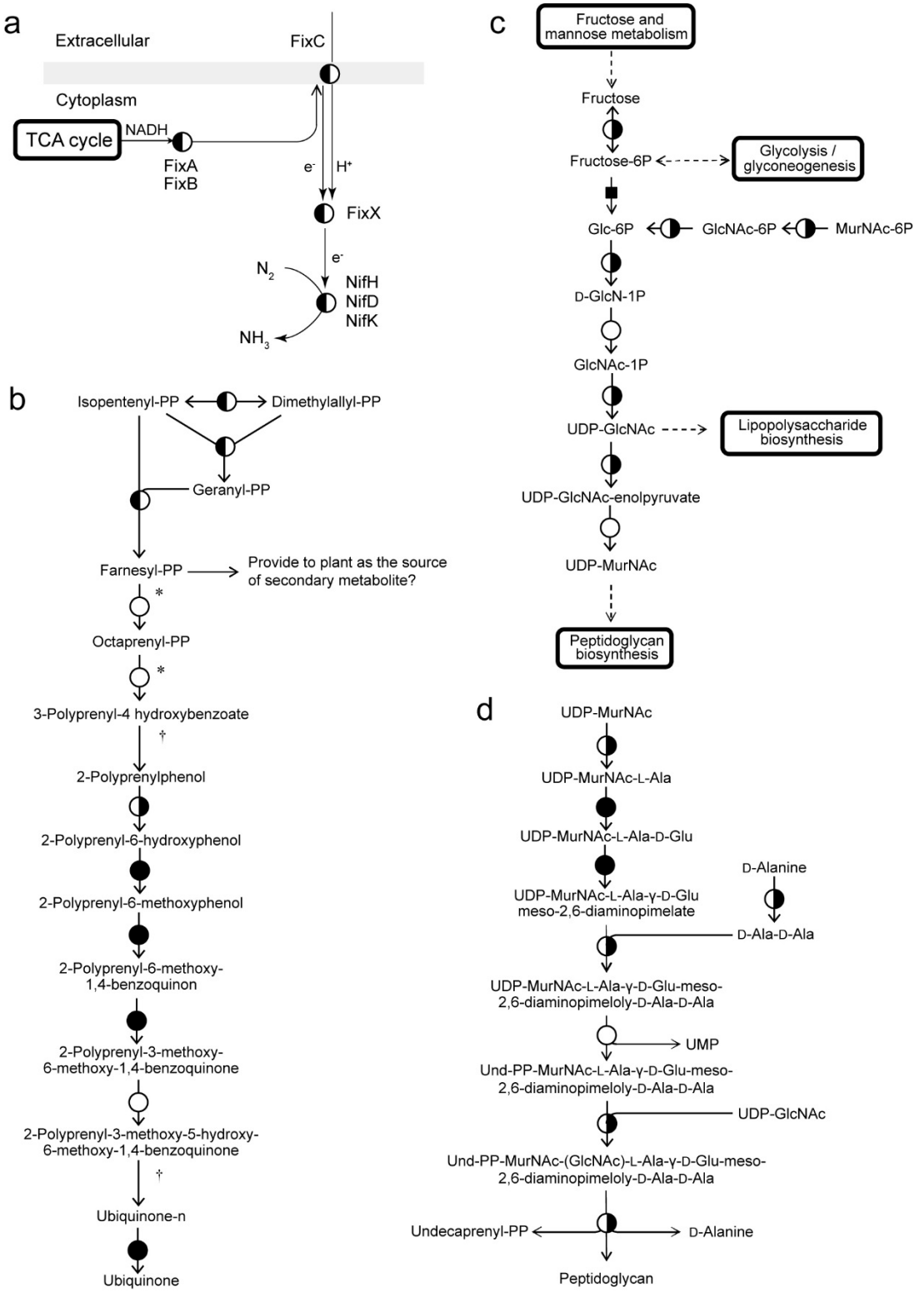

Figure 5 | The map of metabolic pathways under the symbiotic and/or free-living conditions The map of metabolic pathways is shown: (a) Nitrogen fixation, (b) ubiquinone biosynthesis, (c) amino sugar metabolism, (d) peptidoglycan biosynthesis. Circle symbols indicate the same things as in Fig. 4. Daggers (†) indicate the reactions that have universally existed but have not been proposed in *M. loti* by KEGG pathway analysis. Asterisks indicate the focused enzymes discussed in the "Results" section. Abbreviations are as follows: GlcN, Glucosamine; GlcNAc, *N*-acetyl-D-glucosamine, MurNAc, *N*-acetylmuramic acid

and sterols (McGarvey & Croteau, 1995). It is reasonable to suppose that a certain isoprenoid is provided to the host legume from rhizobia.

Nucleotide sugar metabolism and peptidoglycan biosynthesis

On the other hand, the enzymes involved in uridine diphosphate (UDP) sugar metabolism were not produced under the symbiotic condition (Fig. 5c), and lipopolysaccharide (LPS) transporters (mll3197, mll7564, mll7866) were not produced under the symbiotic condition. UDP-*N*-acetylglucosamine is the starting material for LPS biosynthesis. LPS is known as one of the "nod factors," which is secreted by the rhizobial body when it perceives the root through the flavonoid groups secreted from host legume (Denarie et al., 1996). The secretion of LPS is likely unnecessary under the symbiotic condition (after infection). In addition, UDP-*N*-acetylmuramic acid, the end product of this pathway, is the starting material of peptidoglycan biosynthesis. The enzymes of peptidoglycan biosynthesis were uniquely detected under the free-living condition (Fig. 5d).

Flagellum and pilus component

I investigated structural proteins, such as flagellum and pilus component. The flagellum is connected to bacterial motility and attachment of rhizobia to developing root hairs, which is one of the first steps of nitrogen-fixing root nodule symbiosis (Smit et al., 1989). The pilus is a hair-like appendage found on the surface of many bacteria and is related to the process of bacterial conjugation. Rhizobia have not only conjugative pili but also type IV pili, which generate motile forces called twitching motility, in which the pilus works as a grappling hook to bind to a variety of surfaces (Mattick, 2002). The flagellum component proteins, FlaA (mlr2925, mlr2927), FlgL (mlr2939), FlgK (mlr2938), MotB (mlr3926), and FliN (mll2902), were detected only under the free-living condition. DNA microarray analysis has shown that the gene of flagellar L-ling protein (FlgH; mll2921) is repressed at the mRNA level (Uchiumi et al., 2004). Therefore, the obtained protein profile confirmed that under the symbiotic condition, rhizobia repress flagellum genes, and it also indicated that structural proteins of the flagellum are not present under the symbiotic condition. In addition, the pilus assembly proteins, CpaB (mll5595), CpaD (mll5598), and CpaE

(mll5600), were also detected only under the free-living condition. Flagella and pili were lost under the symbiotic condition because rhizobia under the symbiotic condition would have no need for conjugation, infection, and motility in PBM. In contrast, rhizobia under the free-living condition require the flagellum and pilus component proteins.

Discussion

In previous study, transcriptome analysis of *M. loti* by DNA microarray revealed that most of the transposase genes and *nif, fix, fdx,* and *rpoN* on the symbiosis island were highly upregulated under the symbiotic condition, while genes for cell wall synthesis, cell division, DNA replication, and flagella formation were strongly repressed under the symbiotic condition (Uchiumi et al., 2007). However, less information is available about *M. loti* than about other genera of rhizobia, such as *Sinorhizobium meliloti*, *Rhizobium leguminousarum,* and *Bradyrhizobium japonicum*. In addition to transcriptome analysis, proteome analysis has also been applied to rhizobia. Proteome analysis of *M. loti* in mid-growth phase (Kajiwara et al., 2009), *B. japonicum* (Hempel et al., 2009, Sarma & Emerich, 2005, 2006, Nomura et al., 2010, Delmotte et al., 2010), and *S. meliloti* (Chen et al., 2003, Torres-Quesada et al., 2010, Djordjevic, 2004, Barra-Bily et al., 2010, Gao et al., 2007, 2010) have been previously reported with 2-dimensional polyacrylamide gel electrophoresis (2D-PAGE). Another report employed LC-MS/MS combined with multidimensional chromatography (Larrainzar et al., 2007) or gel-based separation (Knief et al., 2011). However gel-based separation and prefractionation steps decreased throughput. Furthermore, all of them included a complicated isolation step of the bacteroid from the nodule, and the step required 1–5 g nodules (Koch et al., 2010).

In this chapter, I used a LC-MS/MS system with a long monolithic silica capillary column and performed high-throughput proteome analysis. By using this system, I identified 847 proteins in *M. loti* under the symbiotic condition from less than 20 mg of root nodules without bacteroid isolation step. The number of identified protein from low amount of crude biological samples guaranteed the performance of my analytical system. On the other hand, I identified 1,533 proteins from free-living *M. loti*. The difference of the number of identified protein between symbiosis and free-living condition derived from following 2 reasons; (i) the variety of rhizobial proteins

would decrease in nodule because *M. loti* reduced the activity of transcription and translation during bacteroid differentiation (discussed in Chapter II) and (ii) the sample crudeness decreased the identification rate of *M. loti* proteins because the peptide sample contained abundant plant proteins and the number of spectra used for rhizobial protein identification were relatively decreased. In total, I identified 1,658 proteins which is corresponding to 22.8 % of all genes encoded on *M. loti* genome. The number of identified protein is superior to the previous reports of rhizobial proteomics (Afroz et al., 2013).

Under the symbiotic condition, rhizobia are differentiated into a bacteroid, and the peribacteroid membrane (PBM)-enclosed bacteroids are essentially a nitrogen-fixing intracellular organelle, termed the 'symbiosome.' In PBM, bacteroids are stationary and become slightly larger than the free-living rhizobia (Kouchi et al., 2010). Scanning electron microscopy (SEM) images confirmed the structural changes in rhizobia between the 2 conditions (Fig. 6). However, the remarkable structural changes have not been confirmed at the protein level. Proteome data could detect the proteins involved in the structural changes, as well as changes in metabolic pathway; thus, I focused on cell surface structure.

From my data, it was predicted that peptidoglycan was not biosynthesized under the symbiotic condition described above (Fig. 5d). Peptidoglycan, which is the main material of bacterial cell wall, plays an important role in the maintenance of structure by providing tolerance to osmotic pressure and mechanical stress, and it is also involved in cell division during growth (Young, 2003). The inactivation of the peptidoglycan biosynthetic pathway under the symbiotic condition is supported by the following: (i) the neogenesis of peptidoglycan is unnecessary because fully symbiotic rhizobia cease their cell division, (ii) symbiotic rhizobia are able to avoid

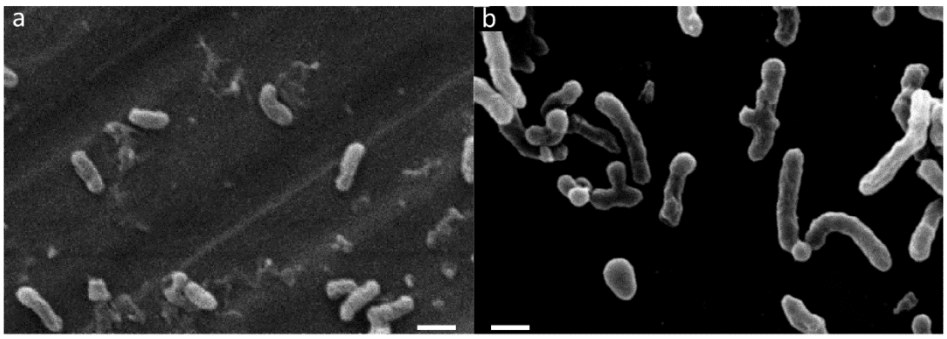

Figure 6 | SEM images of *M. loti* under the symbiotic and free-living conditions The SEM image of (a) *M. loti* under the free-living condition and (b) *M. loti* bacteroid isolated from nodule under symbiotic condition are shown. Scale bars indicate 1 μm.

mechanical stress because of enclosure by PBM and immobility, and (iii) the host legume might control the surrounding environment not to impose an osmotic stress on rhizobia. The protein profile indicates that the interruption of peptidoglycan biosynthesis in symbiotic *M. loti* occurs at the protein level, and rhizobia under the symbiotic condition might lose its cell wall.

From the result of proteome analysis, I focused on the terpenoid biosynthesis. The genes (mlr6368, mlr6371) were encoded on symbiosis island and forms an operon. The operon is consisted by 9 genes (mlr6364-mlr6372), which are 3 cytochrome P450 (mlr6364, mlr6365, mlr6367), short-chain type dehydrogenase/reductase (SDR; mlr6366), geranyltransferase (mlr6368), transport protein (mlr6372), and 3 hypothetical proteins (mlr6369, mlr6370, mlr6371)

To investigate the function of focused operon, I analyzed it from one species from each genus, specifically, examples of species for which complete gemone sequences have been reported, *Sinorhizobium fredii* NGR234 (Schmeisser et al., 2009), *Bradyrhizobium japonicum* USDA110 (Kaneko et al., 2002), and *Rhizobium etli* CFN42 (Gonzalez et al., 2006). Accordingly, the sequence of each gene was used in initial BLAST searches of the Rhizobase database to identify bacteria from the Rhizobiales order that contain homologous genes. By BLAST search, transport protein (mlr6372) was major facilitator superfamily (MSF) transporter, which is a single-polypeptide secondary transporter capable only of transporting small solutes in response to chemiosmotic ion gradient a hypothetical protein (mlr6371) was supposed to be isopentenyl diphosphate isomerase (IDI), and geranyl transferase (mlr6368) presumably synthesized (GGPP).

In addition, homologs to all genes except MFS transporter (mlr6372) were present in *S. fredii*, *B. japonicum*, and *R. etli*, with retention of relative gene order. In particular, homologs to the three cytochrome P450s, an SDR, a geranyltransferase, and three hypothetical proteins (Fig. 7). Although in should be noted that some of these genes were divided and re-combined in certine cases, i.e., mlr6366 were divided into SDR and ferredoxin in *B. japonicum* and *S. fredii*, and ferredoxin moiety were recombined with mlr6365 in *R. etli*, these still exhibited clear homology to the separate genes found elsewhere. And the relevant genes blr2149 and blr2150 in *B. japonicum* were found to be encode *ent*-copalyl diphosphate synthase (CPS) and *ent*-kaurene synthase (KS), respectively (Morrone et al., 2009). Thus, these genes define a core diterpenoid biosynthetic gene cluster/operon that is conserved across all four of the major rhizobial genera, sharing 80 to 95% nucleotide sequence identity. Notably, *M. loti* and *R. etli* have isopentenyl

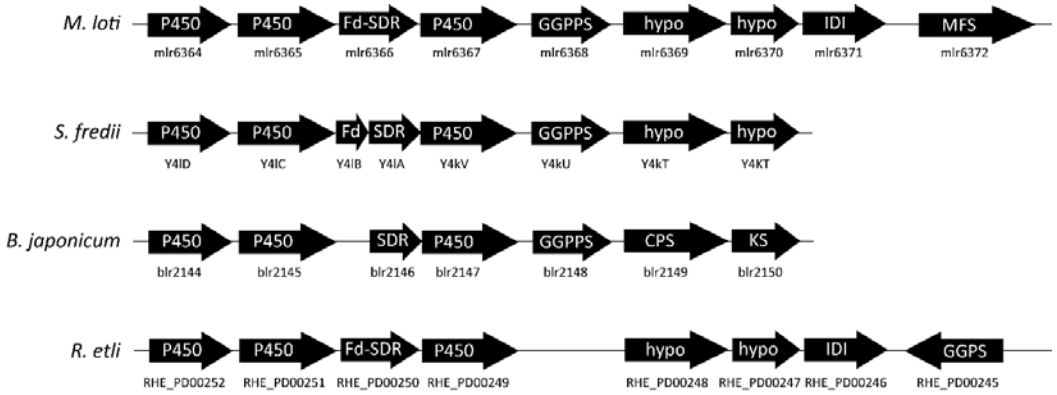

Figure 7 | Schematic of diterpenoid biosynthesis operon from the designated rhizobia The gene designations are described on arrows. The numbers below each allow is accession number of each gene.

---

diphosphate isomerase, which balances the isoprenoid precursor supply and, thus, similarly has a plausible role in terpenoid biosynthesis as well. Intriguingly, *M. loti* uniquely has a gene encoding a MFS transporter immediately downstream of its IDI, and I speculate that this might be involved in secretion of the terpenoid natural product. Accordingly, in *M. loti* and *R. etli* accessory genes appear to have been appended to the core diterpenoid biosynthesis.

Summary

In order to detect the changes in *M. loti* between free-living and symbiotic conditions, I performed proteome analysis of *M. loti*. I used my LC-MS/MS system, equipped with a long monolithic silica capillary column, to successfully identify 1,658 proteins without bacteroid isolation and prefractionation. This analytical system opens up a new horizon for symbiotic proteome analysis from small amounts of unpurified crude biological samples. The protein profile indicated some interesting and unexpected results associated with the cell surface structure and metabolism, in accordance with the external environment of each condition (Fig. 8). The data set revealed that *M. loti* under the symbiotic condition simplifies the components of the cell surface, such as flagellum, pilus, and cell wall. In addition, I found that *M. loti* under the symbiotic condition provided not only a nitrogen source but also isoprenoid, which is a source of secondary metabolism. My data should be helpful in carrying out detailed studies on the change of these 2 conditions of rhizobia.

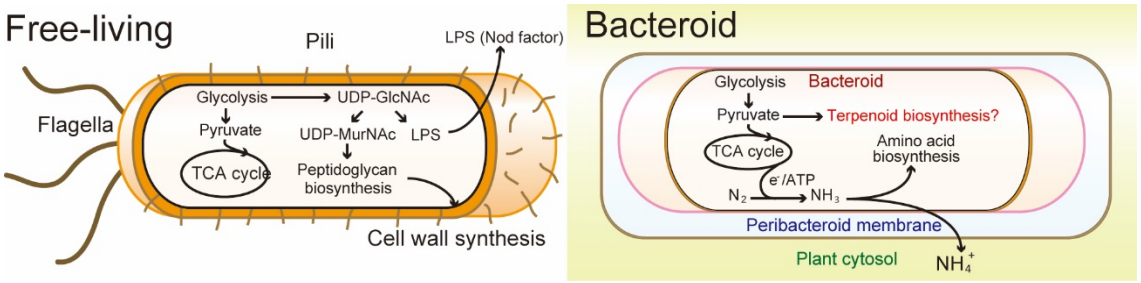

Figure 8 | Schematic representation of the lifestyle under the symbiotic condition compared to the free-living condition The illustration shows the changes in the lifestyles of M. loti: the lifestyle model under the (a) free-living and (b) symbiotic conditions. The central carbon metabolic pathway is essential under both conditions. Under the free-living condition, LPS is secreted extracellularly as a nod factor to infect the host legume. Under the symbiotic condition, nitrogen is fixed by electrons from the TCA cycle or other energy metabolism and is provided to the host legume or used for amino acid biosynthesis. Moreover, terpenoid precursor is synthesized. In contrast, the flagellum and pilus are lost, and the cell wall, which is mainly composed of peptidoglycan, may become thin or disappear.

References

1. Afroz A, Zahur M, Zeeshan N, Komatsu S, Plant-bacterium interactions analyzed by proteomics. *Front. Plant Sci.*, **4**, 1-18 (2013)
2. Barra-Bily L, Fontenelle C, Jan G, Flechard M, Trautwetter A, Pandey SP, Walker GC, Blanco C, Proteomic alterations explain phenotypic changes in *Sinorhizobium meliloti* lacking the RNA chaperone Hfq. *J. Bacteriol.*, **192**, 1719-1729 (2010)
3. Becard G, Fortin JA: Early events of vesicular arbuscular mycorrhiza formation on Ri T-DNA transformed roots. *New. Phytolog.*, 108, 211-218 (1988)
4. Beringer JE, R factor transfer in *Rhizobium leguminosarum*. *J. Gen. Microbiol.*, **84**, 188-198 (1974)
5. Chen H, Teplitski M, Robinson JB, Rolfe BG, Bauer WD, Proteomic analysis of wild-type *Sinorhizobium meliloti* responses to N-acyl homoserine lactone quorum-sensing signals and the transition to stationary phase. *J. Bacteriol.*, **185**, 5029-5036 (2003)
6. Delmotte N, Ahrens CH, Knief C, Qeli E, Koch M, Fischer HM, Vorholt JA, Hennecke H, Pessi G, An integrated proteomics and transcriptomics reference data set provides new insights into the *Bradyrhizobium japonicum* bacteroid metabolism in soybean root nodules. *Proteomics*, **10**, 1391-1400 (2010)

7. Denarie J, Debelle F, Prome JC, Rhizobium lipo-chitooligosaccharide nodulation factors: Signaling molecules mediating recognition and morphogenesis. *Annu. Rev. Biochem.*, **65**, 503-535 (1996)
8. Djordjevic MA, *Sinorhizobium meliloti* metabolism in the root nodule: a proteomic perspective. *Proteomics*, **4**, 1859-1872 (2004)
9. Gao MS, Chen HC, Eberhard A, Gronquist MR, Robinson JB, Connolly M, Teplitski M, Rolfe BG, Bauer WD, Effects of AiiA-mediated quorum quenching in *Sinorhizobium meliloti* on quorum-sensing signals, proteome patterns, and symbiotic interactions. *Mol. Plant Microbe Interact.*, **20**, 843-856 (2007)
10. Gao MS, Chen HC, Eberhard A, Gronquist MR, Robinson JB, Rolfe BG, Bauer WD, sinI- and expR-dependent quorum sensing in *Sinorhizobium meliloti*. *J. Bacteriol*., 187, 7931-7944 (2005)
11. Gibson KE, Kobayashi H, Walker GC, Molecular determinants of a symbiotic chronic infection. *Annu. Rev. Genet.*, **42**, 413-441 (2008)
12. Gonzalez V, Santamaria RI, Bustos P, Hernandez-Gonzalez I, Medrano-Soto A, Moreno-Hagelsieb G, Janga SC, Ramirez MA, Jimenez-Jacinto V, Collado-Vides J et al: The partitioned Rhizobium etli genome: genetic and metabolic redundancy in seven interacting replicons. *Proc. Natl. Acad. Sci. U. S. A.*, **103**, 3834-3839 (2006)
13. Hempel J, Zehner S, Gottfert M, Patschkowski T, Analysis of the secretome of the soybean symbiont *Bradyrhizobium japonicum*. *J. Biotechnol.*, **140**, 51-58 (2009)
14. Kajiwara H, Kaneko T, Ishizaka M, Tajima S, Kouchi H, Protein profile of symbiotic bacteria *Mesorhizobium loti* MAFF303099 in mid-growth phase. *Biosci. Biotechnol. Biochem.*, **67**, 2668-2673 (2003)
15. Kaneko T, Nakamura Y, Sato S, Asamizu E, Kato T, Sasamoto S, Watanabe A, Idesawa K, Ishikawa A, Kawashima K, Kimura T, Kishida Y, Kiyokawa C, Kohara M, Matsumoto M, Matsuno A, Mochizuki Y, Nakayama S, Nakazaki N, Shimpo S, Sugimoto M, Takeuchi C, Yamada M, Tabata S, Complete genome structure of the nitrogen-fixing symbiotic bacterium *Mesorhizobium loti*. *DNA Res*., **7**, 381-406 (2000)
16. Kaneko T, Nakamura Y, Sato S, Minamisawa K, Uchiumi T, Sasamoto S, Watanabe A, Idesawa K, Iriguchi M, Kawashima K, Kohara M, Matsumoto M, Shimpo S, Tsuruoka

H, Wada T, Yamada M, Tabata S, Complete genomic sequence of nitrogen-fixing symbiotic bacterium *Bradyrhizobium japonicum* USDA110. *DNA Res*., **9**,189-197 (2002)

17. Kawaguchi M, *Lotus japonicus* 'Miyakojima' MG-20: An early-flowering accession suitable for indoor handling. *J. Plant Res*., **113**, 507-509 (2000)
18. Knief C, Delmotte N, Vorholt JA, Bacterial adaptation to life in association with plants - A proteomic perspective from culture to *in situ* conditions. *Proteomics*, **11**, 3086-3105 (2011)
19. Koch M, Delmotte N, Rehrauer H, Vorholt JA, Pessi G, Hennecke H, Rhizobial adaptation to hosts, a new facet in the legume root-nodule symbiosis. *Mol. Plant Microbe Interact*., **23**, 784-790 (2010)
20. Kouchi H, Imaizumi-Anraku H, Hayashi M, Hakoyama T, Nakagawa T, Umehara Y, Suganuma N, Kawaguchi M, How Many Peas in a Pod? Legume Genes Responsible for Mutualistic Symbioses Underground. *Plant. Cell Physiol*., **51**, 1381-1397 (2010)
21. Larrainzar E, Wienkoop S, Weckwerth W, Ladrera R, Arrese-Igor C, Gonzalez EM, *Medicago truncatula* root nodule proteome analysis reveals differential plant and bacteroid responses to drought stress. *Plant Physiol*., **144**, 1495-1507 (2007)
22. Masson-Boivin C, Giraud E, Perret X, Batut J, Establishing nitrogen-fixing symbiosis with legumes: how many rhizobium recipes? *Trends Microbiol*., **17**, 458-466 (2009)
23. Mattick JS, Type IV pili and twitching motility. *Annu. Rev. Microbiol*., **56**, 289-314 (2002)
24. McGarvey DJ, Croteau R, Terpenoid metabolism. *Plant Cell*, **7**, 1015-1026 (1995)
25. Miyamoto K, Hara T, Kobayashi H, Morisaka H, Tokuda D, Horie K, Koduki K, Makino S, Núñez O, Yang C, Kawabe T, Ikegami T, Takubo H, Ishihama Y, Tanaka N, High-efficiency liquid chromatographic separation utilizing long monolithic silica capillary columns. *Anal. Chem*., **80**, 8741-8750 (2008)
26. Morisaka H, Matsui K, Tatsukami Y, Kuroda K, Miyake H, Tamaru Y, Ueda M, Profile of native cellulosomal proteins of Clostridium cellulovorans adapted to various carbon sources. *AMB Express*, **2**, 37-41 (2012)
27. Morrone D, Chambers J, Lowry L, Kim G, Anterola A, Bender K, Peters RJ, Gibberellin biosynthesis in bacteria: Separate *ent*-copalyl diphosphate and *ent*-kaurene synthases in *Bradyrhizobium japonicum*. *FEBS Lett*., **583**, 475-480 (2009)
28. Motokawa M, Kobayashi H, Ishizuka N, Minakuchi H, Nakanishi K, Jinnai H, Hosoya K,

Ikegami T, Tanaka N, Monolithic silica columns with various skeleton sizes and through-pore sizes for capillary liquid chromatography. *J. Chromatogr. A.*, **961**, 53-63 (2002)

29. Nomura M, Arunothayanan H, Dao TV, Le HTP, Kaneko T, Sato S, Tabata S, Tajima S, Differential protein profiles of *Bradyrhizobium japonicum* USDA110 bacteroid during soybean nodule development. *Soil Sci. Plant Nutr*., **56**, 579-590 (2010)
30. Prell J, Poole P, Metabolic changes of rhizobia in legume nodules. *Trends Microbiol.*, **14**, 161-168 (2006)
31. Sarma AD, Emerich DW, A comparative proteomic evaluation of culture grown vs nodule isolated *Bradyrhizobium japonicum*. *Proteomics*, **6**, 3008-3028 (2006)
32. Sarma AD, Emerich DW, Global protein expression pattern of *Bradyrhizobium japonicum* bacteroids: a prelude to functional proteomics. *Proteomics*, **5**, 4170-4184 (2005)
33. Schmeisser C, Liesegang H, Krysciak D, Bakkou N, Le Quere A, Wollherr A, Heinemeyer I, Morgenstern B, Pommerening-Roser A, Flores M, Palacios R, Brenner S, Gottschalk G, Schmitz RA, Broughton WJ, Perret X, Strittmatter AW, Streit WR, Rhizobium sp. strain NGR234 possesses a remarkable number of secretion systems. *Appl. Environ. Microbiol.*, **75**, 4035-4045 (2009)
34. Shingler V, Signal sensory systems that impact Sigma 54-dependent transcription. *FEMS Microbiol. Rev*., **35**, 425-440 (2011)
35. Smit G, Kijne JW, Lugtenberg BJ, Roles of flagella, lipopolysaccharide, and a Ca^{2+}-dependent cell surface protein in attachment of *Rhizobium leguminosarum* biovar *viciae* to pea root hair tips. *J. Bacteriol*., **171**, 569-572 (1989)
36. Torres-Quesada O, Oruezabal RI, Peregrina A, Jofre E, Lloret J, Rivilla R, Toro N, Jimenez-Zurdo JI, The *Sinorhizobium meliloti* RNA chaperone Hfq influences central carbon metabolism and the symbiotic interaction with alfalfa. *BMC Microbiol.*, **10**, 71-90 (2010)
37. Uchiumi T, Ohwada T, Itakura M, Mitsui H, Nukui N, Dawadi P, Kaneko T, Tabata S, Yokoyama T, Tejima K, Saeki K, Omori H, Hayashi M, Maekawa T, Sriprang R, Murooka Y, Tajima S, Simomura K, Nomura M, Suzuki A, Shimoda Y, Sioya K, Abe M, Minamisawa K, Expression islands clustered on the symbiosis island of the *Mesorhizobium loti* genome. *J. Bacteriol*., **186**, 2439-2448 (2004)
38. Young KD, Bacterial shape. *Mol. Microbiol*., **49**, 571-580 (2003)

Chapter II Quantitative proteomics of *Mesorhizobium loti* during nodule maturation

Omics analyses are important to characterize dynamic variations in complex biological systems. In particular, proteome analysis is an ideal tool for the characterization of intracellular conditions, as proteins play critical roles in nearly all cellular events (Tyers & Mann, 2003). We reported a qualitative proteome analysis of *M. loti* under both free-living and symbiotic conditions in Chapter I. These analyses revealed distinct protein profiles of *M. loti* and the expression of distinct cell surface structures under each condition. Although the study described the protein profiles between free-living *M. loti* and bacteroid, the specific physiological changes that occur during the transition to the bacteroid state have yet to be fully elucidated.

In this chapter, I aimed to enhance my understanding of metabolic changes which *M. loti* undergoes during the establishment of nitrogen-fixing symbiosis with the host plant *L. japonicus*. To this end, I performed a quantitative time-course proteome analysis of *M. loti* during nodule development to characterize the bacteroid differentiation process.

Materials and Methods

Strains and growth conditions

M. loti MAFF303099 was cultured in tryptone-yeast extract (TY) medium (Beringer, 1974) at 28 °C. Cells were grown to mid log phase (OD_{600} of approximately 0.9–1.1) for 36 h. Cells from this free-living condition were then collected and sample preparation was performed.

To establish symbiotic conditions, *L. japonicus* MG-20 Miyakojima (Kawaguchi, 2000) seeds were sterilized, germinated, grown in minimal medium 1 (MM1) (Becard & Fortin, 1988) medium at 25 °C with a 16 h light/8 h dark cycle, and inoculated with *M. loti*. Root nodules from several plants were harvested at 2, 3, and 4 weeks post-inoculation (WPI), frozen with liquid nitrogen, and stored at −80 °C. Nodules from 3 independently grown pools of plants were collected and processed in parallel.

Bacteroids were isolated and purified from harvested nodules, as previously reported (Kumagai et al., 2007). In brief, nodules were homogenized using a mortar and pestle in 5 mL of 100 mM MOPS-KOH buffer (pH 7.2) containing 375 mM mannitol, 5 mM $MgSO_4$, 10 mM ethylene glycol tetraacetic acid, 3 mM 4-aminobenzamide, 10 mM dithiothreitol, 1% (w/v) polyvinylpyrrolidone-40, 4% (w/v) Dextran T40, and 1% bovine serum albumin. Homogenates were filtered through two layers of Miracloth (Millipore, Billerica, MA, USA), and centrifuged at 4 °C, 100 *g* for 10 min using a Tomy MX-305 refrigerated centrifuge (Tomy Seiko, Tokyo, Japan). The supernatants were harvested and then centrifuged at 4 °C, 700 *g* for 15 min. Pellets were suspended in 200 μL of phosphate-buffered saline (PBS) buffer solution (pH 7.4) (Wakenyaku, Kyoto, Japan), placed on a stepwise gradient of 45%, 60%, and 80% (v/v) Percoll (GE Healthcare, Waukesha, WI, USA), and centrifuged at 4 °C, 4200 *g* for 40 min. The pellets were collected from the interface of 60% and 80% (v/v) Percoll and washed 5 times in 1 mL of PBS buffer solution (pH 7.4). Isolated bacteroids were used for sample preparation.

Sample preparation

Proteins were extracted and digested, as described in Chapter I. The tryptic digests were labeled using the tandem mass tag (TMT) 6-plex labeling kit (Thermo Fisher Scientific, MA, USA), according to the manufacturer's protocol. The TMT labeling reagents were dissolved in 41 μL of acetonitrile and mixed with 30 μL of each tryptic digest, as illustrated in Fig. 1. In brief, the tryptic digests of samples from free-living *M. loti*and bacteroids at 2, 3, and 4 WPI were mixed with TMT 126, 127, 128, and 129, respectively. In addition, a mixture of tryptic digests of samples from free-living and symbiotic organisms was treated with TMT-130 as an internal control for quantification. The reactants were quenched by the addition of 8 μL of 5% hydroxylamine and then lyophilized after mixing all reactants. The dried samples were reconstituted in 30 μL of 0.1% formic acid.

LC–MS/MS analysis

Proteome analyses were performed using a liquid chromatography/mass spectrometry (LC; UltiMate3000, MS; LTQ Orbitrap Velos mass spectrometer, Thermo Fisher Scientific) system

equipped with a long monolithic silica capillary column (500 cm long, 0.1 mm ID) (Matsui et al., 2013). Tryptic digests were injected and separated by reversed-phase chromatography at a flow rate of 500 $nL \cdot min^{-1}$. The gradient was generated by changing the mixing ratio of the 2 eluents: A, 0.1% (v/v) formic acid and B, 80% (v/v) acetonitrile containing 0.1% (v/v) formic acid. The gradient was started with 5% B, increased to 45% B for 600 min, further increased to 95% B to wash the column, then returned to the initial condition, and held for re-equilibration. The separated analytes were detected on a mass spectrometer with a full scan range of 350–1500 *m/z*. For data-dependent acquisition, the apparatus was set to automatically analyze the top 10 most intense ions observed in the MS scan. A normalized collision energy of 40% in higher-energy C-trap dissociation with a 0.1 ms activation time was used. An electrospray ionization voltage of 2.4 kV was applied directly to the buffer end of the LC column using a MicroTee (Upchurch Scientific, Oak Harbor, WA, USA). The ion transfer tube temperature was set to 280 °C. Triplicate analyses were performed for each sample of three biological replicates, and blank runs were inserted between different samples.

Data analyses

The mass spectrometry data from each sample were used for protein identification and quantification. It was performed using Mascot (Matrix Science, London, UK) working on Proteome Discoverer 1.4 (Thermo Fisher Scientific) against the Rhizobase database, containing 7283 sequences, with a precursor mass tolerance of 50 ppm, a fragment ion mass tolerance of 50 mmu, and strict specificity allowing for up to 1 missed cleavage. For trypsin digestion, cysteine carbamidomethylation (+ 57.021 Da), TMT 6-plex of N-term (+ 229.1629 Da), and TMT 6-plex of lysine (+ 229.1629 Da) were set as variable modifications. The data was then filtered at a q-value ≤ 0.01, corresponding to a 1% false discovery rate (FDR) on the spectral level. Protein quantification was performed using the Reported Ions Quantifier with the TMT 6-plex method on Proteome Discoverer software. Three independent biological experiments for each sample were performed, and proteins identified in every replicate with a number of used peptides per protein ≥ 3 were accepted. Proteins that were identified in every replicate were accepted. Global median normalization was carried out to normalize the amount of tryptic digest injected into the

LC–MS/MS.

Non-hierarchical *K*-means clustering, using the Hartigan–Wong algorithm was performed to identify clustered proteome changes. Principal component analysis (PCA) was used to investigate similarities in the production profiles between the three biological replicates. Both analyses were performed using R.

Functional classification of proteins was performed using the Rhizobase (http://genome.microbedb.jp/rhizobase/) at Kazusa DNA Research Institute. The pathway analysis of identified proteins was performed using the KEGG pathway-mapping tool (http://www.genome.jp/kegg/).

To identify proteins that were differentially produced at distinct sampling points, an empirical Bayes moderated *t*-test was performed. To address the issue of multiple comparisons and to control the family-wise error rate, the threshold was set at $P < 0.05$ after adjustment of FDRs, using the Benjamini–Hochberg method.

Results

Protein identification and quantification

To quantify variations in the proteome of *M. loti* bacteroids during nodule maturation, colonized *L. japonicus* nodules were harvested at 2, 3, and 4 WPI. While nodules harvested at 2 WPI, corresponding to the early stage of nodule development, were approximately 1 mm in diameter and were white in color, nodules harvested at 3 and 4 WPI, corresponding to the intermediate stage of nodule development, had grown to approximately 2–3 mm in diameter and were red in color. Bacteroid samples were isolated from harvested nodules, and proteins were extracted, tryptic digested, and TMT-labeled (Fig. 1). Mixtures of each sample (free-living, 2, 3, and 4 WPI, and control) were then subjected to LC–MS/MS analysis, and 537 proteins were successfully identified and quantified. This number of protein identification and quantification is comparable to other reports focused on legume–rhizobium symbiosis (Barra-bily et al., 2010, Chen et al., 2003, Delmotte et al., 2010, Djordevic, 2004, Gao et al., 2007, Hempel et al., 2009, Larrainzar et al., 2007, Sarma & Emerich, 2005, 2006). Correlation analysis and principal com-

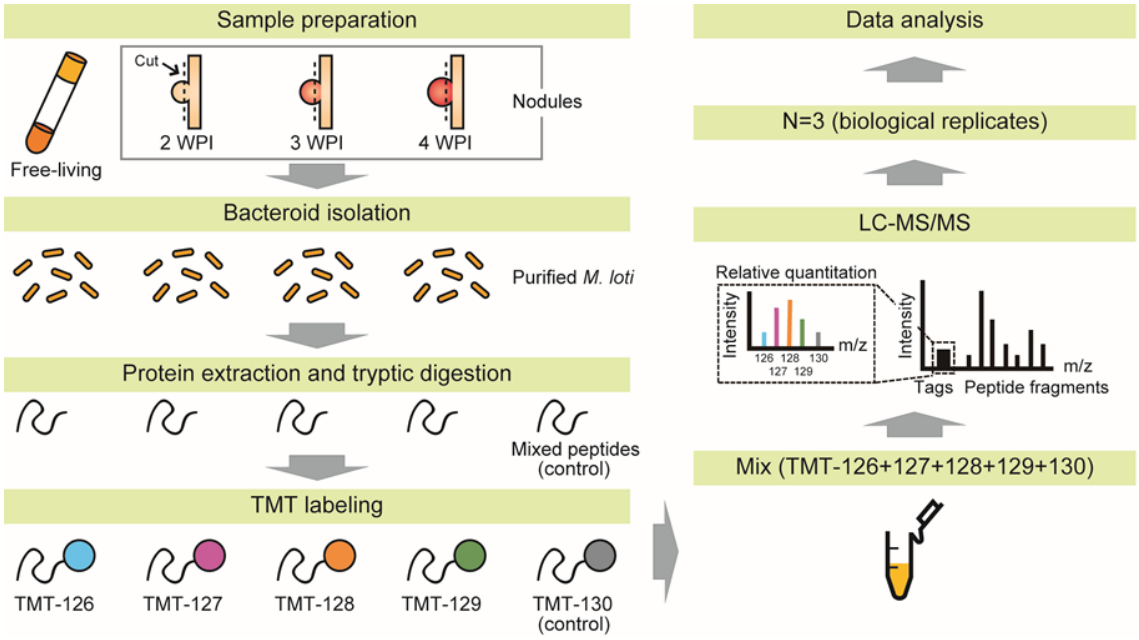

Figure 1 | Experimental workflow for proteome analysis. Samples were harvested from cultured *Mesorhizobium loti* (free-living) and bacteroids isolated from root nodules at 2, 3, and 4 weeks post-inoculation (WPI). Cells were disrupted using glass beads, and the resulting lysates were digested with trypsin. Tryptic peptides were TMT labeled and subjected to LC–MS/MS analysis. A mixture of tryptic digests of samples from free-living and symbiotic cells was used as a control. Details of the experimental workflow are described in the Material and methods.

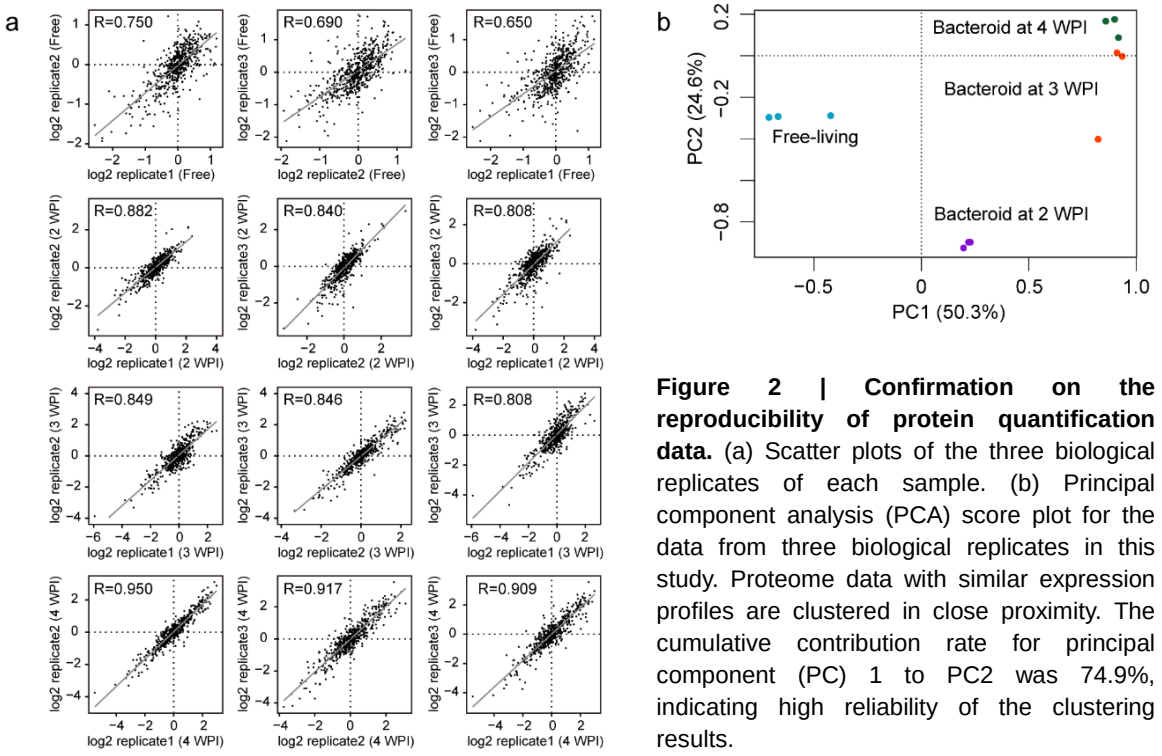

Figure 2 | Confirmation on the reproducibility of protein quantification data. (a) Scatter plots of the three biological replicates of each sample. (b) Principal component analysis (PCA) score plot for the data from three biological replicates in this study. Proteome data with similar expression profiles are clustered in close proximity. The cumulative contribution rate for principal component (PC) 1 to PC2 was 74.9%, indicating high reliability of the clustering results.

ponent analysis (PCA) of the three biological replicates of each sample group were used to evaluate experimental reproducibility. Pearson's correlation analysis (represented as “R”) confirmed the reproducibility (Fig 2a), and plots of PCA scores indicated high levels of similarity between the biological replicates (Fig 2b). These results indicate that I successfully quantified proteome variance with high precision and accuracy.

Clustering analysis

The proteins quantified by LC–MS/MS were classified into five clusters, according to changes in relative abundance to free-living *M. loti*, by non-hierarchical *K*-means clustering (Fig 3a). Relative abundances were calculated by dividing the average abundance of the three biological replicates at each sampling point by the average abundance in free-living *M. loti*. Three protein clusters were up-regulated at 4 WPI during nodule maturation: Group 1 (12-fold), Group 2 (7-fold), and Group 4 (2-fold). Conversely, the Group 5 cluster was down-regulated at 4 WPI

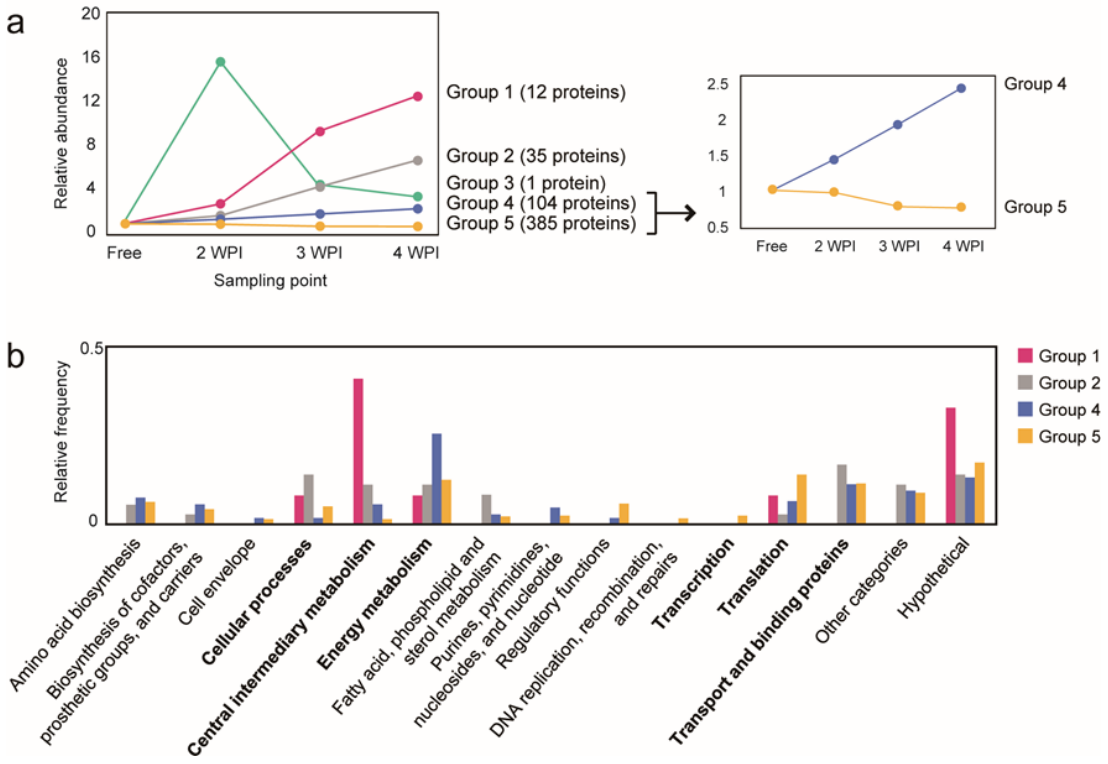

Figure 3 | Functional classification of *K*-means clustered proteome changes. (a) The individual protein profiles classified by *K*-means clustering. Each cluster profile indicates the change in average abundance of clustered proteins. (b) Functional classification of the cluster profiles of Groups 1, 2, 4, and 5. The relative frequencies were calculated by dividing the number of proteins in each category by the total number of proteins identified.

(0.8-fold). Notably, Group 3, which contained only one protein, mll4247, was up-regulated at 2 WPI (16-fold) and then down-regulated at 3 and 4 WPI (5-fold and 4-fold, respectively). Groups 1, 2, 4, and 5 included 12, 35, 104, and 385 proteins, respectively.

To assess the regulation of metabolic processes during bacteroid differentiation, I classified the proteins in Groups 1, 2, 4 and 5 according to their physiological functions, as listed in the rhizobase database (Fig. 3b). This classification revealed that up-regulated proteins (Groups 1, 2, and 4) were generally involved in four functions: central intermediary metabolism, energy metabolism, cellular processes, and transport and binding proteins. The majority of the proteins in Group 1, including the *nif* and *fix* gene products, which are required for nitrogen fixation, were involved in central intermediary metabolism. The expression levels of these proteins markedly increased over the course of nodule maturation (Fig. 3a). These findings are consistent with previous reports that nitrogen fixation by rhizobia occurs only during symbiosis (Uchiumi et al., 2004). The energy metabolism category contained various enzymes involved in central metabolic pathways, including glycolysis and the tricarboxylic acid (TCA) cycle. These findings likely reflect the fact that these processes are crucial for supplying the large amount of ATP and reducing power required for nitrogen fixation (Ronson et al., 1981, Finan et al., 1983). Meanwhile, proteins included in the cellular processes category included enzymes involved in bacterial antioxidant defense. The increase in ATP levels needed for nitrogen fixation by bacteroids requires a concurrent increase in respiration rates, which results in the production of reactive oxygen species (ROS) within the nodules (Hanyu et al., 2009, Becana et al., 2000). Antioxidant defense enzymes would be required to scavenge ROS. Therefore, the observed up-regulation of proteins involved in antioxidant defense is likely a response to prevent oxidative damage during this life stage. Lastly, the transport and binding proteins category included proteins related to iron, sulfur, and phosphorus transport. Iron and sulfur are essential for the proteins involved in nitrogen fixation. Ferredoxins, which transfer electrons from the TCA cycle to the nitrogenase complex, contain [2Fe–2S] clusters, while the nitrogenase complex composed of NifHDK (mlr5905, mlr5906, and mlr5907, respectively) contains [4Fe–4S] clusters, [8Fe–7S] clusters (P-clusters), and [Mo–7Fe–6S] clusters (FeMo cofactors) (Seefeldt et al., 2009). Phosphorus is also required for the production of ATP as an energy source during mutualism. Therefore, these elements likely play

an important role in nitrogen fixation.

Meanwhile, Group 5, which was down-regulated in bacteroids, included multiple proteins involved in transcription and translation. These results indicate that proteins related to gene transcription and mRNA translation, such as RNA polymerases and ribosomal proteins, were repressed during symbiotic growth. The repression of these proteins reflects the reduced multiplication rates of bacteroids during the intermediate stage of nodule development (Ludwig, 1984, Verma, 1992).

Central metabolism

There was a marked change in the central metabolic profile of *M. loti* during the differentiation into bacteroids (Fig. 4). Bacteroids receive carbon and energy sources from hosts in the form of C_4-dicarboxylates, particularly malate and succinate (Prell & Poole, 2006). Because C_4-dicarboxylates are directly incorporated into the TCA cycle, I expected that the expression of proteins involved in this cycle would fluctuate during the course of nodule maturation. Indeed, my proteome analysis indicated that the majority of enzymes involved in the TCA cycle were up-regulated during this period (Fig. 4). The only exception was α-ketoglutarate dehydrogenase (mll4301), which was down-regulated at 2 and 3 WPI, but restored to normal levels at 4 WPI (Fig. 4 box (a)). α-Ketoglutarate dehydrogenase catalyzes the conversion of α-ketoglutarate to S-succinyl-dihydrolipoamide-E. Furthermore, α-ketoglutarate is converted to glutamate by Glutamine oxoglutarate aminotransferase (GOGAT; mll1646) and glutamate dehydrogenase (GDH; mll4104), which were up-regulated at 2 and 4 WPI, respectively (Fig. 5a). My data strongly indicate that the majority of α-ketoglutarate was converted to glutamate by GOGAT or GDH, and then incorporated into amino acid metabolism during symbiotic growth (Fig. 5a). I therefore suggest that biosynthesis of α-ketoglutarate dehydrogenase was down-regulated due to this decrease in α-ketoglutarate.

Phosphoenolpyruvate carboxykinase (PEPCK; mlr5096), which catalyzes the first step in gluconeogenesis, was down-regulated during symbiosis (Fig. 4 box (b)). Reduced PEPCK activity was previously observed in the bacteroids of *Rhizobium leguminosarum*, *S. meliloti*, and *Rhizobium* sp. NGR234 (Mckay et al., 1989, Finan et al., 1991, Saroso et al., 1986). However,

gluconeogenesis appears to be important for symbiotic nitrogen fixation in many rhizobia, including *S. meliloti*, *Rhizobium* sp. NGR234, and *Rhizobium etli*, based on mutation in PEPCK leading to reduced acetylene reduction (Finan et al., 1991, Tate et al., 2004, Osteras et al., 2004). These results suggest that gluconeogenesis was less activated in bacteroids than in free-living *M. loti*, although it was essential for symbiotic nitrogen fixation.

The expression level of branched-chain amino acid transferase (mll2664), which catalyzes the synthesis of the branched-chain amino acids valine, leucine, and isoleucine, decreased during nodule maturation (Fig. 4 box (c)). It has been reported that transporters for branched-chain amino acids were required for effective nitrogen fixation in *R. leguminosarum* (Lodwig et al., 2003, Hosie et al., 2002). These findings therefore suggest that rhizobia must obtain the branched-chain amino acids from the host.

A previous report demonstrated that bacteroids provide ammonium as well as the amino acids alanine and/or aspartate for the host (Allaway et al., 2000). The expression levels of two aspartate aminotransferases, which produce aspartate from oxaloacetate, were quantified (Fig. 4 box (d)). One of these aminotransferases, mlr5883, is encoded within the *M. loti*symbiosis island, and was up-regulated at 3 and 4 WPI (the intermediate stage of nodule development) (Kaneko et al., 2000). The other, mlr2541, is encoded in a region outside the symbiosis island and was constitutively produced. It was reported that expression of the symbiosis island is highly up-regulated during symbiotic growth (Uchiumi et al., 2004). While bacteroids likely used both of the aspartate aminotransferases, aspartate aminotransferase mlr5883 was specially produced

---

Figure 4 | Map of central metabolic pathways. The relative abundances of proteins involved in glycolysis, the Entner-Doudoroff (ED) pathway, the pentose phosphate (PP) pathway, the tricarboxylic acid cycle, and amino acid synthesis at each sampling point were shown. Values were calculated by dividing the average abundance of the three biological replicates at each sampling point by the average abundance in free-living *Mesorhizobium loti*. The values are presented as means ± standard error of the mean (SEM), based on three independent experiments. To compare the individual protein abundances in bacteroids at each sampling point with those in free-living *M. loti*, false discovery rate (FDR)-adjusted *P*-values were determined using an empirical Bayes moderated *t*-test and the Benjamini-Hochberg method: * $P < 0.05$, ** $P < 0.01$. The vertical axes indicate the relative abundances of proteins at each sampling point. The relative abundances of isozymes of each protein are depicted in thin-lined boxes. The relative abundances of specific proteins examined in this study are shown in gray boxes as follows: (a) phosphoenolpyruvate carboxykinase (mlr5096); (b) α-ketoglutarate dehydrogenase (mll4301); (c) branched-chain amino acid transferase (mll2664); (d) alanine dehydrogenase (mll9089); (e) two aspartate aminotransferases (mlr2541, and mlr5883).

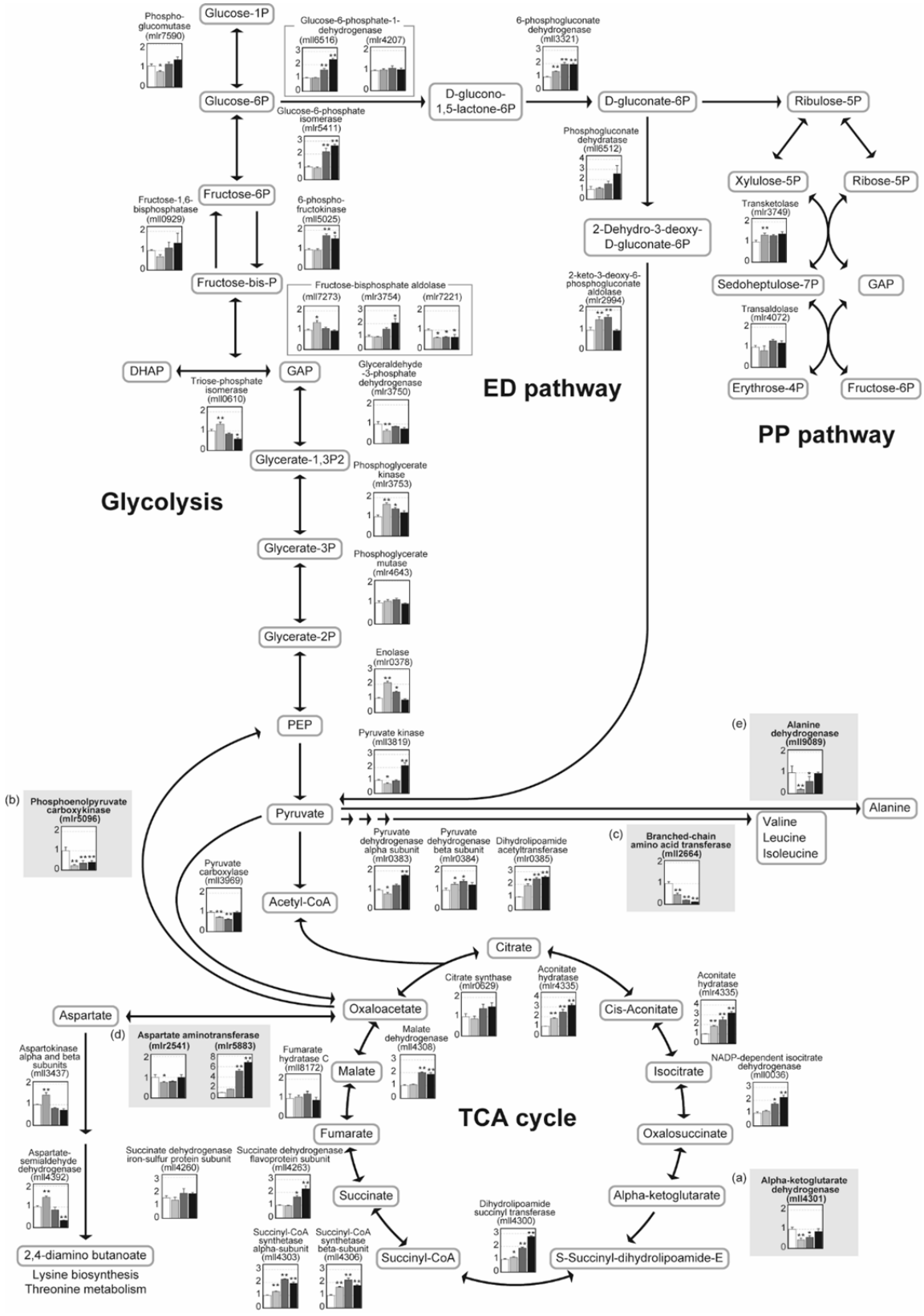
Glucose-1P
Phospho-glucomutase (mlr7590)
Glucose-6P
Glucose-6-phosphate-1-dehydrogenase (mll6516) (mlr4207)
Glucose-6-phosphate isomerase (mlr5411)
D-glucono-1,5-lactone-6P
6-phosphogluconate dehydrogenase (mll3321)
D-gluconate-6P
Ribulose-5P
Phosphogluconate dehydratase (mll6512)
Xylulose-5P
Ribose-5P
Transketolase (mlr3749)
Fructose-6P
Fructose-1,6-bisphosphatase (mll0929)
6-phospho-fructokinase (mll5025)
2-Dehydro-3-deoxy-D-gluconate-6P
Fructose-bis-P
Fructose-bisphosphate aldolase (mll7273) (mlr3754) (mlr7221)
2-keto-3-deoxy-6-phosphogluconate aldolase (mlr2994)
Sedoheptulose-7P
GAP
Transaldolase (mlr4072)
DHAP
GAP
Triose-phosphate isomerase (mll0610)
Glyceraldehyde -3-phosphate dehydrogenase (mlr3750)
ED pathway
Erythrose-4P
Fructose-6P
PP pathway
Glycerate-1,3P2
Phosphoglycerate kinase (mlr3753)
Glycolysis
Glycerate-3P
Phosphoglycerate mutase (mlr4643)
Glycerate-2P
Enolase (mlr0378)
PEP
Pyruvate kinase (mll3819)
(e)
Alanine dehydrogenase (mll9089)
(b)
Phosphoenolpyruvate carboxykinase (mlr5096)
Pyruvate
Alanine
Valine
Leucine
Isoleucine
(c)
Branched-chain amino acid transferase (mll2664)
Pyruvate dehydrogenase alpha subunit (mlr0383)
Pyruvate dehydrogenase beta subunit (mlr0384)
Dihydrolipoamide acetyltransferase (mlr0385)
Pyruvate carboxylase (mll3569)
Acetyl-CoA
Citrate
Citrate synthase (mlr0629)
Aconitate hydratase (mlr4335)
Aconitate hydratase (mlr4335)
Aspartate
Oxaloacetate
Cis-Aconitate
(d)
Aspartate aminotransferase (mlr2541) (mlr5883)
Malate dehydrogenase (mll4308)
Aspartokinase alpha and beta subunits (mll3437)
Fumarate hydratase C (mll8172)
Malate
Isocitrate
NADP-dependent isocitrate dehydrogenase (mll0036)
TCA cycle
Fumarate
Oxalosuccinate
Aspartate-semialdehyde dehydrogenase (mll4392)
Succinate dehydrogenase iron-sulfur protein subunit (mll4260)
Succinate dehydrogenase flavoprotein subunit (mll4263)
Succinate
Alpha-ketoglutarate
(a)
Alpha-ketoglutarate dehydrogenase (mll4301)
Dihydrolipoamide succinyl transferase (mll4300)
Succinyl-CoA synthetase alpha-subunit (mll4303)
Succinyl-CoA synthetase beta-subunit (mll4306)
Succinyl-CoA
S-Succinyl-dihydrolipoamide-E
2,4-diamino butanoate
Lysine biosynthesis
Threonine metabolism

specifically produced at the intermediate stage of nodule development. Conversely, the biosynthesis of alanine dehydrogenase (mll9089), which produces alanine from pyruvate, decreased at the early stage of nodule development. However, production of this protein was restored to levels similar to that observed in free-living *M. loti* at the intermediate stage of nodule development (Fig. 4 box (e)). The fold change (symbiosis/free-living) of aspartate aminotransferase (mlr5883) was higher than that of alanine dehydrogenase (mll9089) (Fig. 4 boxes (d, e)). As a result, bacteroids likely biosynthesized excessive amounts of aspartate during symbiosis, and may therefore secrete larger amounts of aspartate than alanine in the host. This idea is supported by previous reports that aspartate aminotransferase mutants of *S. meliloti* did not fix nitrogen in nodules (Lodwig et al., 2003, Watson et al., 1993).

Nitrogen-deficiency at the early stage of nodule development

The loading scatter plot displays the principal components of the loadings, which are the correlation between the original variables and the factors, and therefore the key to understand the underlying nature of a particular factor (Fig. 5b). Analysis of this figure indicated that the

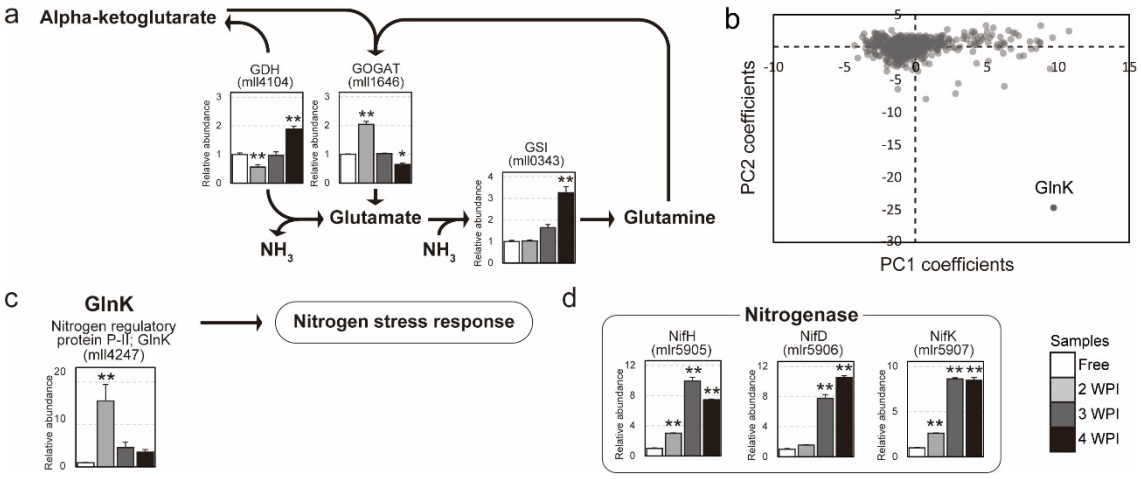

Figure 5 | Adaptation of nitrogen metabolism to symbiotic conditions. (a) The relative abundances of proteins involved in ammonium assimilation. (b) The loading scatter plots corresponding to PCA sore plots in Fig. 2b. (c) The relative abundance of the nitrogen regulatory protein P-II; GlnK. (d) The relative abundances of nitrogenase complex core subunits (NifHDK). Values were calculated by dividing the average abundances of three biological replicates at each sampling point by the average abundance in free-living *Mesorhizobium loti*. The values are presented as means ± SEM, based on three independent experiments. To compare individual protein abundances in bacteroids at each sampling point with those in free-living *M. loti*, false discovery rate (FDR)-adjusted *P*-values were determined using an empirical Bayes moderated *t*-test and the Benjamini–Hochberg method: **P* < 0.05, ***P* < 0.01. Abbreviations are as follows: GDH, glutamate dehydrogenase; GOGAT, glutamine oxoglutarate aminotransferase; GSI, glutamine synthase I.

nitrogen regulatory protein P-II; GlnK (mll4247) had the largest effect on bacteroid development at 2 WPI (Fig. 5c). GlnK is uridylylated under nitrogen-deficiency resulting in the activation of nitrogen stress response (Patriarca et al., 2002, Coutts et al., 2002, Bueno et al., 1985, Atkinson & Ninfa 1998). Previous studies in *E. coli* demonstrated that GlnK production was enhanced under nitrogen-deficient conditions (Atkinson & Ninfa 1998, van Heeswijk et al., 1996). In *Corynebacterium glutamicum*, GOGAT production was enhanced under nitrogen-deficient conditions. Conversely, GOGAT and GDH were down- and up-regulated under nitrogen-rich conditions, respectively (Beckers et al., 2001). Interestingly, my data demonstrated that GlnK and GOGAT were up-regulated in bacteroids at 2 WPI (the early stage of nodule development). Then GlnK expression returned to the levels observed in free-living *M. loti* at 3 and 4 WPI (the intermediate stage of nodule development) (Fig. 5c). Meanwhile, the expression levels of GOGAT and GDH were low and high in bacteroids at 4 WPI compared to the levels present in free-living *M. loti*, respectively (Fig. 5a). Accordingly, my results strongly indicate that *M. loti* may enter a nitrogen-deficient condition at the early stage of nodule development, and then change to a nitrogen-rich condition at the intermediate stage of nodule development.

Discussion

This study aimed to characterize variations in the physiological conditions of bacteroids during nodule maturation. To the best of my knowledge, this is the first report describing a time-course of proteome variations in *M. loti* bacteroids. I quantitatively identified 537 proteins, which comprise only 32.3% of a total of identified proteins in a qualitative proteome analysis of *M. loti* in chapter I. However, my data provide novel insights into molecular mechanisms of *L. japonicus–M. loti* symbiosis because I described the intracellular variations of *M. loti* bacteroids during nodule maturation, which have never been revealed.

My quantitative proteome analysis demonstrated that GlnK and GOGAT, which have been reported to be produced at high levels under nitrogen-deficiency (Atkinson & Ninfa 1998, van Heeswijk et al., 1996, Beckers et al., 2001), were up-regulated in bacteroids at 2 WPI (Fig, 5a, c). These results suggest that *M. loti* undergoes nitrogen-deficiency during the early stage of nodule

development. While nodules harvested at 3 and 4 WPI were red, the nodules harvested at 2 WPI were white. This white phenotype is a strong indicator that at 2 WPI, nodules contained significantly less leghemoglobin than at 3 and 4 WPI. In the nitrogen-fixing nodules, leghemoglobin is induced by host plants to avoid inactivation of oxygen-labile nitrogenase and to maintain a sufficient oxygen flux for respiration (Appleby, 1984, Ott 2005). In addition, nitrogenase complex core subunits (NifHDK) were slightly up-regulated (less than 3-fold) at 2 WPI, but highly up-regulated (more than 7-fold) at 3 and 4 WPI (Fig. 5d). These results indicated that bacteroids were associated with lower levels of nitrogenase activity during the early stage of nodule development than during the intermediate stage of nodule development. Therefore, nitrogen-deficiency would likely occur in the nodule at the early stage of development. Meanwhile, nitrogen fixation resulted in nitrogen-rich conditions in bacteroids at the intermediate stage of nodule development. Furthermore, GlnK and GOGAT levels were similar to those in free-living *M. loti* at this stage of nodule development (Fig. 5a, c).

Although it was generally accepted that bacteroids shut down ammonium assimilation during the symbiotic growth stage (Prell & Poole, 2006, Patriarca et al., 2002), I observed high expression levels of enzymes involved in ammonium assimilation during the intermediate stage of nodule development, indicating that bacteroids assimilated ammonia during this period. Ammonium assimilation occurs through the glutamine synthase (GS)/GOGAT or GDH/GS pathways (Patriarca et al., 2002). GS plays an important role in ammonium assimilation by catalyzing the condensation of glutamate and ammonia to yield glutamine. GSI (mll0343) deficiency in *M. loti* has been reported to reduce nitrogen-fixing activity per nodule and induce early nodule senescence (Chungopast et al., 2014). My data indicated up-regulations of GSI (mll0343) and GDH (mll4104) production in bacteroids at 4 WPI (Fig. 5a). These results suggest that *M. loti* assimilates ammonia through the GDH/GS pathway during the intermediate stage of nodule development.

Summary

In conclusion, quantitative time-course proteome analysis of *M. loti* bacteroids revealed that the protein production profiles of *M. loti* varied greatly over the course of bacteroid differentiation, and provides a comprehensive characterization of the intracellular conditions of bacteroids (Fig. 6). Based on these data, I propose three characteristics regarding the cellular conditions of *M. loti* during mutualism. First, *M. loti* experiences nitrogen-deficiency at the early stage of nodule development resulting from low levels of nitrogenase expression. Second, high levels of nitrogenase production induce nitrogen-rich conditions in *M. loti* at the intermediate stage of nodule development. Third, *M. loti*assimilates ammonia produced by nitrogen fixation at the intermediate stage of nodule development. These characteristics were hard to find by previous individual researches focused on several genes or proteins. I found some important phenomena by using proteomics approach, and next I have to prove these phenomena at gene or protein level analysis.

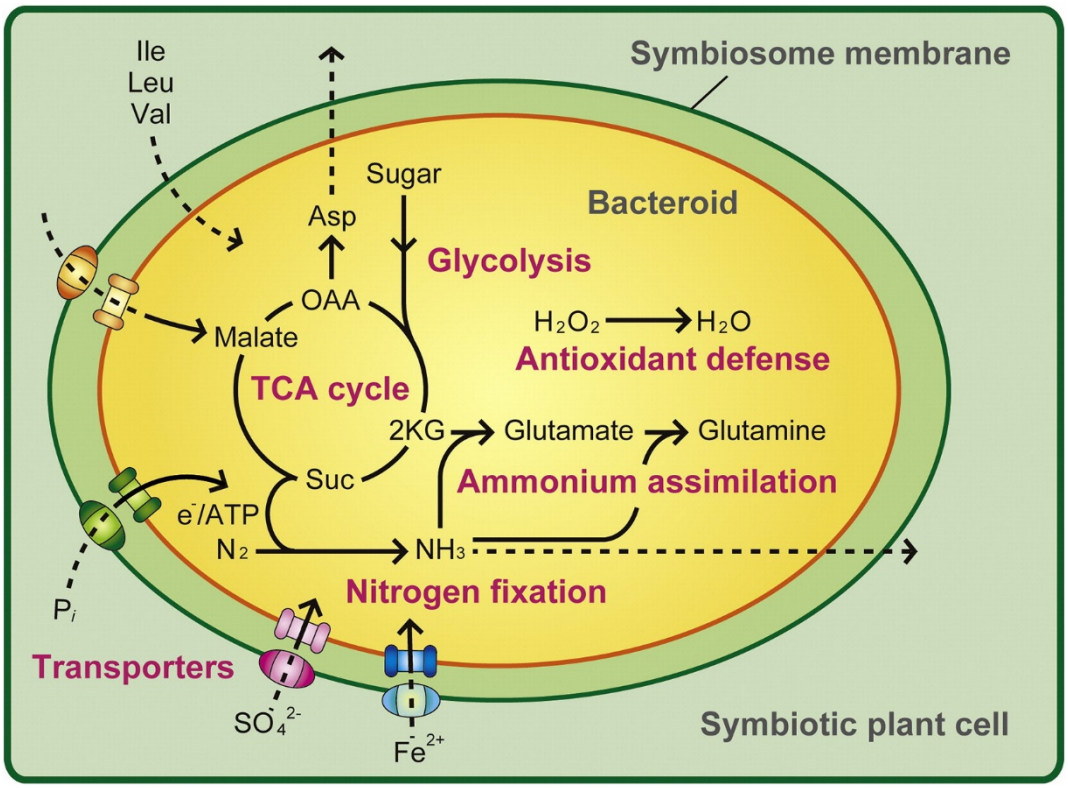

Figure 6 | Overview of transport and metabolism in *Mesorhizobium loti* bacteroids. The production of proteins involved in nitrogen fixation, antioxidant defense, iron, sulfur, and phosphorus transporters, the tricarboxylic acid cycle, glycolysis, and nitrogen assimilation were enhanced in *M. loti* bacteroids. Red words indicate metabolic pathways focused in this study.

References

1. Allaway D, Lodwig EM, Crompton LA, Wood M, Parsons R, Wheeler TR, Poole PS, Identification of alanine dehydrogenase and its role in mixed secretion of ammonium and alanine by pea bacteroids, *Mol. Microbiol*., **36**, 508–515 (2000)
2. Appleby CA, Leghemoglobin and Rhizobium respiration, *Annu. Rev. Plant Physiol. Plant Mol. Biol*., **35**, 443–478 (1984)
3. Atkinson MR, Ninfa AJ, Role of the GlnK signal transduction protein in the regulation of nitrogen assimilation in *Escherichia coli*, *Mol. Microbiol*., **29**, 431–447 (1998)
4. Barra-Bily L, Fontenelle C, Jan G, Flechard M, Trautwetter A, Pandey SP, Walker GC, Blanco C, Proteomic alterations explain phenotypic changes in *Sinorhizobium meliloti* lacking the RNA chaperone Hfq. *J. Bacteriol.*, **192**, 1719-1729 (2010)
5. Becana M, Dalton DA, Moran JF, Iturbe-Ormaetxe I, Matamoros MA, Rubio MC, Reactive oxygen species and antioxidants in legume nodules, *Physiol. Plant*., **109**, 372–381 (2000)
6. Becard G, Fortin JA: Early events of vesicular arbuscular mycorrhiza formation on Ri T-DNA transformed roots. *New. Phytolog*., **108**, 211-218 (1988)
7. Beckers G, Nolden L, Burkovski A, Glutamate synthase of *Corynebacterium glutamicum* is not essential for glutamate synthesis and is regulated by the nitrogen status, *Microbiology*, **147**, 2961–2970 (2001)
8. Beringer JE, R factor transfer in *Rhizobium leguminosarum*. *J. Gen. Microbiol*., **84**, 188-198 (1974)
9. Bueno R, Pahel G, Magasanik B, Role of *glnB* and *glnD* gene products in regulation of the *glnALG* operon of *Escherichia coli*, *J. Bacteriol*., **164**, 816–822 (1985)
10. Chen H, Teplitski M, Robinson JB, Rolfe BG, Bauer WD, Proteomic analysis of wild-type *Sinorhizobium meliloti* responses to N-acyl homoserine lactone quorumsensing signals and the transition to stationary phase, *J. Bacteriol*., **185**, 5029–5036 (2003)
11. Chungopast S, Thapanapongworakul P, Matsuura H, Van Dao T, Asahi T, Tada K, Tajima S, Nomura M, Glutamine synthetase I-deficiency in *Mesorhizobium loti* differentially affects nodule development and activity in *Lotus japonicus*, *J. Plant Physiol*., **171**, 104–108 (2014)

12. Coutts G, Thomas G, Blakey D, Merrick M, Membrane sequestration of the signal transduction protein GlnK by the ammonium transporter AmtB, *EMBO J.*, **21**, 536–545 (2002)
13. Delmotte N, Ahrens CH, Knief C, Qeli E, Koch M, Fischer HM, Vorholt JA, Hennecke H, Pessi G, An integrated proteomics and transcriptomics reference data set provides new insights into the *Bradyrhizobium japonicum* bacteroid metabolism in soybean root nodules. *Proteomics*, **10**, 1391-1400 (2010)
14. Djordjevic MA, *Sinorhizobium meliloti* metabolism in the root nodule: a proteomic perspective, *Proteomics*, **4**, 1859–1872 (2004)
15. Finan TM, Mcwhinnie E, Driscoll B, Watson RJ, Complex symbiotic phenotypes result from gluconeogenic mutations in *Rhizobium meliloti*, *Mol. Plant Microbe Interact*., **4**, 386–392 (1991)
16. Finan TM, Wood JM, Jordan DC, Symbiotic properties of C4-dicarboxylic acid transport mutants of *Rhizobium leguminosarum*, *J. Bacteriol*., **154**, 1403–1413 (1983)
17. Gao MS, Chen HC, Eberhard A, Gronquist MR, Robinson JB, Connolly M, Teplitski M, Rolfe BG, Bauer WD, Effects of AiiA-mediated quorum quenching in *Sinorhizobium meliloti* on quorum-sensing signals, proteome patterns, and symbiotic interactions. *Mol. Plant Microbe Interact*., **20**, 843-856 (2007)
18. Hanyu M, Fujimoto H, Tejima K, Saeki K, Functional differences of two distinct catalases in *Mesorhizobium loti* MAFF303099 under free-living and symbiotic conditions, *J. Bacteriol*., **191**, 1463–1471 (2009)
19. Hempel J, Zehner S, Gottfert M, Patschkowski T, Analysis of the secretome of the soybean symbiont *Bradyrhizobium japonicum*. *J. Biotechnol*., **140**, 51-58 (2009)
20. Hosie AHF, Allaway D, Galloway CS, Dunsby HA, Poole PS, *Rhizobium leguminosarum* has a second general amino acid permease with unusually broad substrate specificity and high similarity to branched-chain amino acid transporters (Bra/LIV) of the ABC family, *J. Bacteriol*., **184**, 4071–4080 (2002)
21. Kaneko T, Nakamura Y, Sato S, Asamizu E, Kato T, Sasamoto S, Watanabe A, Idesawa K, Ishikawa A, Kawashima K, Kimura T, Kishida Y, Kiyokawa C, Kohara M, Matsumoto M,

Matsuno A, Mochizuki Y, Nakayama S, Nakazaki N, Shimpo S, Sugimoto M, Takeuchi C, Yamada M, Tabata S, Complete genome structure of the nitrogen-fixing symbiotic bacterium *Mesorhizobium loti*. *DNA Res*., **7**, 381-406 (2000)

22. Kawaguchi M, *Lotus japonicus* 'Miyakojima' MG-20: An early-flowering accession suitable for indoor handling. *J. Plant Res*., **113**, 507-509 (2000)
23. Kumagai H, Hakoyama T, Umehara Y, Sato S, Kaneko T, Tabata S, Kouchi H, A novel ankyrin-repeat membrane protein, IGN1, is required for persistence of nitrogen-fixing symbiosis in root nodules of *Lotus japonicus*, *Plant Physiol*., **143**, 1293–1305 (2007)
24. Larrainzar E, Wienkoop S, Weckwerth W, Ladrera R, Arrese-Igor C, Gonzalez EM, *Medicago truncatula* root nodule proteome analysis reveals differential plant and bacteroid responses to drought stress. *Plant Physiol.*, **144**, 1495-1507 (2007)
25. Lodwig EM, Hosie AH, Bourdes A, Findlay K, Allaway D, Karunakaran R, Downie JA, Poole PS, Amino-acid cycling drives nitrogen fixation in the legume–rhizobium symbiosis, *Nature*, **422**, 722–726 (2003)
26. Ludwig RA, Rhizobium free-living nitrogen fixation occurs in specialized nongrowing cells, *Proc. Natl. Acad. Sci. U. S. A*., **81**, 1566–1569 (1984)
27. Matsui K, Bae J, Esaka K, Morisaka H, Kuroda K, Ueda M, Exoproteome profiles of *Clostridium cellulovorans* grown on various carbon sources, *Appl. Environ. Microbiol*., **79**, 6576–6584 (2013)
28. Mckay IA, Dilworth MJ, Glenn AR, Carbon catabolism in continuous cultures and bacteroids of *Rhizobium leguminosarum* Mnf-3841, *Arch. Microbiol*., **152**, 606–610 (1989)
29. Osteras M, Finan TM, Stanley J, Site-directed mutagenesis and DNA sequence of pckA of Rhizobium NGR234, encoding phosphoenolpyruvate carboxykinase: gluconeogenesis and host-dependent symbiotic phenotype, *Mol. Gen. Genet*., **230**, 257–269 (1991)
30. Ott T, van Dongen JT, Gunther C, Krusell L, Desbrosses G, Vigeolas H, Bock V, Czechowski T, Geigenberger P, Udvardi MK, Symbiotic leghemoglobins are crucial for nitrogen fixation in legume root nodules but not for general plant growth and development, *Curr. Biol*., **15**, 531–535 (2005)
31. Patriarca EJ, Tate R, Iaccarino M, Key role of bacterial NH_4^+ metabolism in rhizobium-plant

symbiosis, *Microbiol. Mol. Biol. Rev*., **66**, 203–222 (2002)

32. Prell J, Poole P, Metabolic changes of rhizobia in legume nodules, *Trends Microbiol*., **14**, 161–168 (2006)
33. Ronson CW, Lyttleton P, Robertson JG, C4-dicarboxylate transport mutants of *Rhizobium trifolii* form ineffective nodules on *Trifolium repens*, *Proc. Natl. Acad. Sci. U. S. A.*, **78**, 4284–4288 (1981)
34. Sarma AD, Emerich DW, A comparative proteomic evaluation of culture grown vs nodule isolated *Bradyrhizobium japonicum*. *Proteomics*, **6**, 3008-3028 (2006)
35. Sarma AD, Emerich DW, Global protein expression pattern of *Bradyrhizobium japonicum* bacteroids: a prelude to functional proteomics. *Proteomics*, **5**, 4170-4184 (2005)
36. Saroso S, Dilworth MJ, Glenn AR, The use of activities of carbon catabolic enzymes as a probe for the carbon nutrition of snakebean nodule bacteroids, *J. Gen. Microbiol*., **132**, 243–249 (1986)
37. Seefeldt LC, Hoffman BM, Dean DR, Mechanism of Mo-dependent nitrogenase, *Annu. Rev. Biochem*., **78**, 701–722 (2009)
38. Tate R, Ferraioli S, Filosa S, Cermola M, Riccio A, Iaccarino M, Patriarca EJ, Glutamine utilization by *Rhizobium etli*, *Mol. Plant Microbe Interact*., **17**, 720–728 (2004)
39. Tyers M, Mann M, From genomics to proteomics, *Nature*, **422**, 193–197 (2003)
40. Uchiumi T, Ohwada T, Itakura M, Mitsui H, Nukui N, Dawadi P, Kaneko T, Tabata S, Yokoyama T, Tejima K, Saeki K, Omori H, Hayashi M, Maekawa T, Sriprang R, Murooka Y, Tajima S, Simomura K, Nomura M, Suzuki A, Shimoda Y, Sioya K, Abe M, Minamisawa K, Expression islands clustered on the symbiosis island of the *Mesorhizobium loti* genome. J. Bacteriol., **186**, 2439-2448 (2004)
41. Verma D, Signals in root nodule organogenesis and endocytosis of Rhizobium, *Plant Cell*, **4**, 373–382 (1992)
42. van Heeswijk WC, Hoving S, Molenaar D, Stegeman B, Kahn D, Westerhoff HV, An alternative PII protein in the regulation of glutamine synthetase in *Escherichia coli*, *Mol. Microbiol*., **21**, 133–146 (1996)
43. Watson RJ, Rastogi VK, Cloning and nucleotide sequencing of *Rhizobium meliloti*

aminotransferase genes: an aspartate aminotransferase required for symbiotic nitrogen fixation is atypical, *J. Bacteriol.*, **175**, 1919–1928 (1993)

Chapter III Rhizobial gibberellin negatively regulates host nodule number

Rhizobia establish symbiotic relationships with legumes in host nodules. The number of nodules is controlled to balance the cost (carbon provision)-to-benefit (nitrogen taking) ratio of the host. In *Lotus japonicus*, the nodule number has been considered to be tightly regulated by phytohormones, and glycopeptides produced by the host plant (Caetano-Anolles & Gresshoff, 1991, Ferguson et al., 2010, Ferguson and Mathesius, 2014, Oka-Kira & Kawaguchi, 2006, Ryu et al., 2012).

While nodule number is presumed to be under control of host plant-derived signal molecules, I have discovered a 'symbiont-driven' mechanism for the regulation of nodulation in *Mesorhizobium loti*. I have found that terpenoid synthetic enzymes encoded on an operon were produced in bacteroid by proteomic study in Chapter I. In this chapter, I characterized the function of the enzymes, and found that *M. loti* synthesized gibberellin (GA) with symbiosis-specific expressing operon. Furthermore, I found that the GA produced by already-incorporated rhizobia have the function to reduce the host nodule number. Moreover, I found the clear relationships between distribution of GA-synthetic genes and host nodule types. My results suggest that rhizobial GA negatively regulates the host nodule number to be beneficial to already-incorporated rhizobia. This is the first report suggesting that incorporated rhizobia negatively affect the nodule number via synthesis of phytohormone.

Materials and Methods

Strains, culture media and culture conditions

M. loti MAFF303099 and *L. japonicus* MG-20 Miyakojima (Kawaguchi, 2000) were purchased from National Institute of Technology and Evaluation (Japan) and National BioResource Project (Japan), respectively. Signature-tagged mutagenesis (STM) mutant of mlr6364 (Clone ID: 36T01f03), mlr6365 (Clone ID: 10T05d07), mlr6367 (Clone ID: 05T04e11),

mlr6368 (Clone ID: 10T01h01 as *gib*$^{-}$ mutant), mlr6370 (Clone ID: 01T03h03) and mlr6371 (Clone ID: 14T06b04) were purchased from F1National BioResource Project (Japan). Bacterial cells were grown in Trypton–Yeast extract (TY) medium at 28 °C. Phosphomycin (100 μg/mL), tetracyclin (5 μg/mL), spectinomycin (100 μg/mL), streptomycin (100 μg/mL) and isopropyl β-D-1-thiogaractopyranoside (IPTG; 1 mM) were added if needed. For nodule collection to perform fractured nodule assay, *L. japonicus* MG-20 Miyakojima seeds were sterilized, germinated and inoculated with M. loti and grown in MM1 (Becard & Fortin 1988) medium at 25 °C with a 16-h light/8-h dark cycle.

Plant assays

M. loti wild-type and STM mutants were cultured in TY medium with suitable antibiotics until the OD_{600} reached approximately 1.0. Cells were washed and resuspended in B & D nitrogen-free medium to an OD_{600} of 1.0, then 20 mL of bacterial suspension was inoculated at 3 week after *L. japonicus* seedlings were planted on vermiculite in Incu tissue (SPL Life Sciences, Korea). To measure the colony forming unit (CFU), roots from each plant were homogenized in PBS and plated onto TY agar plates containing phosphomycin. Colonies were counted on the plates after 7 days of incubation at 28 °C. Nodule number was visually confirmed. For addition of GA_3, water-dissolved GA_3 was exogenously added at 10^{-7} mole per Incu Tissue at 2WPI. Significant differences between two groups were determined by student *t*-test. Multiple comparisons were corrected using the Holm–Bonferroni *t*-test. Nodule positions were measured using over 200 nodules from 20 (*gib*$^{-}$) and 30 (WT) plants. Significant difference was determined by Mann-Whitney *U*-test.

Genetic recombination of M. loti

Insertion of the *lac* promoter cassette in front of the gibberellin operon was performed using the suicide vector pSUP202 and primers (Table 1). Six hundred base pair regions just upstream of the translation-initiating sequence of the target operon were amplified from *M. loti* genomic DNA using primers gibpromoter-f/r, and 1466 base *lac* promoter cassette were cloned from pMAL-pIII vector (New England Biolabs, MA, USA) with the primers lac-f/r. PCR products were then cloned into the pSUP202 EcoRI site by In-Fusion HD Cloning Kit (Takara-Bio, Japan)

Table 1 | Primers used in this chapter

Primer	Sequence (from 5' to 3')
plasmid construction	
gibpromoter-f	CAGGAAACAGCCAGTATGTCCGAACAACCCTTGCCGAC
gibpromoter-r	TTTCATTGCCATACGCTTGTCCCACATCTTGCCGCG
lac-f	ATGAATGCTCATCCGTGGTGCAAAACCTTTCGCGGTATGG
lac-r	ACTGGCTGTTTCCTGTGTGAAATTGTTATCC
pET21a-mlr6364-f	AGAAGGAGATATACATATGTCCGAACAACCCTTGCCGAC
pET21a-mlr6364-r	GTGGTGGTGGTGGTGCCAGAGCACCGGGAACTCCTC
pET21a-mlr6365-f	AGAAGGAGATATACATATGGACGTGCAAGAAACCACGGC
pET21a-mlr6365-r	GTGGTGGTGGTGGTGGCCCCCCTGAGCATGCAGTC
pET21a-mlr6366-f	AGAAGGAGATATACATATGCGCGTCGTGATCGATCAGG
pET21a-mlr6366-r	GTGGTGGTGGTGGTGGCAGCGCGGCCCCGC
pET21a-mlr6367-f	AGAAGGAGATATACATATGGACATGCTGCTCAACCCGC
pET21a-mlr6367-r	GTGGTGGTGGTGGTGTGAGAATCCGATGCGGATTTTCATGGAC
pET21a-mlr6368-f	AGAAGGAGATATACATGTGAACGCGCTGTCCGAACAG
pET21a-mlr6368-r	GTGGTGGTGGTGGTGTGGCGCCGCTCCTGCTCC
pET21a-mlr6369-f	AGAAGGAGATATACATATGATCCAGACCGAACGCGCGC
pET21a-mlr6369-r	GTGGTGGTGGTGGTGGGCGGGCGCACGCTGG
pET21a-mlr6370-f	AGAAGGAGATATACATGTGGGCGGGGAGAAATCTCATAC
pET21a-mlr6370-r	GTGGTGGTGGTGGTGACGCCGGAAAAAGAACCGCATCG
pET21a-mlr6371-f	AGAAGGAGATATACATATGTCCGAACAACCCTTGCCGAC
pET21a-mlr6371-r	GTGGTGGTGGTGGTGCCAGAGCACCGGGAACTCCTC
RT-qPCR	
mlr2466-f	GCCAGATGCTGCACGAGAT
mlr2466-r	TTCAAGACCTTGCGCACTTTT
mlr6364-f	GAAAATCCGCACCTGACGTT
mlr6364-r	CGCCATGCCGATGCA
mlr6365-f	TGGACCTGCATTGGGAATTC
mlr6365-r	GAGCCCGAACATGTCATCCT
mlr6366-f	CATGCCGCGAAAGACCAA
mlr6366-r	GGTCACCACGGCCACCTT
mlr6367-f	CCTGGTATGGCTGGAAATGG
mlr6367-r	CCCCGGCCTTGTGCAT
mlr6368-f	GGCGCGTGCTTGAACAG
Primer	**Sequence (from 5' to 3')**
mlr6368-r	GGAACGGTTGGCGCAGAT
mlr6369-f	TCTGGCCGATCAATGTGTTC
mlr6369-r	GCCCGGCCAGATGCA
mlr6370-f	TGCACAACGGCATCGATT
mlr6370-r	AGCAACGACAGGCAACAGAA
mlr6371-f	TGGAGGCCGATGGACTCA
mlr6371-r	CCGGCTGTACCGCTTCCT
mlr6372-f	CGGAGCGCGCTTCACT
mlr6372-r	ACCGCGGGCAATTGCT
LjATPS-f	ACATGCTTGCACCATACCAA
LjATPS-r	TCCCCAACTCCAGCAAATAC
NSP2-f	CATCGACTCCATGATTGACG
NSP2-r	GGTTGTTGTTGTCGTGGTTG

and confirmed by sequencing. pSUP202 constructs were transferred from *E. coli* strain S17-1 into *M. loti* by conjugation, and transconjugants were selected on TY + phosphomycin (100 μg/mL) + tetracyclin (10 μg/mL) agar plate 3 times before confirmation by sequencing of genomic DNA.

Isolation of RNA and preparation of cDNA

M. loti bacteroids were prepared using the method of Uchiumi et al. (2004). Total RNAs were extracted from bacterial cells at log phase (OD_{600} = 1.0), and 50 mg of plant roots using the RNeasy Mini Kit (QIAGEN, Hilden, Germany) or RNeasy Plant Mini Kit (QIAGEN), respectively, according to the manufacturer's protocol. cDNA synthesis was performed using a High Capacity DNA Reverse Transcription kit (Applied Biosystems by Life Technologies, Carlsbad, CA, USA) with 2 μg of the total RNAs as a template. The reaction was performed according to the manufacturer's protocol.

Real-time reverse transcription polymerase chain reaction (RT-PCR) analysis

For the quantitative PCR, *sigA* (mll2466) or *LjATPS* (ATP synthase) was used as an endogenous control for bacteria or plants to normalize the expression data for each gene, respectively. The primers (Table 1) were designed using Primer Express software (Applied Biosystems, Foster City, CA). Amplification was performed using Power SYBR Green PCR Master Mix (Applied Biosystems) in the 7500 Real-Time PCR System (Applied Biosystems). The reporter signals were analysed using the 7500 Real-Time PCR System.

Identification and quantification of GAs by LC-MS

From the 10 mL of *M. loti* (WT and *gib*$^+$) culture supernatant, organic compounds were extracted using equal volumes of ethylacetate (EtOAc) thrice after acidification to pH 3 by HCl. The organic phase was collected, dried by evaporation and dissolved in 100 μL of water containing 1% acetic acid. Approximately 50 mg of nodules was ground in 3 mL of 80% (v/v) acetone containing 1% (v/v) acetic acid, and incubated for 24 h at 4 °C and then centrifuged at 3000 × *g* for 20 min at 4 °C. The supernatant was concentrated to dryness, dissolved in 0.5 mL of water containing 20% methanol and 1% acetic acid and analysed by LC–MS. Exact mass analysis

was performed using a nano-LC (Ultimate 3000, DIONEX)–MS system (LTQ Orbitrap Velos, Thermo Fisher Scientific). Extracts (5 μL) were injected and separated by reversed-phase chromatography using a monolithic column (Miyamoto et al., 2008) (2000 mm, 0.1 mm I.D., Kyoto Monotech Co., Ltd., Kyoto) at a flow rate of 500 nL/min. The gradient was 10% (0–10 min), 10–99% (10–40 min) and 99–100% (40–45 min) 80% acetonitrile/water containing 0.1% formic acid in water containing 0.1% formic acid. The MS was operated with an ESI voltage of 2.3 kV and a transfer tube temperature of 280 °C. MS data acquisition was set from 20 to 65 min. For non-target analysis, the acquired data were delimited by each 50 spectra and 1.0 Th at mass-to charge ratio, and the intensities in each compartment were totaled up. Then the data were analyzed by principal component analysis (PCA) after global median normalization. Kazusa MFSearcher (http://webs2.kazusa.or.jp/mfsearcher/index_jp.html) was used for prediction of molecules picked up by PCA. For acquinsion of extracted ion chromatogram, the chromatograms of mass range at m/z = 315.155–315.165 and m/z = 345.165–345.175are extracted to focus on GA_9 and GA_{24}.

Plasmid construction and protein production in E. coli

The full-length coding sequences of 8 genes were amplified using each primer pair (Table 1). The PCR products were cloned into the pET-21a expression vector (Novagen) using the In-Fusion HD Cloning Kit (Takara Bio) to generate fusions with 6-His-tags at the C termini. The vectors were then introduced into *E. coli*cells strain BL21 Star (DE3) (Stratagene). For protein production, the culture (5 mL) was incubated at 37 °C to OD 0.5 at 600 nm. The temperature was then decreased to 16 °C, and IPTG (0.1 mM) was added. The culture was incubated for 24 h and then centrifuged at 4 °C. The pellet was washed using phosphate buffer (100 mM, pH 7.0) and then resuspended in lysis buffer (50 mM HEPES pH 7.4, 10% (w/v) glycerol, 5 mM $MgCl_2$). The samples were sonicated and the supernatants were used for the reactions. Protein concentration was measured by Protein Assay Bicinchoninate Kit (Nacalai Tesque, Kyoto, Japan)

Reaction conditions of enzyme assays

For functional validation of mlr6uchi mlr6369, mlr6370 and mlr6371, *in vitro* enzyme assays were performed in the following buffer: 50 mM HEPES (pH7.4), 10% (w/v) glycerol and

5 mM $MgCl_2$. For each assay, 100 µL of *E. coli* lysate (containing 10 mg/mL protein) was incubated in 0.5 mL buffer with 20 µM of each substrate [isopropyl pyrophosphate, dimethylallyl pyrophosphate, geranyl pyrophosphate (GPP), farnesyl pyrophosphate (FPP), and geranylgeranyl pyrophosate (GGPP); Sigma-Aldrich] and incubated at 37 °C for 6 h. The reaction products were dephosphorylated by adding 20 units of alkaline phosphatase (intestinal calf; New England Biolabs) for 1 h at 37 °C. Terpene alcohols produced by dephosphorylation were then extracted with an equal volume of hexane. The organic phase was then dried, resuspended in hexane and analysed using a gas chromatography-mass spectrometry (GC/MS; GCMS-QP2010 Ultra, Shimadzu, Japan) in electron ionization (70 eV) mode, equipped with a 30 m × 0.25-mm diameter with 0.25 µm film of HP-1 MS column (Agilent Technologies, Santa Clara, CA). Samples (1 µL) were injected in splitless mode at 50 °C. After holding for 3 min at 50 °C, the oven temperature was raised at a rate of 14 °C/min to 300 °C, where it was held for an additional 3 min. MS data were collected by selected-ion monitoring mode focused on m/z corresponding to each product. Geranylgeraniol (GGOH) and *ent*-kaurene were identified by comparison of their mass spectra retention times with authentic standards (GGOH, Sigma Aldrich; *ent*-kaurene, Olchemim Ltd., Czech Republic). Selected ion monitoring (SIM) mode were used to draw the chromatogram of GGOH and *ent*-kaurene. SIM parameters were set at m/z 290 for GGOH, and 272 for *ent*-kaurene.

For the functional validation of MlP450-1,2,3 and MlSdr, *in vitro* enzyme assays were performed using the following procedure. *E. coli* lysates (100 µL) were mixed with 3.5 µM spinach ferredoxin, 0.1 U spinach ferredoxin reductase, 2 mM NADPH and 2 mM $NADP^+$ (Sigma-Aldrich) in a final volume of 1 mL of 100 mM Tris-HCl, pH 7.5. Substrates were added at a final concentration of 100 µM, and the reaction was incubated overnight at 30 °C. Control incubations were performed with the addition of *E. coli* lysates bearing the empty pET21a vector. The reactions were stopped by adding 50 µL HCl and 1 mL EtOAc and centrifuged at 3000 rpm for 10 min. Kaurenoic acid and gibberellic acids were methylated using trimethylsilyl-diazomethane (TMS, Nacalai Tesque) in toluene containing 20% methanol. Samples were then trimethylsilylated using *N*-methyl-*N*-(trimethylsilyl)trifluoroacetamide for addition to hydroxyl groups. GC–MS analysis was performed as described in bacteroid assays using authentic standards (GA_3, Sigma-Aldrich; Kaurenoic acid (KA), GA_1, GA_4, GA_7, GA_9, GA_{12}, GA_{15} and GA_{24}; Olchemim Ltd.).

Reactions using fractured nodules

Isolated nodules (1 g) were homogenized in a mortar with extraction buffer (10 mL, 50 mM $KHPO_4$ pH 7.0, 200 mM sodium ascorbate and 1.2 g polyvinyl pirrolidone). The homogenate was centrifuged at 8500 × g for 20 min, washed and resuspended in reaction buffer (50 mM TES pH 7.5, 2.5 mM $MgCl_2$ and 1 mM $KHPO_4$). Substrates (100 μM) were then added to the 1-mL suspensions and incubated for 48 h at 28 °C with shaking at 200 rpm. For product extraction, suspensions were extracted with an equal volume of EtOAc after acidification to pH 3.0. The extracts were methylated using TMS-diazomethane and measured by GC–MS as described above. SIM parameters were set at m/z 418, 506, 416 and 504 to detect GA_4, GA_1, GA_7 and GA_3, respectively.

Acetylene reduction assay

The whole-plant nitrogenase activity was determined by acetylene reduction assay. An individual plant was packed into a 5-mL headspace vial (GL Science, Tokyo, Japan) in which 20% of the air was replaced by acetylene gas generated by CaC_2 (Sigma-Aldrich). After a 3-h reaction at 25 °C, the atmosphere (1 mL) was injected into a GC–MS (30 m × 0.32-mm diameter HP-PLOT Q column with 0.20 μm film) (Agilent Technologies) at 40 °C, followed by a gradient from 40 °C to 80 °C at 5 °C/min and then from 80 °C to 180 °C at 50 °C/min.

Co-inoculation assays

Wild-type and *gib*$^-$ were cultured in TY + phosphomycin medium until the OD_{600} reached approximately 1.0. Cells were then washed and resuspended in B & D nitrogen-free medium (Broughton & Dilworth, 1971) to an OD_{600} of 1.0. Both wild-type and *gib*$^-$ suspensions were mixed, and 20 mL of bacterial mixture was inoculated into the culture. To measure the CFU, roots from each plant were homogenized in PBS and plated onto TY agar plates containing phosphomycin with or without streptomycin and spectinomycin. Colonies were counted on the plates after 7 days of incubation at 28 °C. The percentage of *gib*$^-$ in the population was calculated as (output streptomycin and spectinomycin-resistant colony count)/(output of all colony count).

Phylogenetic trees

The phylogenetic trees were referred from Doyle (1998). The bacterial phylogeny which was based on the 16S rRNA gene sequence (Table 2) was constructed by neighbour-joining method using Clustal X (http://www.clustal.org/). The parameters were set to 111 for 'random number generator seed' and 1000 for 'number of bootstrap trials'. Whether a bacterial species has GA-synthetic genes was determined by the presence of both *ent*-copalyl pyrophosphate synthase (mlr6369) and *ent*-kaurene synthase (mlr6370) by BLAST search (Table 3). On the other hand, phylogenetic relationships of legumes (and some non-legumes) which are based on *rbcL* sequence (Table 3) were also constructed using Clustal X.

Table 2 | Bacterial strains and sequences used for phylogeny

name	strain	Source of 16S rRNA sequence	
		NCBI RefSeq	Genbank
Strains described in Figure 4			
Rhizobium trpoici	CIAT 889	R_102511.1	
Agrobacterium rhizogenes	IFO 13257	NR_043398.1	
Rhizobium leguminosarum bv. *viciae*	USDA 2370	NR_044774.1	
Rhizobium leguminosarum bv. *trifolii*	R6-1		AB721425.1
Rhizobium leguminosarum bv. *phaseoli*	LPA1410		JF792192.1
Rhizobium etli	CFN42	NR_074499.1	
Agrobacterium fabrum	C58	NR_074266.1	
Rhizobium galegae	LMG6214	NR_118990.1	
Agrobacterium vitis	LMG8750	NR_118989.1	
Sinorhizobium fredii	NGR234	NR_102919.1	
Sinorhizobium fredii	USDA205	NR_112784.1	
Sinorhizobium meliloti	LMG6133	NR_118988.1	
Mesorhizobium loti	MAFF303099	NR_074162.1	
Bradyrhizobium japonicum	USDA110		L23331.1
Rhodopseudomonas palustris	J		EU531568.1
Bradyrhizobium elkanii	USDA61		AB231916.1
Azorhizobium caulinodans	NBRC14845	NR_113675.1	
Aquabacter spiritensis	SPL-1	NR_104747.1	

name	16S rRNA sequence
Strains not described in Figure 4	
Brucella abortus	X13695
Bartonella bacilliformis	Z11683
Agrobacterium rubi	X67228
Rhizobium aggregatum	X73041
Sinorhizobium saheli	X68390
Sinorhizobium terangae	X68387
Mesorhizobium ciceri	U07934
Mesorhizobium huakuii	D12797
Phyllobacterium myrsinacearum	D12790
Mycoplana dimorpha	D12786
Afipia clevelandensis	M69186
Afipia felis	M65248
Nitrobacter hamburgensis	L11663
Nitrobacter winogradskyi	L11661
Bradyrhizobium denitrificans	S46917
Methylobacterium organophilum	D32226
Beijerinckia indica	M59060
Starkeya novella	D32247
Ancylobacter aquaticus	M62790
Rhodoplanes elegans	D25311
Blastochloris viridis	D25314
Rhodomicrobium vannielii	M34127
Rhodospirillum rubrum	D30778

Table 3 | Plants and their *rbcL* sequences used for phylogeny

genus	species	Genbank
Galega	*officinalis*	KM360795.1
Vicia	*sativa*	NC_027155.1
Pisum	*sativum*	NC_014057.1
Melilotus	*officinalis*	JX848463.1
Trifolium	*subterraneum*	NC_011828.1
Medicago	*truncatura*	NC_003119.6
Lotus	*japonicus*	NC_002694.1
Anthyllis	*vulneraria*	KF602115.1
Sesbania	*vesicaria*	KJ773882.1
Phaseolus	*vulgaris*	NC_009259.1
Vigna	*unguiculata*	NC_018051.1
Glycine	*max*	NC_007942.1
Cajanus	*cajan*	Z95535.1
Lupinus	*albus*	NC_026681.1
Leucaena	*trichandra*	NC_028733.1
Parasponia	*parviflora*	AF500342.1

Results

Functional analysis of a putative GA operon in M. loti

I have found that *M. loti* possesses a putative GA-synthetic operon. I found a terpenoid biosynthetic operon with symbiosis-specific expression in Chapter I (Fig. 1a). The operon exists on 'symbiosis island', which is horizontally-transferable chromosomal region existing in all rhizobia and contains many genes required for symbiosis such as nodulation (*nod*) genes and nitrogen fixation (*nif*) genes (Uchiumi et al., 2004, Freiberg et al., 1997, Kaneko et al., 2000). Real-time RT-PCR and quantitative proteomics also validated the symbiosis-specific expression of the genes (Fig. 1b,c). Thus, I hypothesized that these symbiosis-specific genes play some important roles in legume–rhizobia symbiosis. This operon was predicted to control GA synthesis because some rhizobia are reported to produce GA (Atzorn et al., 1988, Boiero et al., 2007), and four enzymes (encoded by mlr6368, mlr6369, mlr6370 and mlr6371) were confirmed to participate in the synthesis of *ent*-kaurene, a major GA intermediate, from dimethylallyl

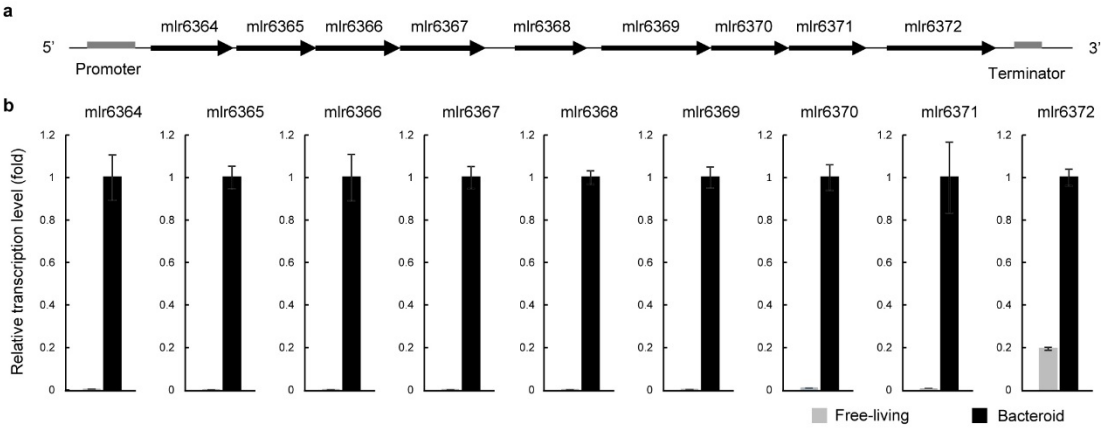

c

Accession number	2WPI	3WPI	4WPI
mlr6364	1 ± 0.36	1.85 ± 0.20	2.43 ± 0.27
mlr6365	1 ± 0.07	2.06 ± 0.36	2.38 ± 0.16
mlr6366	1 ± 0.13	1.59 ± 0.49	1.49 ± 0.26
mlr6369	1 ± 0.20	1.68 ± 0.09	3.09 ± 0.27
mlr6371	1 ± 0.03	2.19 ± 0.26	3.92 ± 0.39

Figure 1 | Symbiosis-specific expression of GA-synthetic operon in *M. loti* (**a**) The operon consists of 9 genes with accession numbers mlr6364–mlr6372. (b) Relative expression levels of the operon genes. The fold-change values are relative to *M. loti* bacteroids at 4 weeks post-inoculation (WPI) (expression level = 1). Error bars indicate the SEMs from 3 independent experiments. (c) Protein expression levels from quantitative proteomics in Chapter II. Expression levels are relative to *M. loti* at 2 WPI (expression level = 1). Values show mean ± SEM.

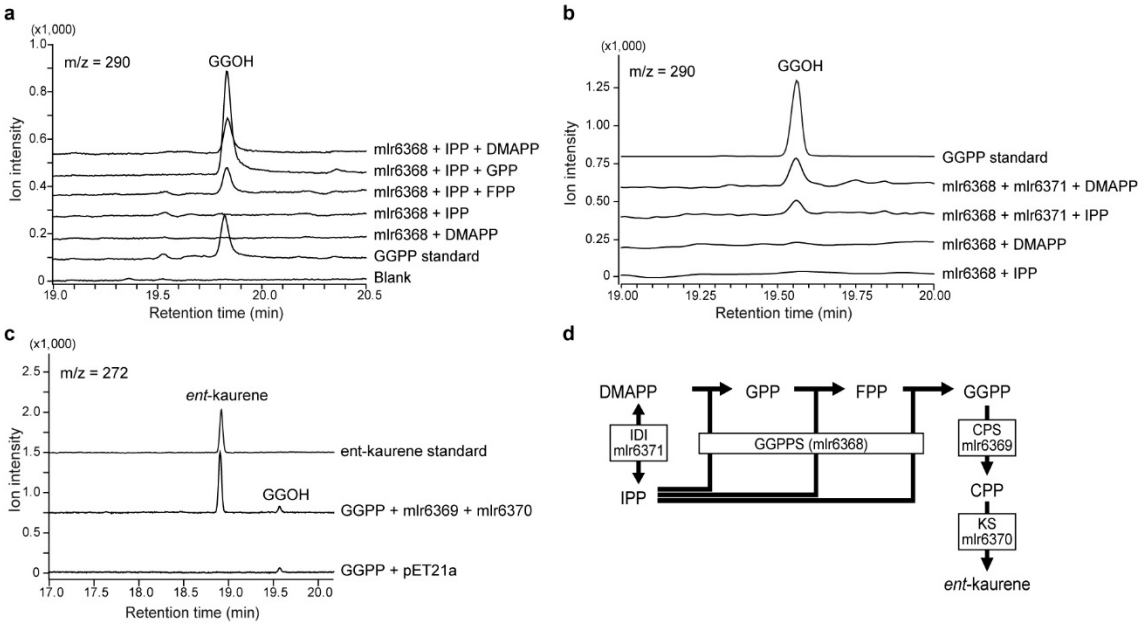

Figure 2 | *In vitro* confirmation of the enzymes encoded by mlr6368, mlr6369, mlr6370 and mlr6371
(a, b) GC–MS analysis (SIM; m/z = 290) of dephosphorylated products resulting from *in vitro* assays using prenyl alcohols as a substrate and lysates isolated from mlr6368-expressing *E. coli* (a) and mlr6371-expressing *E. coli* (b). (c) GC–MS analysis (SIM; m/z = 272) of *ent*-kaurene rom *in vitro* assays using GGPP as a substrate and lysates isolated from mlr6369- and mlr6370-expressing *E. coli*. (d) The confirmed *ent*-kaurene synthetic pathway reported by Hershey *et al*. (2014) (mlr6369 and mlr6370) and predicted by genetic information (mlr6368 and mlr6371). Note that GGPP was dephosphated to GGOH by alkaline phosphatase to detect by GC-MS, because GGPP is hard to be detected by GC-MS. GGOH, geranylgeraniol; DMAPP, dimethylallyl pyrophosphate; IPP, isopentenyl pyrophosphate; GPP, geranyl pyrophosphate; FPP, farnesyl pyrophosphate; GGPP, geranylgeranyl pyrophosphate; CPP, *ent*-copalyl pyrophosphate; IDI, isopentenyl-diphosphate isomerase; GGPPS, geranylgeranyl pyrophosphate synthase; CPS, *ent*-copalyl pyrophosphate synthase; KS, *ent*-kaurene synthase.

---

pyrophosphate (DMAPP) and isopentenyl pyrophosphate (IPP) (Fig. 2) (Hersheys et al., 2014).

Next, I found that GA produced by rhizobia negatively regulates the host nodule number. To investigate the effect of this putative rhizobial GA on the host plant, six *M. loti* STM mutants (Shimoda et al., 2008) with transposon insertions into the operon (Fig. 3a) were inoculated into host *L. japonicus*. Hosts inoculated with STM mutants increased its nodule number without affecting their growth (Fig. 3b–c). For further investigation, an STM mutant with a transposon insertion into mlr6368 (*gib*$^{-}$ mutant; Fig. 3a) was inoculated into host *L. japonicus*, and the phenotypic changes were observed from 2 to 8 WPI. In these plants, the number of days taken to flower, the length of the shoot and the number of rhizobial cells per plant were unchanged (Fig. 3d–f). However, from 4 WPI, nitrogen fixation activity per nodule and nodule weight significantly decreased, the nodule number significantly increased, and nodules formed at significantly lower

position. (Fig. 3g–j). These results suggest that putative rhizobial GA is the symbiont-derived signal for regulation of nodule number to reject delayed infection and that the optimal nodule environment for nitrogen fixation is established by GA-associated regulation of the host nodule number.

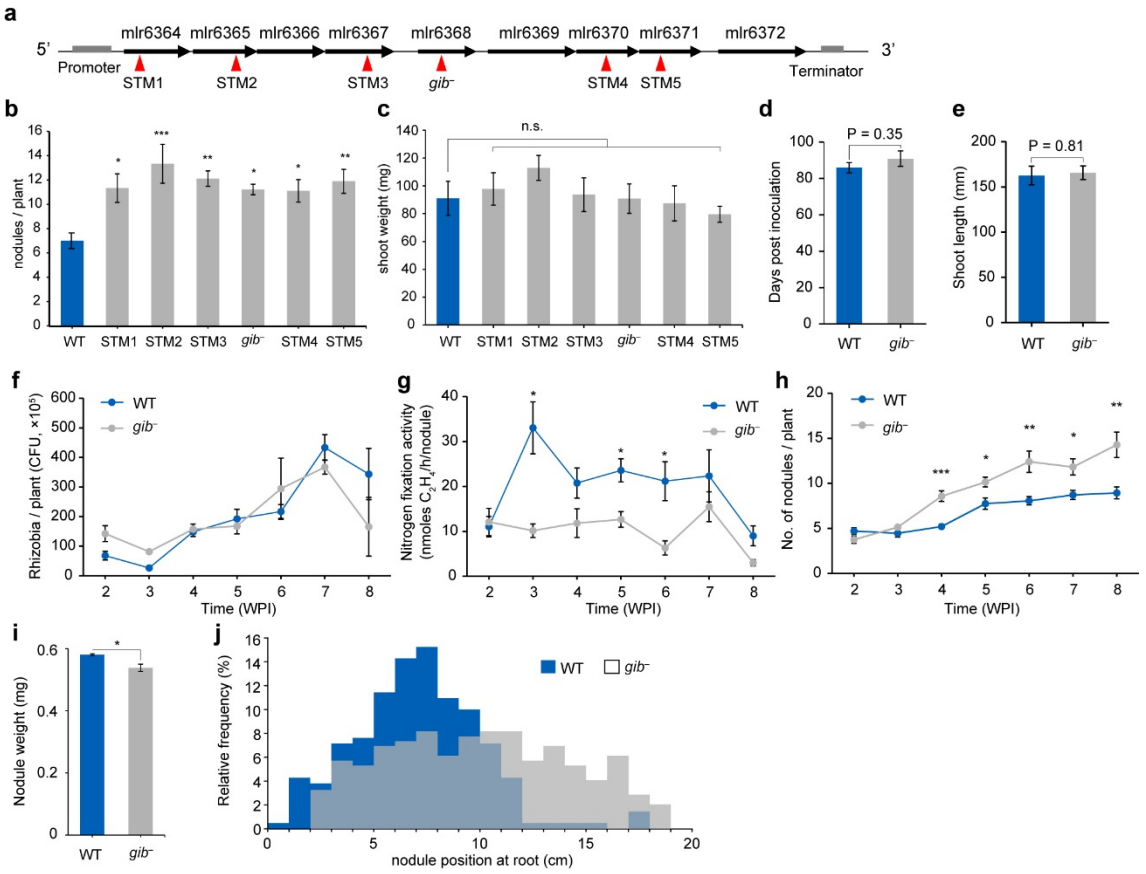

Figure 3 | GA-synthetic operon in *M. loti* and time-course plant assays (a) The operon consists of 9 genes with accession numbers mlr6364–mlr6372. The arrowhead indicates the transposon insertion site of each STM mutant. (b) Number of nodules and (c) Shoot weight of the host plants inoculated with 6 STM mutants were measured at 5WPI. (d) Flowering period from the day of inoculation. (e) Shoot length of the host plant when flowering. (f) Number of rhizobia grown in roots. (g) Nitrogen fixation activity determined by acetylene reduction assay. (h) Number of nodules. (i) Weight per nodule at 5WPI. Bars indicate the average weights of 30 nodules. (j) Relative frequency of nodule position from root-stem boundary at 8WPI. Significance was determined by Mann-Whitney *U*-test (p-value = 5.52×10^{-13}). Relative frequencies were calculated by 210 for wild-type and 245 nodules for *gib*$^{-}$ mutant, respectively. Significances were determined by student *t*-test (d,e,i). Multiple comparisons were corrected using the Dunnett's test (b,c) and the Holm–Bonferroni *t*-test (f,g,h). *p < 0.05, **p < 0.01, ***p < 0.001. WPI, weeks post inoculation. Error bars indicate SEMs from 3 plants (f), 8-9 plants (b,c,g), >15 plants (d,e,h) and 3 biological replicates (i).

Identification of GA produced in nodule

Candidate GAs produced by *M. loti* under symbiosis are numerous because >130 GAs have been found thus far (Hedden & Sponsel, 2015). To identify the rhizobial GA product, I constructed an *M. loti* mutant in which the operon was inductively expressed by IPTG-inducible promoter cassette in front of the gene operon (*gib*$^+$ strain, Fig. 4a–c). After gene induction by 1 mM IPTG and cultivation for 24 h, the secreted products in liquid media were extracted with acidic ethyl acetate and analyzed using LC–MS equipped with a long monolithic column. Non-target metabolomics approach revealed that the metabolic profile of the induced *gib*$^+$ strain was differ from the other three profiles (Fig. 4d), and the characteristic components in the secreted product of induced *gib*$^+$ strain were corresponding to the peaks of m/z = m/z = 315.16 $[M\text{-}H]^-$ at 56.5 min and m/z = 345.17 $[M\text{-}H]^-$ at 53.7 min (Fig. 4e-g), which were finally identified as GA_9 and GA_{24} by comparison with authentic standards (Fig. 4h,i). GA_9 and GA_{24} are both intermediates in GA synthesis in plants and fungi (Bomke & Tudzynski, 2009) and are produced by *M. loti* bearing a symbiosis-specific gene set.

Identification of GA synthetic pathway

Next, I sought to identify the GA-synthetic pathway in *M. loti*. Although plants and fungi synthesize various GAs using various pathways (Bomke & Tudzynski, 2009), GA_9 and GA_{24} are synthesized by almost similar pathway and I predicted that the pathway used by *M. loti* would be similar. To identify the pathway, lysates from *E. coli* expressing each of the functionally unknown 4 enzymes (encoded by mlr6364–mlr6367) were assayed *in vitro* with potential substrates. Three of the 4 enzymes were cytochrome P450s, and the other was a short-chain dehydrogenase reductase. For convenience, I named these enzymes MlP450-1 (mlr6364), MlP450-2 (mlr6365), MlSdr (mlr6366) and MlP450-3 (mlr6367). The products were analysed by (GC–MS). MlP450-3 converted *ent*-kaurene into KA, indicating that it functions as an *ent*-kaurene oxidase (Fig. 5a,f). Assays of MlP450-2 and MlSdr together converted KA into GA_{12}, whereas MlP450-2 or MlSdr alone did not (Fig. 5b,g). This result indicates that GA_{12} is synthesized from KA by the cooperative function of MlP450-2 and MlSdr, although KA oxidases from plants and fungi enzymatically convert KA into GA_{12}. MlP450-1 converted GA_{12} into GA_9 through GA_{15} and GA_{24},

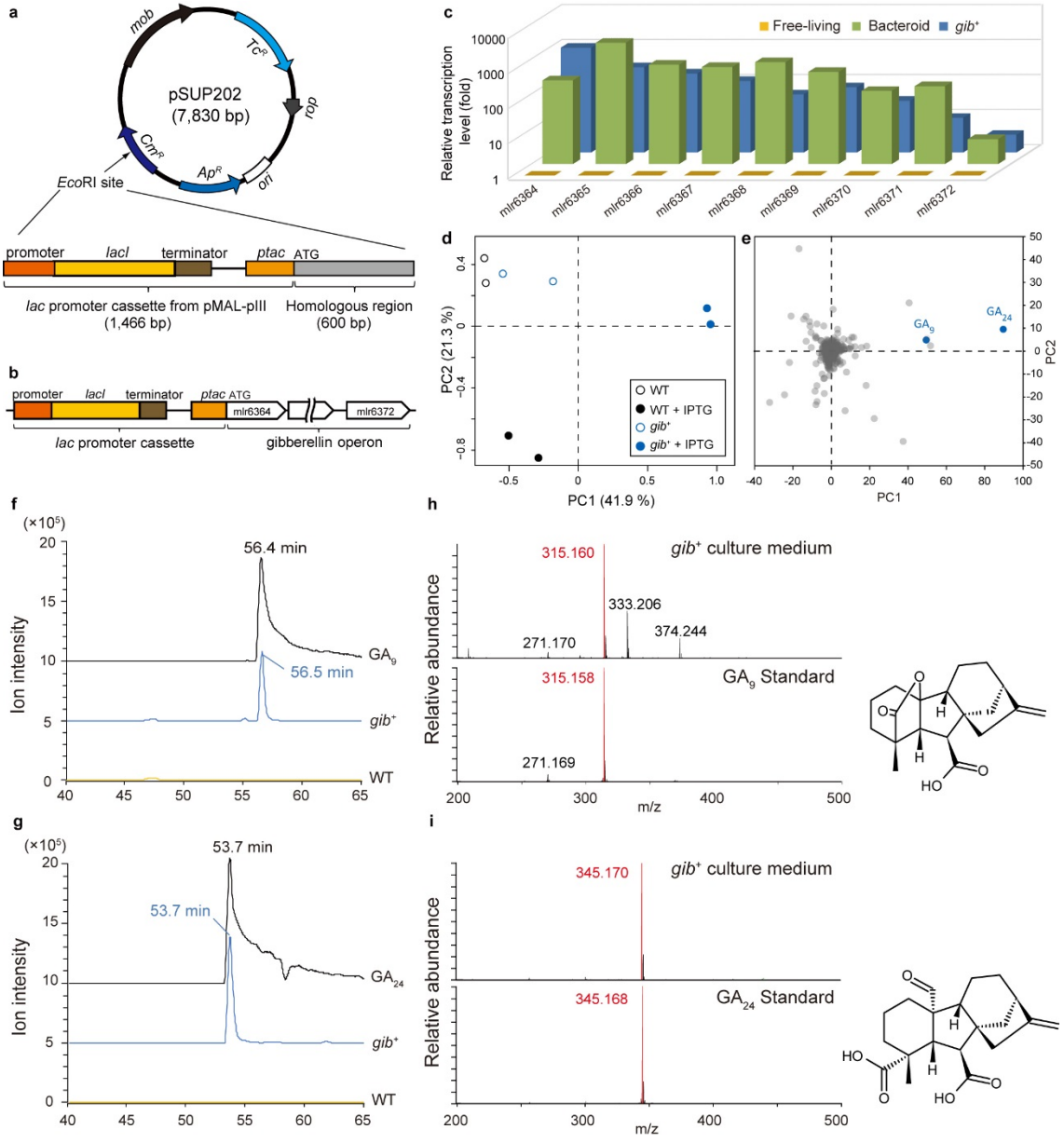

Figure 4 | GA-synthetic operon in *M. loti* and time-course plant assays (a) Plasmid vector for homologous recombination of the *M. loti* genome. *Lac* promoter cassette in front of the homologous region (600 bp) is inserted into *Eco*RI restriction site. (b) *Lac* promoter insertion site. Note that *gib*$^+$ mutant is a single-crossover mutant. (c) Relative expression levels of the operon genes. The fold-change values are relative to wild-type grown in liquid culture with 1 mM isopropyl β-D-1-thiogaractopyranoside (expression level = 1). Error bars indicate the standard error from 3 independent experiments. (d,e) Principal component analysis (PCA) of the metabolic profiles of wild-type and *gib*$^+$ supernatant. Scatter plot (d) and loading plot (e) of PCA are shown. (f,g) NanoLC–MS chromatograms of culture medium of wild-type and *gib*$^+$ mutant and authentic GAs. The chromatograms of mass range at m/z = 315.155–315.165 (f) and m/z = 345.165–345.175 (g) are extracted to focus on GA_9 and GA_{24}. (h,i) Mass spectra of *gib*$^+$ culture medium and GA standards at 56.5 min (h) and 53.7 min (i). Insets show the structure of GA_9 and GA_{24}.

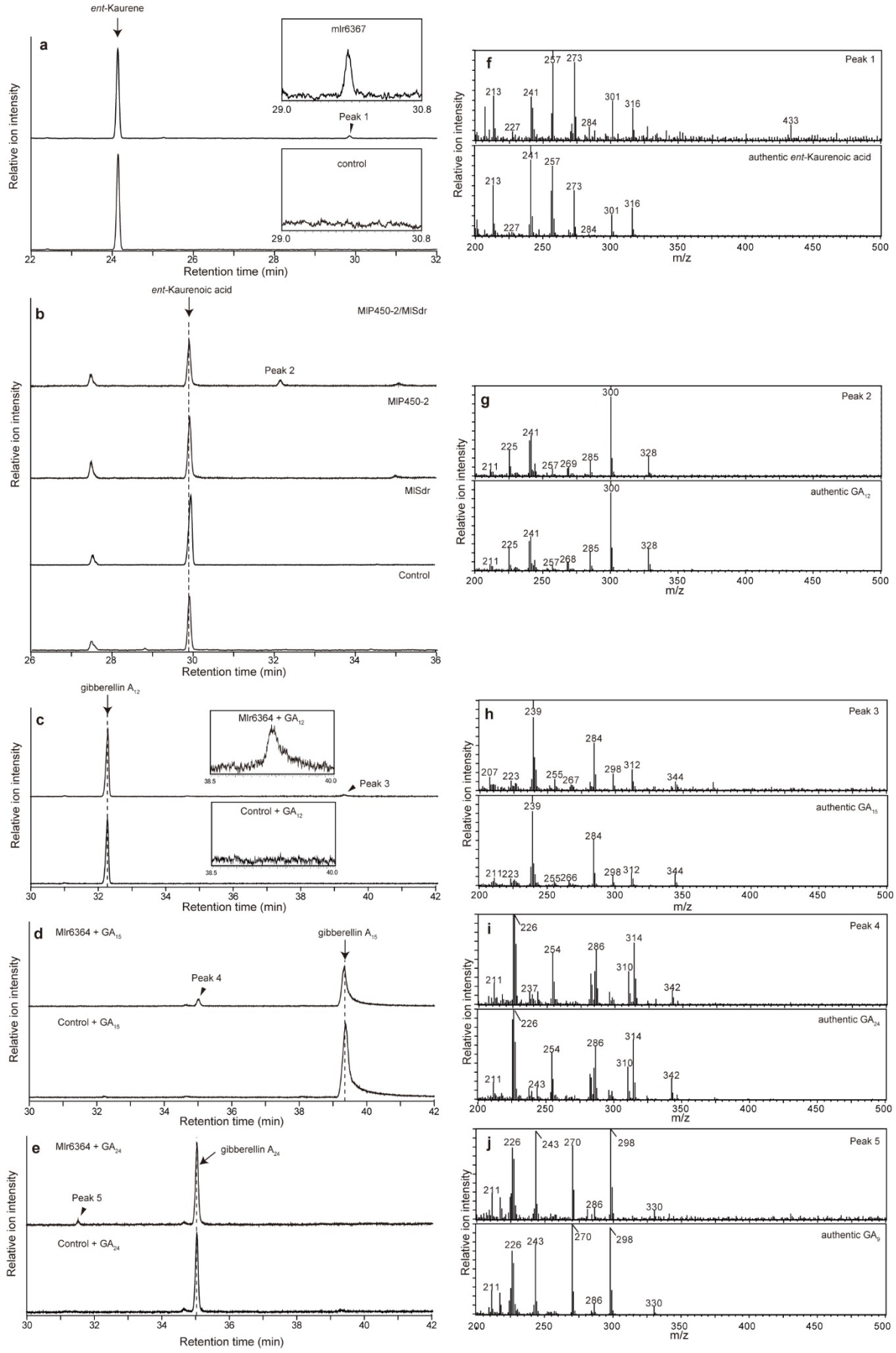
a
ent-Kaurene
mlr6367
Peak 1
control
Relative ion intensity
Retention time (min)
b
ent-Kaurenoic acid
MIP450-2/MISdr
Peak 2
MIP450-2
MISdr
Control
c
gibberellin A12
MIr6364 + GA12
Peak 3
Control + GA12
d
MIr6364 + GA15
gibberellin A15
Peak 4
Control + GA15
e
MIr6364 + GA24
gibberellin A24
Peak 5
Control + GA24
f
Peak 1
authentic ent-Kaurenoic acid
g
Peak 2
authentic GA12
h
Peak 3
authentic GA15
i
Peak 4
authentic GA24
j
Peak 5
authentic GA9
m/z

Figure 5 | *In vitro* enzymatic assays of MlP450s and MlSdr. (a−e) Total ion chromatograms of reaction products from *in vitro* assays. (a) Reaction of *ent*-kaurene with lysates isolated from MlP450-3-expressing *E. coli* and empty-vector control *E. coli*. (b) Reaction of *ent*-kaurenoic acid with lysates isolated from MlP450-2 and/or MlSdr-expressing *E. coli* and empty-vector control *E. coli*. (c−e) Reaction of GA_{12} (c), GA_{15} (d) and GA_{24} (e) with lysates isolated from MlP450-1-expressing *E. coli* and empty-vector control *E. coli*. (f−j) Mass spectra of peaks 1–5 compared with authentic gibberellin or *ent*-kaurenoic acid.

indicating that MlP450-1 functions as a GA20-oxidase (Fig5, c-e,h-j). These results show that *M. loti* synthesizes GA_9 via a pathway similar to that of higher plants and fungi with a slightly different enzymatic function (Fig. 6a, inside the broken-line box).

How do rhizobia regulate nodulation by GA_9? Although GAs are major phytohormones that affect various plant development events, including nodulation, GA_9 is one of the inactive GAs in higher plants. Only 3-hydroxylated GAs (GA_1, GA_3, GA_4 and GA_7) are known to be bioactive in higher plants, so I predicted that rhizobial GA_9 was converted into bioactive GAs in nodules using the GA-synthetic pathway. *In vitro*, GA_9 incubated with fractured nodule was converted into GA_1 and GA_3 via GA_4 (Fig. 6a-e). GA_1 and GA_3 were elevated in plants inoculated with wild-type *M. loti* and not with the *gib*$^{-}$ mutant (Fig. 7a). Therefore, I concluded that rhizobial GA_9 functions in the host through its conversion into GA_1 and GA_3 mediated by the cooperative

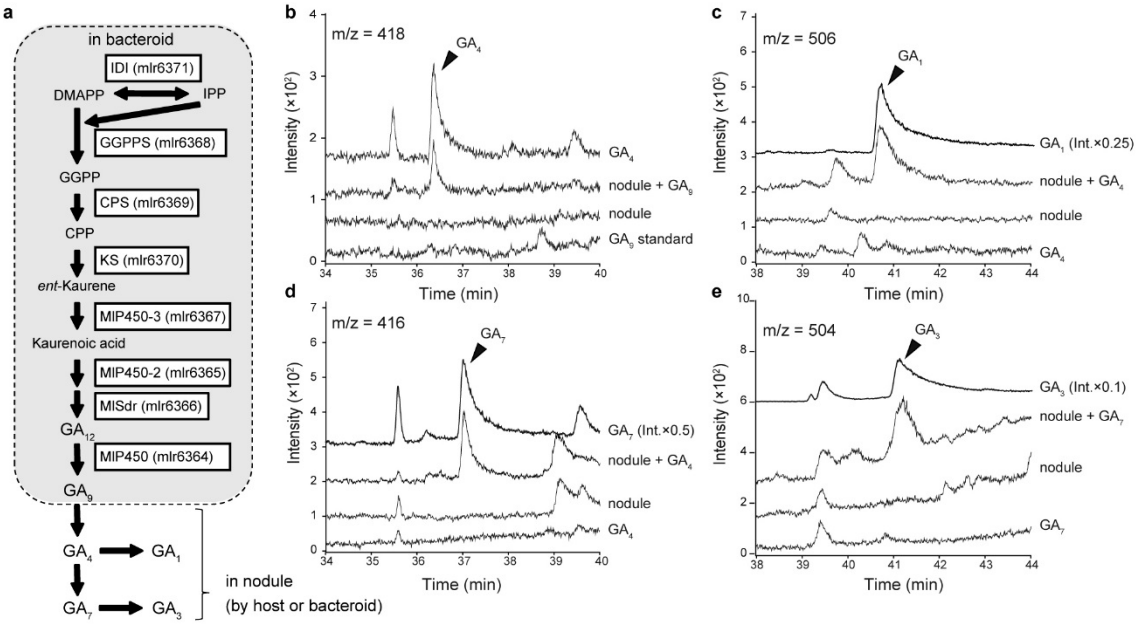

Figure 6 | GA synthesis mechanism in nodules. (a) GA-synthetic pathway in nodules. Reactions mediated by enzymes encoded on the GA-synthetic operon are shown inside the broken-lined box. Fractured nodules were incubated with substrate (GA_9, GA_4 or GA_7). (b-e) GAs were extracted with acidic ethylacetate. Extracts were methylated and trimethylsilylated and measured by GC–MS. Selected ion monitoring modes of m/z = 418 (b), 506 (c), 416 (d) and 504 (e) were used to detect GA_4, GA_1, GA_7 and GA_3, respectively.

action of host and symbiont enzymes. Moreover, addition of GA_3 to host with *gib*⁻mutant decreased the nodule number (Fig. 7b).

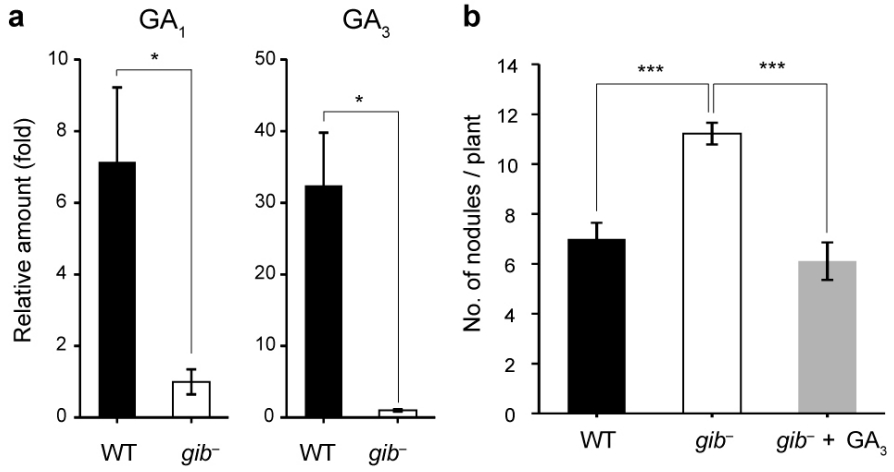

Figure 7 | GA quantification and exogenous application of GA (a) The amount of GA_1 and GA_3 in plants inoculated with wild-type and *gib*⁻ mutant rhizobia were determined by LC–MS. GA_4 and GA_7 were below the detection limit under both conditions. Significant differences were determined using student *t*-test. *p < 0.05. Error bars indicate SEMs from 3 biological replicates. (b) Number of nodules. Water-dissolved GA_3 was exogenously added at 10^{-7} mole per Incu Tissue at 2WPI. Multiple comparisons were corrected using the Holm-Bonferroni *t*-test. ***p < 0.001. WPI, weeks post inoculation. Error bars indicate SEMs from 9 plants.

Distribution of GA synthetic gene

To investigate the gene distribution among various rhizobial species, I performed BLAST (http://blast.ncbi.nlm.nih.gov/Blast.cgi) homology search against the genes in GA operon. I searched amino acid sequence similarities against two key genes for GA synthesis; *ent*-copalyl pyrophosphase synthase (mlr6369) and *ent*-kaurene oxidase (mlr6370). I chose these genes because *ent*-kaurene synthesis is powerful indicator for gibberellin synthesis and soil bacteria have some cytochrome P-450s irrelevant to GA synthesis (Kelly SL & Kelly DE, 2013). Interestingly, the genes for GA synthesis are found in species of rhizobia that inhabit the host in determinate nodules, including *M. loti*, *Bradyrhizobium japonicum*, *Sinorhizobium* (*Ensifer*) *fredii* and *Rhizobium etli*. Such genes are not found in rhizobial species, such as *S. meliloti* and *R. leguminosarum* biovar. *viciae*, which construct indeterminate nodules (Fig. 8). Among *R. leguminosarum*, GA synthetic genes were found only in *R. leguminosarum* biovar. *phaseoli*, but not in *R. leguminosarum* biovar. *viciae* and *R. legumino-*

sarum biovar. *trifoliae* although they belong to the same species. This result indicated that existence of GA-synthetic genes strongly correlated with the host nodule type.

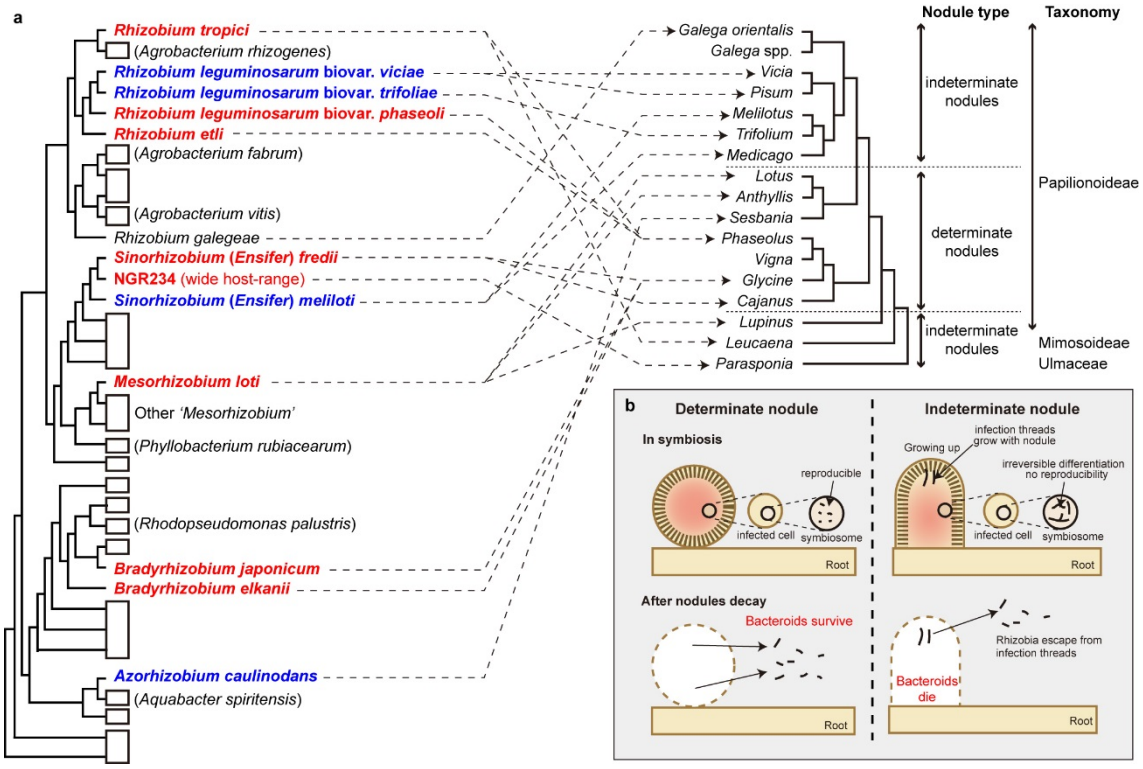

Figure 8 | Phylogenies of legumes and bacteria, nodule types and distribution of GA synthetic genes (**a**) Phylogenetic trees are modified from Doyle (1998). The bacterial phylogeny (left) is based on the 16S rRNA gene sequence. Representative symbiotic bacteria are shown; lineages of non-symbiotic bacteria are indicated by boxes. The bacteria possessing putative GA synthetic genes are shown in red bold characters and the bacteria without are shown in blue bold characters. Whether a bacterial species has GA-synthetic genes was determined by the presence of both *ent*-copalyl pyrophosphate synthase and *ent*-kaurene synthase by BLAST search. The phylogenetic relationships of legumes (and some non-legumes) based on *rbcL* sequence (right) are indicated for selected legume genera nodulated by bacteria that are shown on the bacterial tree. Nodule type and taxonomy are shown to the right of the tree. Arrows connect bacterial symbionts with their plant host. The wide host-range of NGR234 is shown by its ability to nodulate *Parasponia*. (**b**) Nodule structure of determinate and indeterminate nodules. Rhizobia lose the ability to reproduce after differentiation into bacteroids in indeterminate but not determinate nodules. Rhizobia typically possess the gibberellin operon only in hosts with determinate nodules.

Competition assay of wild-type and gib⁻ mutant

GA-synthetic genes are held by the rhizobia which construct determinate nodules (Fig. 8a). However, GA-synthetic genes are not necessary for symbiosis with host forming determinate nodules, because *gib*⁻ mutant which lacks the function of GA synthesis could infect into *L. japonicus* (Figs 3d–f and 7). Therefore, I hypothesized that possession of GA-synthetic genes

bring some advantages over non-possessor of the genes. To demonstrate the advantage of possessing GA-synthetic genes, wild-type and *gib*⁻strains were used in competition assays. Co-inoculation of equal amount of wild-type and *gib*⁻ mutants demonstrated that the *gib*⁻mutant gradually decreased in the population, without increasing nodule number (Fig. 9a,b), although such co-culture in liquid medium did not show this result (Fig. 9c) and individual inoculation assays of wild-type and *gib*⁻ mutants showed similar patterns of increasing numbers of rhizobial cells (Fig. 3f). These results show that possession of GA-synthetic genes is beneficial for growth in nodule.

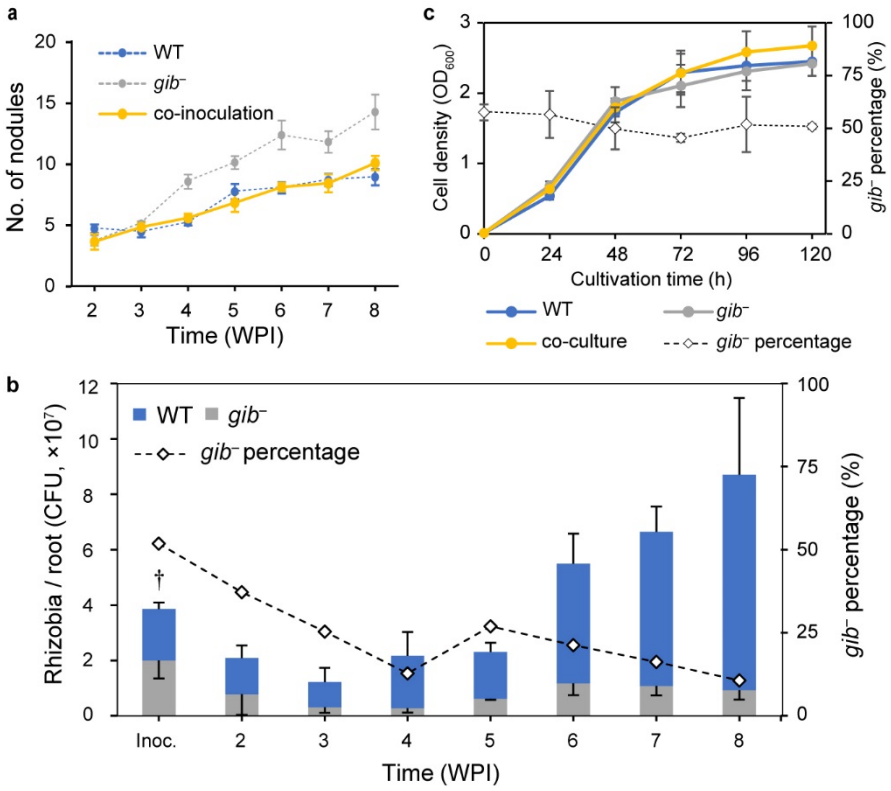

Figure 9 | Competition between *M. loti* WT and *gib*⁻ (a) Number of nodules in co-inoculation assays. Nodule numbers for *gib*⁻ are shown in grey, taken from Fig. 3h. Error bars represent SEMs from > 8 plants. (b) The number and percentage of rhizobia in roots. The number above each bar indicates the percentage of *gib*⁻colonies compared with the total colonies. Error bars indicate the SEMs from 3 plants. †: at this point, bacteria are isolated from soil (1 g) immediately after co-inoculation of WT and *gib*⁻. (c) Co-cultivation assay in liquid medium. Error bars indicate the SEMs from 3 independent experiments.

Discussion

In this chapter, I showed the phytohormonal regulation of nodule number from already-incorporated rhizobia in legume-rhizobia symbiosis. Nod factors (NFs) or exopolysaccharides are symbiont-derived signals for nodulation (Spaink, 1995, Kawaharada, 2015), however, rhizobial GA-dependent regulation of nodule number is different from the signals of NFs. Rhizobial GA regulates the nodule number under symbiotic condition, in contrast, NFs mainly initiate the nodulation process (Limpens, 2003). NFs are produced in response to flavonoid secreted from legume root hair, then induce the host nodule formation. There is a report that *nodC and nodD* genes were expressed during nodulation in *S. meliloti* (Sharma & Singer, 1990). It may play some roles in nodule development, however, the function of these bacterial genes inside the nodule are still functionally unknown, even if the NF receptors MtNFP and MtLYK3 were shown to be produced and required for bacterial release in the nodule, as Moling *et al*. (2014) mentioned. Okazaki *et al*. (2013) showed that *Bradyrhizobium elkanii* used type III secretion system to promote symbiosis by independent pathway of NF-dependent manner. This system also affects nodule number by activating host symbiosis signalling, however it is used when free-living rhizobia infect into host. Tian *et al*. found that already-incorporated *Sinorhizobium meliloti* inhibited the formation of infection thread by using cAMP signalling cascade (Tian et al., 2012). This study showed that rhizobia played an active role in the control of infection, however, defective mutant of cAMP signalling did not show the significant difference in nodule number. Thus I conclude that regulation of nodule number by rhizobial GA is a new regulation mechanism which benefits the already-incorporated rhizobia.

Then what is the meaning of negative regulation of host nodule formation by rhizobia? Results of time-course nodulation assay (Fig. 3h) showed that rhizobial GA decreased the nodule number at 4 WPI when primary nodules developed into a mature state, and nodule formed at lower position in *gib*$^{-}$ mutant (Fig. 3j). Lower nodule positions in *gib*$^{-}$ indicate that nodules were formed at younger portion of root, i.e. delayed nodule formation. These results suggest that rhizobia in mature nodules prevented the delayed nodule formation. This hypothesis is supported by my previous quantitative proteomic data in Chapter II, showing that the amount of protein

produced through the operon gradually increased during nodule maturation (Fig. 1c). Evolutionarily, the acquisition of nodule number control by rhizobia is presumed to be driven by the obstructive effects of delayed nodule formation by the following reasons: (i) too many nodules result in the decreased distribution of the carbon source per nodule from the host and (ii) rhizobia infecting the host after primary nodule maturation differ in genotype from those in primary nodules (Sullivan et al., 1995). Thus, I considered that already-incorporated rhizobia are likely to reject delayed infection by other rhizobia, leading to the evolutionary acquisition of nodule number regulation.

How rhizobia regulate the host nodule number by synthesizing GA? Previous report showed that exogenously-added GA_3 decreased the nodule number in *L. japonicus* (Maekawa et al., 2009). The root hair curling triggered by rhizobia was inhibited by exogenous GA treatment. Exogenously added GA suppressed gene expression of nodule signalling pathway 2 (*NSP2*), which functions upstream of *NIN*, a gene required for the onset of nodule development (Schauser et al., 1999). In this study, the expression level of *NSP2* in hosts inoculated with *gib*$^{-}$ *M. loti* was just slightly higher than that in hosts with wild-type *M. loti* at 5 WPI (Fig. 10) like Maekawa et al. (2009). The result suggests that rhizobial GA inhibits infection of other rhizobia via similar pathway which exogenous GA does. On the other hand, the relationship between rhizobial GA-dependent regulation of nodule number and AON is still obscure. In *P. sativum*, regulation of nodulation by host GA is predicted to act independently of AON (Ferguson et al., 2011). If it is applicable to *Lotus japonicus*, regulation by rhizobial GA also predicted to be independent from AON.

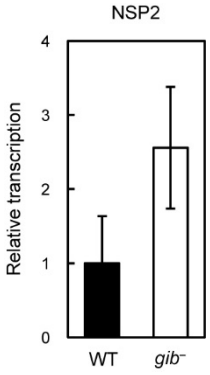

Figure 10 | Relative expression levels of NSP2 Fold-change values are relative to host inoculated with *M. loti* wild-type (expression level = 1) at 5 WPI. Error bars indicate the standard error from 3 plants.

Then why are GA-synthetic genes distributed among rhizobia which inhabit determinate nodule? The answer to this question lies in the developmental process of determinate and indeterminate nodules. Within indeterminate nodules, bacteroids are deprived of duplication capability by nodule-specific, cysteine-rich peptides secreted by the host (Kaneko et al., 2000, Atzorn et al., 1988). In contrast, bacteroids in determinate nodules still have the capacity for duplication, and they can escape from the nodule after the host plant dies (Fig. 8b) (Denison, 2000). The characteristic of determinate nodule gives rhizobia advantage to reject delayed nodulation and to increase the population in nodule. Therefore, GA synthesis in rhizobia is presumably acquired in symbiont pairs involving a rhizobium and a host legume that does not kill its symbiont. This hypothesis of evolutionary acquisition of the genes is supported by the process of leguminous evolution. Now, the origin of nodulation is predicted to be approximately 60 million years ago, when all nodules were indeterminate nodules (Doyle, 2011). Determinate nodules arose from indeterminate-type ancestor in legume evolution, supporting that GA-synthetic genes were evolutionarily acquired after rhizobial symbiotic modules (symbiotic island or plasmid) were developed. Moreover, it was reported that the cytochrome P-450 cluster on NGR234 was 10% richer in G + C content than the rest of the symbiotic plasmid (Freiberg et al., 1997), and had proteins with >80% similarity to those of other rhizobia (e.g. Table 4), indicating that these genes have been selectively integrated into the symbiotic modules of rhizobia constructing determinate nodule. Furthermore, the micromolar concentrations of exogenously applied GA were reported to decrease the nodule number in *L. japonicus*, which forms determinate nodules (Maekawa et al., 2009), but increase the nodule number in *P. sativum*, which forms indeterminate nodules (Ferguson et al., 2005). These observations indicate that GA plays opposing roles in the formation of the two types of nodules. The negative effect of host with determinate nodule by GA allows rhizobia to decrease the nodule number.

Table 4 | Distribution of GA synthetic genes among rhizobia

species	ent-copalyl pyrohposphase synthase		ent-kaurene oxidase	
name	NCBI Reference Sequence ID	homology(%)	NCBI Reference Sequence ID	homology(%)
Mesorhizobium loti (reference)	WP_010913996.1	100	WP_010913997.1	100
Rhizobum tropici	WP_004120019.1	90	WP_004120017.1	88
Rhizobium leguminosalum bv. *viciae*	–	–	–	–
Rhizobium leguminosalum bv. *trifoliate*	–	–	–	–
Rhizobium leguminosalum bv. *phaseoli*	WP_037145548.1	86	WP_037145551.1	88
Rhizobium etli	WP_040140636.1	88	WP_020923331.1	91
Sinorhizobium fredii	WP_014857759.1	95	WP_014857758.1	94
NGR234 (wide host-range)	WP_010875301.1	94	WP_010875302.1	94
Sinorhizobium meliloti	–	–	–	–
Bradyrhizobium japonicum	WP_026312707.1	93	WP_028153675.1	93
Bradyrhizobium elkanii	WP_028350654.1	93	WP_028350655.1	94
Azorhizobium coulinodans	–	–	–	–

Co-inoculation assay revealed that rhizobia which lacks GA synthesis were decreased gradually (Fig. 9b), although the growth rate in liquid medium was similar to wild-type (Fig. 9c). The mechanism of this phenomenon remains obscure, but I suggest that the rhizobial GA also affects rhizobial population in nodules. As many studies indicate plant-derived GA plays an important role in nodule formation reviewed in Hayashi *et al*. (2014), rhizobial GA might also affect proper nodule formation. Reduction of nitrogen fixing activity (Fig. 3g) and slightly smaller nodules in *gib*$^{-}$ mutant (Fig. 3i) support this idea. In *gib*$^{-}$ dominant nodule, nitrogen fixing activity maybe lower or nodule formation maybe slower than wild-type dominant nodule, then sanctioned by host plant when considering the sanction hypothesis (Denison, 2000, Kiers et al., 2003). Or rhizobial gibberellin may promote the bacterial release from the infection threads. Yet, this hypothesis have to be further experimentally proved.

Summary

In this chapter, I show for the first time that *M. loti* synthesizes GA during symbiosis using enzymes unique to this condition and that synthesized GA maintains optimal nodule number and eventually optimizes the amount of nitrogen fixation per nodule. This finding is the first demonstration that a symbiont-derived hormonal signal regulates the host nodule number. These results enable me to propose a model of nodule number regulation by rhizobial GA (Fig. 11) and suggest that GA synthesis gives an evolutionary advantage for rhizobia in determinate nodules as

it enables indigenous rhizobia to restrain delayed infection by other rhizobia. My findings show the potential of symbionts to co-evolutionarily acquire the ability to regulate the host's phenotype.

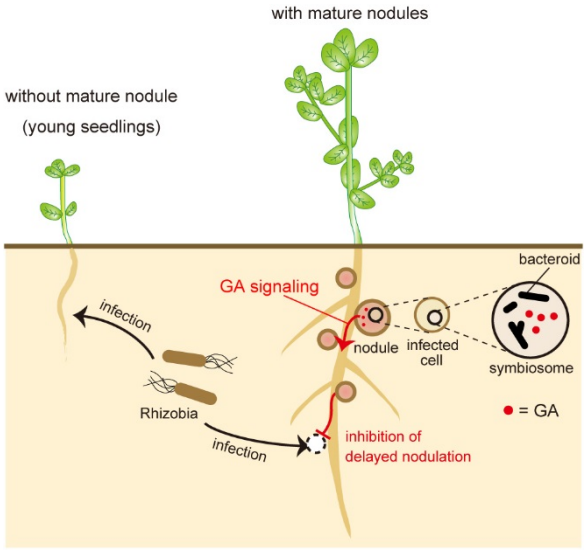

Figure 11 | Model of nodule number regulation by rhizobial gibberellin In the early developmental stage (no mature nodules), rhizobia inoculate into host plants only under host-derived control (e.g. auto-regulation of nodulation). After nodules have matured, the symbiont-derived regulation via rhizobial gibberellin also works to inhibit delayed infection by other rhizobia.

References

1. Atzorn R, Crozier A, Wheeler CT, Sandberg G, Production of gibberellins and indole-3-acetic acid by *Rhizobium phaseoli* in relation to nodulation of *Phaseolus vulgaris* roots. *Planta*, **175**, 532–538 (1988)
2. Becard G, Fortin JA, Early events of vesicular-arbuscular mycorrhiza formation on Ri T-DNA transformed roots. *New Phytol.*, **108**, 211–218 (1988)
3. Boiero L, Perrig D, Masciarelli O, Penna C, Cassán F, Luna V, Phytohormone production by three strains of *Bradyrhizobium japonicum* and possible physiological and technological implications. *Appl. Microbiol. Biotechnol.*, **74**, 874–880 (2007)
4. Bomke C, Tudzynski B, Diversity, regulation, and evolution of the gibberellin biosynthetic pathway in fungi compared to plants and bacteria. *Phytochemistry*, **70**, 1876–1893 (2009)
5. Broughton WJ, Dilworth MJ, Control of leghaemoglobin synthesis in snake beans. *Biochem. J.*, **125**, 1075–1080 (1971)
6. Caetano-Anolles G, Gresshoff PM, Plant genetic control of nodulation. *Annu. Rev. Microbiol.*, **45**, 345–382 (1991)

7. Denison RF, Legume sanctions and the evolution of symbiotic cooperation by rhizobia. *Am. Nat*., **156**, 567–576 (2000)
8. Doyle JJ, Phylogenetic perspectives on nodulation: evolving views of plants and symbiotic bacteria. *Trends Plant Sci*., **3**, 473–478 (1998)
9. Doyle JJ, Phylogenetic perspectives on the origins of nodulation. *Mol. Plant-Microbe Interact*., **24**, 1289–1295 (2011)
10. Ferguson BJ, Foo E, Ross JJ, Reid JB, Relationship between gibberellin, ethylene and nodulation in *Pisum sativum*. *New Phytol*., **189**, 829–842 (2011)
11. Ferguson BJ, Indrasumunar A, Hayashi S, Lin MH, Lin YH, Reid DE, Gresshoff PM, Molecular analysis of legume nodule development and autoregulation. *J. Integr. Plant Biol*., **52**, 61–76 (2010)
12. Ferguson BJ, Mathesius U, Phytohormone regulation of legume-rhizobia interactions. *J. Chem. Ecol*., **40**, 770–790 (2014)
13. Freiberg C, Fellay R, Bairoch A, Broughton WJ, Rosenthal A, Perret X, Molecular basis of symbiosis between *Rhizobium* and legumes. *Nature*, **387**, 394–401 (1997)
14. Hedden P, Sponsel V, A century of gibberellin research. *J. Plant Growth Regul*., **34**, 740–760 (2015).
15. Hershey DM, Lu X, Zi J, Peters RJ, Functional conservation of the capacity for *ent*-kaurene biosynthesis and an associated operon in certain rhizobia. *J. Bacteriol*., **196**, 100–106 (2014)
16. Kaneko T, Nakamura Y, Sato S, Asamizu E, Kato T, Sasamoto S, Watanabe A, Idesawa K, Ishikawa A, Kawashima K, Kimura T, Kishida Y, Kiyokawa C, Kohara M, Matsumoto M, Matsuno A, Mochizuki Y, Nakayama S, Nakazaki N, Shimpo S, Sugimoto M, Takeuchi C, Yamada M, Tabata S, Complete genome structure of the nitrogen-fixing symbiotic bacterium *Mesorhizobium loti*. *DNA Res*., **7**, 331–338 (2000)
17. Kawaguchi M, *Lotus japonicus* 'Miyakojima' MG-20: An early-flowering accession suitable for indoor handling. *J. Plant Res*., **113**, 507–509 (2000)
18. Kawaharada Y, Kelly S, Nielsen MW, Hjuler CT, Gysel K, Muszyński A, Carlson RW, Thygesen MB, Sandal N, Asmussen MH, Vinther M, Andersen SU, Krusell L, Thirup S, Jensen KJ, Ronson CW, Blaise M, Radutoiu S, Stougaard J, Receptor-mediated exopolysaccharide perception controls bacterial infection. *Nature*, **523**, 308-312 (2015)

19. Kelly SL, Kelly DE, Microbial cytochromes P450: biodiversity and biotechnology. Where do cytochromes P450 come from, what do they do and what can they do for us? *Philos. Trans. R. Soc. Lond. B. Biol. Sci*., **368**, 20120476 (2013)
20. Kiers ET, Rousseau RA, West SA, Denison RF, Host sanctions and the legume-rhizobium mutualism. *Nature*, **425**, 78–81 (2003)
21. Limpens E, Bisseling T, Signaling in symbiosis. *Curr. Opin. Plant Biol*., **6**, 343–350 (2003)
22. Maekawa T, Maekawa-Yoshikawa M, Takeda N, Imaizumi-Anraku H, Murooka Y, Hayashi M, Gibberellin controls the nodulation signaling pathway in *Lotus japonicus*. *Plant J*., **58**, 183–194 (2009)
23. Miyamoto K, Hara T, Kobayashi H, Morisaka H, Tokuda D, Horie K, Koduki K, Makino S, Núñez O, Yang C, Kawabe T, Ikegami T, Takubo H, Ishihama Y, Tanaka N, High-efficiency liquid chromatographic separation utilizing long monolithic silica capillary columns. *Anal. Chem*., **80**, 8741–8750 (2008)
24. Moling S, Pietraszewska-Bogiel A, Postma M, Fedorova E, Hink MA, Limpens E, Gadella TW, Bisseling T, Nod factor receptors form heteromeric complexes and are essential for intracellular infection in *Medicago* nodules. *Plant Cell*, **26**, 4188–4199 (2014)
25. Oka-Kira E, Kawaguchi M, Long-distance signaling to control root nodule number. *Curr. Opin. Plant Biol*., **9**, 496–502 (2006)
26. Okazaki S, Kaneko T, Sato S, Saeki K, Hijacking of leguminous nodulation signaling by the rhizobial type III secretion system. *Proc. Natl. Acad. Sci. U. S. A.*, **110**, 17131–17136 (2013)
27. Ryu H, Cho H, Choi D, Hwang I, Plant hormonal regulation of nitrogen-fixing nodule organogenesis. *Mol. Cells*, **34**, 117–126 (2012)
28. Schauser L, Roussis A, Stiller J, Stougaard J, A plant regulator controlling development of symbiotic root nodules. *Nature*, **402**, 191–195 (1999)
29. Sharma SB, Signer ER, Temporal and spatial regulation of the symbiotic genes of *Rhizobium meliloti* in planta revealed by transposon Tn5-gusA. *Genes Dev*., **4**, 344–356 (1990)
30. Shimoda Y, Mitsui H, Kamimatsuse H, Minamisawa K, Nishiyama E, Ohtsubo Y, Nagata Y, Tsuda M, Shinpo S, Watanabe A, Kohara M, Yamada M, Nakamura Y, Tabata S, Sato S, Construction of signature-tagged mutant library in *Mesorhizobium loti* as a powerful tool for functional genomics. *DNA Res*., **15**, 297–308 (2008)

31. Spaink HP, The molecular basis of infection and nodulation by rhizobia: the ins and outs of sympathogenesis. *Annu. Rev. Phytopathol*., **33**, 345–368 (1995)
32. Sullivan JT, Patrick HN, Lowther WL, Scott DB, Ronson CW, Nodulating strains of *Rhizobium loti* arise through chromosomal symbiotic gene transfer in the environment. *Proc. Natl. Acad. Sci. U. S. A.*, **92**, 8985–8989 (1995)
33. Tian CF, Garnerone AM, Mathieu-Demaziere C, Masson-Boivin C, Batut J, Plant-activated bacterial receptor adenylate cyclases modulate epidermal infection in the *Sinorhizobium meliloti-Medicago* symbiosis. *Proc. Natl. Acad. Sci. U. S. A.*, **109**, 6751–6756 (2012)
34. Uchiumi T, Ohwada T, Itakura M, Mitsui H, Nukui N, Dawadi P, Kaneko T, Tabata S, Yokoyama T, Tejima K, Saeki K, Omori H, Hayashi M, Maekawa T, Sriprang R, Murooka Y, Tajima S, Simomura K, Nomura M, Suzuki A, Shimoda Y, Sioya K, Abe M, Minamisawa K, Expression islands clustered on the symbiosis island of the *Mesorhizobium loti* genome. *J. Bacteriol*., **186**, 2439–2448 (2004)

Conclusion

The present study has been performed to describe the symbiotic phenotype of *M. loti* under symbiosis with *L. japonicus* with my original analytical system of proteomics. I first found 'symbiont-driven' control of nodulation in *L. japonicus*-*M. loti* symbiosis.

In Chapter I, I compared the protein profile of *M. loti* MAFF303099 under free-living conditions to its profile under symbiotic conditions by using small amounts of crude extracts. The obtained protein profiles appeared to reflect differences in the phenotypes under both conditions. In addition, KEGG pathway analysis revealed that the cell surface structure of rhizobia was largely different under each condition, and surprisingly, that rhizobia might provide some kinds of terpenoid to the host as a source of secondary metabolism. *M. loti* changed its metabolism and cell surface structure in accordance with the surrounding conditions.

In Chapter II, I performed quantitative proteomics of *M. loti* during nodule maturation. The results revealed significant changes in the carbon and amino acid metabolisms of *M. loti* upon differentiating into bacteroids. Furthermore, my findings suggested that *M. loti* enters into a nitrogen-deficient condition during the early stages of nodule development, and then a nitrogen-rich condition during the intermediate stages of nodule development. In addition, my data indicated that *M. loti* assimilated ammonia during the intermediate stages of nodule development.

In Chapter III, I studied the symbiosis specific expressing operon which was found in my previous proteomics. I showed for the first time that *M. loti* synthesizes gibberellic acid (GA) during symbiosis using enzymes unique to this condition and that synthesized GA maintains an optimal nodule number and eventually optimizes the amount of nitrogen fixation per nodule. This finding is the first demonstration that a symbiont-derived hormonal signal regulates the host nodule number. These results enable us to propose a model of nodule number regulation by rhizobial GA and suggest that GA synthesis gives an evolutionary advantage for rhizobia in determinate nodules as it enables indigenous rhizobia to restrain delayed infection by other rhizobia.

In summary, the findings of the present study revealed that *M. loti* under symbiosis shows various responses other than nitrogen fixation and controls the host nodulation.

Acknowledgments

This thesis is submitted by the author to Kyoto University for the Doctor degree of Agriculture. The studies presented here have been carried out under the direction of Professor Mitsuyoshi Ueda in the Laboratory of Biomacromolecular Chemistry, Division of Applied Life Sciences, Graduate School of Agriculture, Kyoto University, during 2011-2017.

I would like to express my sincere gratitude to Professor Mitsuyoshi Ueda for his continuous guidance and helpful discussions throughout the course of this study. I deeply thank Associate Professor Kouichi Kuroda for his critical comments throughout my study. And I am also deeply grateful to Assistant Professor Wataru Aoki for his valuable comments and discussion. I express my appreciation to Secretary Fukuko Suzuki for her support of my laboratory life. My deepest appreciation goes to all the members in this laboratory for their constant encouragement and support throughout this work.

I am deeply grateful to the late ex-Assistant Professor Hironobu Morisaka for his guidance, encouragement, understanding, experimental suggestion, and skilled technical supports.

I am grateful to Research Fellowship of the Japan Society for the Promotion of Science for Young Scientists and Teijin-Kumura scholarship foundation for financial support.

Lastly, I express my great gratitude to my family for all their help and warm encouragement.

Yohei TATSUKAMI

Laboratory of Biomacromolecular Chemistry
Division of Applied Life Sciences
Graduate School of Agriculture
Kyoto University

Publication

Chapter I

Tatsukami Y, Nambu M, Morisaka H, Kuroda K, Ueda M, Disclosure of the differences of *Mesorhizobium loti* under the free-living and symbiotic conditions by comparative proteome analysis without bacteroid isolation. *BMC Microbiol.*, **13**, 180 (2013)

Chapter II

Nambu M*, Tatsukami Y*, Morisaka H, Kuroda K, Ueda M, Quantitative time-course proteome analysis of *Mesorhizobium loti* during nodule maturation. *J. Proteomics*, **125**, 112–120 (2015) *co-first author

Chapter III

Tatsukami Y and Ueda M, Rhizobial gibberellin negatively regulates host nodule number. *Sci. Rep.*, **6**, 27998 (2016)

Other publications

Morisaka H, Matsui K, Tatsukami Y, Kuroda K, Miyake H, Tamaru Y, Ueda M, Profile of native cellulosomal proteins of *Clostridium cellulovorans* adapted to various carbon sources. *AMB Express*, **2**, 37 (2012)

Aoki W, Ueda T, Tatsukami Y, Kitahara N, Morisaka H, Kuroda K, Ueda M, Time-course proteomic profile of *Candida albicans* during adaptation to a fetal serum. *Pathog. Dis.*, **67**, 67-75 (2013)

Miura N, Shinohara M, Tatsukami Y, Sato Y, Morisaka H, Kuroda K, Ueda M, Spatial reorganization of *Saccharomyces cerevisiae* enolase to alter carbon metabolism under hypoxia. *Eukaryot. Cell*, **12**, 1106-19 (2013)

Aoki W, Tatsukami Y, Kitahara N, Matsui K, Morisaka H, Kuroda K, Ueda M,

Elucidation of potential virulent factors of *Candida albicans* during serum adaptation by using quantitative time-course proteomics. *J. Proteomics*, **91**, 417-429 (2013)

Takagi T, Morisaka H, Aburaya S, Tatsukami Y, Kuroda K, Ueda M, Putative alginate assimilation process of the marine bacterium *Saccharophagus degradans* 2-40 based on quantitative proteomic analysis. *Mar. Biotechnol*., **18**, 15-23 (2016)

Japanese publications

立上陽平, 植田充美, 第三章 水素キャリアの研究開発 7. 微生物の合成生物学的改質育種に向けて, 『バイオ水素とキャリア開発の最前線』, シーエムシー出版, 162-169 (2015)

立上陽平, 植田充美, 根粒菌の新たな機能を発見：ジベレリン生合成と根粒数制御, 『バイオサイエンスとインダストリー』, バイオインダストリー協会, 第 75 巻, 第 1 号 (2017)